

國立交通大學

電信工程研究所

博士論文

適用於多輸入多輸出與多輸入多輸出中
繼系統中最大似然接收機之前置編碼器
設計

Precoder Designs for Maximum-Likelihood
Detectors in MIMO and MIMO Relay
Systems

研究生：林鈞陶

指導教授：吳文榕 博士

中華民國 101 年 8 月

適用於多輸入多輸出與多輸入多輸出中繼系統中
最大似然接收機之前置編碼器設計

Precoder Designs for Maximum-Likelihood Detectors
in MIMO and MIMO Relay Systems

研究生：林鈞陶

Student: Chun-Tao Lin

指導教授：吳文榕 博士

Advisor: Dr. Wen-Rong Wu

國立交通大學

電信工程研究所

博士論文



A Dissertation

Submitted to Institute of Communication Engineering
College of Electrical and Computer Engineering

National Chiao Tung University

in Partial Fulfillment of the Requirements
for the Degree of Doctor of Philosophy

in

Communication Engineering

Hsinchu, Taiwan

2012 年 8 月

適用於多輸入多輸出與多輸入多輸出中繼系統中最大似然接收機之前置編碼器設計

研究生：林鈞陶

指導教授：吳文榕 博士

國立交通大學

電信工程研究所博士班



前置編碼已被認為是一種可以有效改善多輸入多輸出 (Multiple-input multiple-output ; MIMO)系統中傳輸品質的技術。一般而言，前置編碼的設計與接收機的類型有關。對於最大似然 (Maximum-likelihood ; ML)接收機而言，最佳的前置編碼設計準則是最大化系統的自由距離，然而最佳解的導出相當困難，因此目前多數文獻僅討論其次佳解，本論文旨在探討對應 ML 接收機的前置編碼器設計問題。在論文的第一部分，我們首先考慮簡化之前置編碼，也就是傳送端天線選擇，最佳的天線選擇準則必需透過高運算量的窮舉法才能得到，為了避免此問題，研究者利用奇異值分解(Singular value decomposition ; SVD)以及 QR 分解 (QR decomposition ; QRD)推導出自由距離的下界。我們提出以 QRD 為基礎之天線選擇方法，我們證明了 QRD 選擇法會優於傳統的 SVD 法，此外我們進一步提出基底轉換的方法使得 QRD 選擇法能夠更接近最佳解。除了傳送端天線選擇之外，我們提出的方法也可適用於其他應用，例如接收端天線選擇、傳送端與接收端聯合天線選擇、以及在 MIMO 中繼系統中天線選擇。模擬結果顯示，

我們提出的方式在上述應用中均能提供接近最佳的表現。

除了天線選擇之外，最近有研究者提出一種基於 X-架構之次佳前置編碼方式，此方法的概念在於先利用 SVD 得到平行子通道，再利用兩兩配對的方式得到多個 2×2 的子系統，這樣的作法允許我們僅需設計 2×2 的子前置編碼器，因而得以在降低編碼的複雜度，此外 X-架構前置編碼的方式同時可提供一個低複雜度的 ML 接收機。然而，目前現有文獻中所提出的 X-架構前置編碼器的設計均仰賴數值法以及查表的方式，使得現有的方法在實際應用上困難度與複雜度均相對增加。在論文的第二部分我們提出一個簡單但有效的方法來解決此問題，我們的方法所得到的前置編碼矩陣具有解析解，另外，我們也探討如何將 X-架構前置編碼延伸至 MIMO 中繼系統中聯合前置編碼器設計的問題。模擬結果顯示我們提出的方法比現有的前置編碼法可以更有效的改善系統效能。



前置編碼器的計算需要完整的通道資訊，因此一般都在接收端完成，在實際系統中，前置編碼的實現是透過從碼書中選取一個最佳的碼字，再經由迴授通道將該碼字的索引回傳至傳送端。在論文的最後一個部分，我們將討論如何建構 X-架構前置編碼所需要的碼書，有別於傳統的前置編碼，X-架構前置編碼器需要兩種碼書，一種是用於一么正矩陣，另一種是用於子編碼器的矩陣，使用於么正矩陣的碼書所面臨的問題在於量化的矩陣不能讓系統保有 X 的架構，低複雜度 ML 接收機也因此不復存在，針對此問題，我們先證明我們所提出的 X-架構前置編碼器仍然有效，接著我們提出一個低複雜的接收機架構來解決偵測的問題。模擬結果顯示，我們所提出的方法除了可以使用低複雜度的接收機外同時也可有效改善系統效能。

Precoder Designs for Maximum-Likelihood Detectors in MIMO and MIMO Relay Systems

Student: Chun-Tao Lin

Advisor: Dr. Wen-Rong Wu

National Chiao Tung University

Institute of Communication Engineering



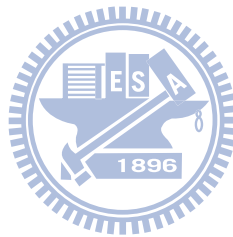
Precoding has been considered a promising technique in multiple-input multiple-output (MIMO) transmission. In general, the design criterion depends on the detector used at the receiver. For the maximum-likelihood (ML) detector, the criterion is known to maximize the free distance. Unfortunately, the derivation of the optimum solution is difficult, and suboptimum solutions have then been developed. In this dissertation, we study the precoder design for the ML detector in MIMO and MIMO relay systems. In the first part of this dissertation, we consider a simplified precoding scheme, namely, transmit antenna selection. To maximize the free distance, it is necessary to conduct exhaustive search for the selection pattern. To avoid the problem, lower bounds of the free distance derived with the singular value decomposition (SVD) or QR decomposition (QRD) were developed. We propose a QRD-based selection method maximizing the corresponding lower bound. With some matrix properties, we theoretically prove that the lower bound yielded by the QRD is tighter than that by the SVD. We then further propose a

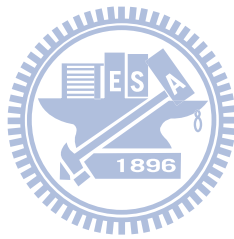
basis-transformation method so that the lower bound yielded by the QRD can be further tightened. The proposed method is also extended to antenna selection in amplify-and-forward (AF) MIMO relay systems, and other types of selections such as receive antenna selection, and joint transmit and receive antenna selection. Simulations show that the lower bound that the proposed methods evaluate can approach the true free distance closely.

As mentioned, the optimum precoder for the ML detector is difficult to derive. Recently, a simple design method, referred to as X-structured precoding, was proposed to solve the problem. This method first adopts the SVD to transform the MIMO channel into parallel subchannels. Then, the subchannels are paired to obtain a set of 2×2 subsystems and 2×2 subprecoders can be designed. Due to this special structure, the ML detection in the receiver can be conducted on 2×2 subsystems, reducing computational complexity significantly. Several methods have been developed to solve the X-structured precoder. However, most of them use numerical searches to find their solutions and require table look-ups during the run time. In the second part of this dissertation, we propose a simple but effective method to solve the problems. The proposed precoder has a simple closed-form expression and no numerical searches and table look-ups are required. We also extend the proposed method in joint source/relay precoders design in two-hop AF MIMO relay systems. With the proposed source subprecoder, the joint design problem can be significantly simplified. Simulations show that the proposed X-structured precoding for MIMO relay systems significantly outperforms other types of precoding methods.

Calculation of the precoder requires full channel state information and is conducted in the receiver in general. In real-world applications, a codebook is designed for the precoder, and only the index of the codeword is fed back. In the final part of this dissertation, we investigate the codebook design problem in X-structured precoding. Unlike the conventional precoding, X-structured precoding requires two codebooks, one for a unitary matrix and the other for 2×2 subprecoders. The challenges are that the quantized unitary matrix cannot yield the X-structure and the receiver cannot conduct ML detection on 2×2 subsystems. We show that the proposed

X-structure precoding scheme can still be used, and propose low-complexity detection schemes to solve the detection problem. Simulation results show that the proposed method can effectively reduce the computational complexity of the receiver and at the same time improve the system performance.





Acknowledgements

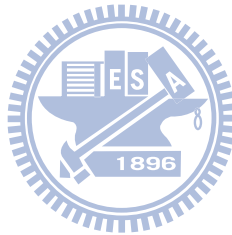
During my Ph.D. program, I would like to show my gratitude to many people. First, I would like to deeply thank my advisor, Prof. Wen-Rong Wu, for his kindly guidance. He spent a lot of time in discussing the problems I encountered in my research, providing valuable suggestions, and teaching me how to write technical papers. Under his enthusiastic instruction, I have learned not only the method to do research, but also the optimistic attitude. At this moment, I have to say Prof. Wu is the key person whom I am most grateful to.

Second, I am grateful to all the members in our Lab for their valuable discussions and help in academic research; they are Chun-Fang Lee, Din-Hwa Huang, Chi-Han Lee, Sheng-Lung Cheng, and all other master students. Especially, I deeply appreciate Dr. Chao-Yuan Hsu, Dr. Fan-Shuo Tseng, and Dr. Hung-Tao Hsieh for their encouragement and suggestions. Besides, thank you all who help me prepare my oral defense; you are Jacky, Yangyang, Wranky, and other master students. Also, I would like to thank all my friends who ever encouraged or helped me. Thank you Hsueh-Shu Huang for your kindly help in preparing travel information about conferences.

Last, but not least, I would like to show my deep gratitude to my family, especially my dear mother. Thank you all for your economic and spirit support in the period. Without your supports and encouragements, I cannot finish my Ph.D. program.

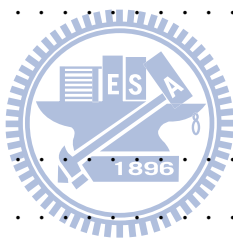
Contents

Chinese Abstract		iii
English Abstract		v
Acknowledgements		x
Contents		xi
List of Tables		xvi
List of Figures		xvii
1 Introduction		1
2 Antenna Selection for ML Detectors in Spatial-Multiplexing MIMO and MIMO Relay Systems		9
2.1 Lower bounds for free distance		10
2.1.1 <i>System and Signal Models</i>		10
2.1.2 <i>Lower Bound with SVD-Based Method</i>		11
2.1.3 <i>Lower Bound with QRD-Based Method</i>		12
2.2 Proposed Basis-Transformation Method		15
2.2.1 <i>Permutation Matrix</i>		17
2.2.2 <i>Transformation Matrix in Lattice Reduction</i>		18



2.2.3	<i>Cascade of Permutation and LR Matrices</i>	20
2.3	Implementation Issues and Complexity Comparisons	21
2.3.1	<i>Givens Rotations Method</i>	21
2.3.2	<i>Efficient Permutations</i>	22
2.3.3	<i>Complexity Comparisons</i>	23
2.4	Other Applications	23
2.4.1	<i>Receive and Joint Transmit/Receive Antenna Selection</i>	23
2.4.2	<i>Antenna Selection in MIMO Relay Systems</i>	25
2.4.3	<i>Sphere Decoding Algorithm</i>	27
2.5	Simulations and Discussions	28
3	X-Structured Precoding for ML Detectors in Spatial-Multiplexing MIMO and MIMO Relay Systems	43
3.1	System Models and Problem Formulation	44
3.2	Existing Subprecoders for MIMO Systems	46
3.2.1	<i>Complex-Valued Subprecoder Design</i>	46
3.2.2	<i>Real-Valued Subprecoder Design</i>	48
3.2.3	<i>Orthogonal Subprecoder Design</i>	49
3.3	Proposed Subprecoders for MIMO Systems	49
3.3.1	<i>GMD-Based Subprecoder with Rank-Deficiency</i>	50
3.3.2	<i>Extension to MIMO Systems for $M > 2$</i>	52
3.3.3	<i>Complexity Comparisons</i>	53
3.4	Joint Precoders Design for MIMO Relay Systems	54
3.4.1	<i>Problem Formulation and Source Precoder Design</i>	54
3.4.2	<i>Relay Precoder Design</i>	57
3.5	Simulations and Discussions	66
3.5.1	<i>Performance Comparisons for MIMO Systems</i>	66
3.5.2	<i>Performance Comparisons for MIMO Relay Systems</i>	67

4 Limited-Feedback for X-Structured Precoding in Spatial-Multiplexing MIMO Systems	77
4.1 System Models and Problem Formulation	78
4.2 Quantization for X-Structured Precoding	79
4.3 Low-Complexity MIMO Detection	84
4.4 Simulation Results	87
5 Conclusions	95
Appendix A	99
A.1 SVD-Based Lower Bound with Transformed Symbol Vectors	99
A.2 Evaluation of (2.27)	100
A.3 Proof of (2.28)	101
Appendix B	105
B.1 Proof of (3.57)	105
B.2 Proof of (3.58)	107
B.3 Derivation of (3.68)	108
B.4 Derivation of (3.80)	109
Bibliography	111



List of Tables

2.1	Algorithm of proposed QRD-based BT-P method	31
2.2	Operations of CLLL algorithm	33
2.3	Algorithm of proposed QRD-based BT-C method	34
2.4	Algorithm of proposed QRD-based BT-E method	35
2.5	Complexity comparisons for different antenna selection methods	36
3.1	Complexity comparisons for X-structured precoding	69
3.2	Detection complexity comparisons for X-structured precoding	70
3.3	Joint source/relay precoders design with source power allocation	76
4.1	Complexity comparisons for detection methods	89

List of Figures

2.1	System model for transmit antenna selection in a spatial-multiplexing MIMO system.	31
2.2	LR for $M = 2$	32
2.3	$[\mathbf{R}_i]_{\min}$ computations for $M = 3$	34
2.4	System model of a two-hop AF MIMO relay system.	35
2.5	BER performance comparison for transmit antenna selection ($N_t = 6, N_r = 3,$ and $M = 3$).	37
2.6	BER performance comparison for receive antenna selection ($N_t = 3, N_r = 6,$ and $M = 3$).	38
2.7	BER performance comparison for joint transmit/receive antenna selection ($N_t =$ $5, N_r = 4,$ and $M = 3$).	39
2.8	BER performance comparison for antenna selection in a two-hop MIMO relay system ($N_t = 4, N_{re} = 4, N_r = 4,$ and $M = 3$).	40
2.9	BER performance comparison for transmit antenna selection with SDA ($N_t =$ $6, N_r = 3,$ and $M = 3$).	41
3.1	System model for a precoded spatial-multiplexing MIMO system.	69
3.2	System model for a precoded spatial-multiplexing MIMO relay system.	70
3.3	BLER performance comparisons for MIMO systems with $N_t = 2, N_r = 2,$ and $M = 2$	71

3.4	BLER performance comparisons for MIMO systems with $N_t = 4$, $N_r = 4$, and $M = 4$	72
3.5	BLER performance comparisons for MIMO relay systems with 4-QAM ($N_t = 4$, $N_r = 4$, $N_d = 4$, and $M = 4$).	73
3.6	BLER performance comparisons for MIMO relay systems with 16-QAM ($N_t = 4$, $N_r = 4$, $N_d = 4$, and $M = 4$).	74
3.7	Algorithm 3.1: Joint source/relay precoders design without source power allocation Υ	75
4.1	System model for a limited-feedback precoding MIMO system.	89
4.2	Performance comparisons for different sizes of \mathcal{F}_1	90
4.3	Performance comparisons for different values of K_c	91
4.4	Performance comparisons for unprecoded and precoded systems with $N_t = 4$, $N_r = 4$, and $M = 4$	92
4.5	Detection complexity comparisons for unprecoded systems with different values of M	93
A1	Symbol constellations in which $d_{\min}(\mathcal{X}_{LR}^1) = d_{\min}(\mathcal{X}^M)$ ($M = 2$, \times : original constellation, \bullet : transformed constellation).	101

Chapter 1

Introduction

IN recent years, the multiple-input multiple-output (MIMO) technique has been widely adopted in wireless communication systems. In MIMO systems, it is well-known that transmission with spatial multiplexing can provide higher spectral efficiency without bandwidth expansion [1]. However, its performance heavily depends on the condition number of the channel matrix [2]. For ill-conditioned channels, the performance of a MIMO system can be degraded seriously. Precoding is an effective method to overcome this problem.

The precoder design problem has been extensively studied in the literature. With the mutual information criterion, a power allocation method referred to as mercury/water-filling [3] was proposed for parallel Gaussian channels, and the obtained precoder, being diagonal, is shown to be the optimum power allocation scheme. For general MIMO channels, the optimum precoder has also been studied in [4]. However, the computational complexity of the optimum precoder can be very high in solving a so-called fixed-point equation. Except for mutual information, there are also other criteria used for the precoder design. Precoders that maximize the signal-to-noise ratio (SNR) or achieve minimum mean square error (MMSE) were developed for linear receivers in [5–8]. Although the computational complexity of linear receivers is low, the performance is often not satisfactory. Two non-linear receivers are well known: successive interference cancellation (SIC) and maximum-likelihood (ML) detection. The optimum precoder

for the QR-SIC receiver, minimizing the block error rate (BLER), has been solved with geometric mean decomposition (GMD) [9, 10]. In addition, the optimum precoder for the MMSE-SIC receiver was also solved with uniform channel decomposition (UCD) [11]. To further improve the performance, bit loading was jointly considered with precoding in MIMO transceiver design in [12, 13]. It is known that the performance of an ML receiver is dominated by the minimum distance of received signal constellations, referred to as free distance. This suggests that the design criterion for the ML detector is equivalent to maximizing the free distance. Unfortunately, this optimization problem is known to be difficult; the optimum ML precoder remains unsolved. In this dissertation, we study the precoder design for the ML detector in MIMO and MIMO relay systems.

In the first part of this dissertation, we first consider a simplified precoding scheme, namely, transmit antenna selection. Consider a MIMO system with N_t transmit antennas, N_r receive antennas, and M transmitted bit-streams. In transmit antenna selection, only M antennas are selected for signal transmission though there are N_t antennas. The idea of this scheme comes from the fact that the cost of antennas is low while that of radio-frequency (RF) chains is relatively high. With a feedback channel, the transmitter can conduct the optimum selection such that the performance of the $M \times N_r$ system can approach that of the un-selected $N_t \times N_r$ system. Since the number of the RF chains is reduced, the implementation cost of the MIMO system can be reduced. Many methods for antenna selection have been proposed. In [14], antenna selection maximizing the capacity was considered and performance was analyzed. Several selection criteria for linear receivers were proposed in [15], including post signal-to-noise ratio (SNR) maximization and mean-square-error (MSE) minimization. It is known that nonlinear receivers can outperform linear receivers. However, antenna selection for a nonlinear receiver is also more involved. In [16], a selection method for ordered-successive-interference-cancellation (OSIC) was proposed, and in [17], a selection method for the ML receiver was proposed. The method in [17] minimizes the union bound of the error rate and its computational complexity can be very high. As mentioned, the performance of the ML receiver is determined by the free dis-

tance, and we can then maximize the free distance in the selection problem. With this method, the authors in [18] conjectured that the diversity for antenna selection in the ML receiver is $N_r + N_t - M$. Unfortunately, finding the free distance requires an exhaustive search, and the computational complexity can be prohibitively high. To reduce the computational complexity, a singular value decomposition (SVD) based method was proposed in [18]. The SVD-based method selects the antenna subset that maximizes the smallest singular value of the channel matrix. It was shown that this singular value can serve as a lower bound of the free distance. An alternative lower bound using QR decomposition (QRD) was also derived in the literature [10]. It is obtained with the smallest diagonal entry in the R-factor of the channel matrix, where the R-factor is the upper-triangular matrix obtained with the QRD of the channel matrix. Although the computational complexity of the SVD-based or QRD-based method is low, the tightness of the lower bounds have not been analyzed before.

To improve the performance of the selection, we propose a QRD-based selection method maximizing the smallest diagonal entry in the R-factor of the channel matrix. We theoretically prove that the lower bound achieved with the QRD-based method is tighter than that with the SVD-based one. The tightness of the lower bound is related to the spread of the diagonal entries in the R-factor. If the spread is smaller, the lower bound is tighter. This property motivates us to propose a basis-transformation method further tightening the lower bound of the QRD-based method. The idea is to find a basis transformation for the transmitted symbol vector so that the spread can be reduced. We propose two basis-transformation matrices to do the work. The first one is the permutation matrix, and the second one is the transformation matrix used in lattice reduction (LR) [19, 20]. The LR technique has been used in antenna selection [21] for performance improvement. The selection method in [21] is designed for a linear detector operating in the basis-transformed domain. In our method, LR is used only for the derivation of the transformation matrix. An ML detector operating in the original basis is used at the receiver. Therefore, the role of LR is much different from that in [21]. We theoretically prove that the proposed basis transformations can further tighten the lower bound obtained with the original

QRD-based method. The basis-transformation method needs extra QRDs, and the computational complexity will be increased. We propose an efficient permutation method and the use of Givens rotations to reduce the computational complexity of our selection methods. Except for transmit antenna selection, we also consider the applications of the proposed algorithms in other scenarios which include receive antenna selection [22–24], joint transmit/receive antenna selection [25], and antenna selection in amplify-and-forward (AF) MIMO relay systems. For receive antenna selection, no feedback is required and this will be a great advantage in high mobility environments. In some scenarios, the number of receive antenna elements may be limited due to the size constraint. Joint transmit/receive antenna selection provides a solution to this problem. MIMO relay systems have been extensively studied recently since they can provide range extension or diversity enhancement for MIMO systems [26,27]. In general, it is desirable to minimize the hardware complexity in a relay. Antenna selection is then a good candidate for the performance enhancement in the system.

As mentioned, the optimum precoder for the ML detector is difficult to derive. Recently, a simple suboptimum method was proposed to solve the problem. It first uses SVD to transform the MIMO channel into parallel subchannels. Then, the subchannels are paired to obtain a set of 2×2 MIMO subsystems, and 2×2 subprecoders are designed to maximize the free distance in the MIMO subsystems. We refer this approach as precoding with X-structure which has been considered in [28–30]. Precoding with X-structure not only facilitates the precoder design, but also yields a low-complexity ML receiver since only 2×2 MIMO subsystems have to be dealt with. For 4-QAM, the optimum complex-valued subprecoder was first found in [31]. The result was extended to higher QAM constellations in [32], but the optimality is no longer held. An orthogonal subprecoder derived from a rotation matrix was proposed in [29]. The advantage of this approach is that the precoder has a simple closed-form expression. However, the closed-form expression of the optimum rotation angle is available only for 4-QAM. A numerical search is required for the angle in higher QAM constellations. Recently, an optimum real-valued subprecoder was developed [30]. It also requires the numerical search for the optimum precoder

though simpler. Note that both orthogonal and real-valued precoders require table look-ups during run time. In the second part of this dissertation, we propose a design method for the X-structured precoder. The main idea is using the GMD method in the subprecoder design. With the proposed method, no numerical searches are required in the design phase and no table look-ups are required during run time. In addition, the existing subprecoders are only valid for 2×2 subsystems. In other words, the subprecoder designed for more than 2×2 has to be numerically resolved [33]. On the contrary, the GMD solution can be easily extended to the subprecoder with higher dimension. Simulation results show that the performance of the proposed method is almost as good as the existing methods.

In recent years, cooperative communications have been considered a promising method to improve the performance of point-to-point MIMO systems [26, 27]. By employing relays between the source and destination, the signal can be transmitted via the source-to-relay and then relay-to-destination link. Multiple antennas can be equipped at each node to form a MIMO relay system. In the MIMO relay system, both the source and relay nodes can conduct precoding, referred to as joint source/relay precoding. Several joint precoders designs for AF MIMO relay systems have been proposed. In [34, 35], the precoders maximizing the channel capacity were developed. In [36–42], the precoders using the MMSE criterion were designed for the linear receivers. To the best of our knowledge, the joint precoders design in the MIMO relay system with an ML receiver has not been considered before. We then extend the proposed methods for MIMO systems to MIMO relay systems. However, the problem becomes much more involved in this case and a closed-form solution is difficult to obtain. We then propose iterative methods to derive the source and relay precoders, individually and repeatedly. First assume that the relay precoder is given; the source precoder design can then be easily solved by the proposed MIMO precoder. Then with the solved source precoder, the relay precoder can be solved and updated. The derivation of the relay precoder for a given source precoder, however, is much more complicated due to the fact that the MIMO relay channel is a nonlinear and complicated function of the relay precoder. We then propose two methods overcoming the problem such that

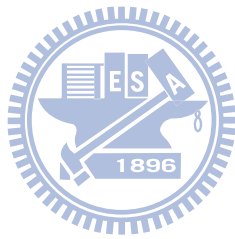
the relay precoder can be efficiently solved with Karash-Kuhn-Tucker (KKT) conditions [43]. Simulation results show that the proposed method significantly outperform existing methods.

To derive a precoder, CSI is generally required. The precoder can be calculated in the transmitter or receiver. If it is calculated in the transmitter, CSI must be fed back, and if it is calculated in the receiver, the coefficients of the precoder must be fed back. In real-world applications, feedback of the perfect CSI or precoder is difficult. To have lower distortion, the feedback of the precoder is generally preferred. In general, the coefficients of the precoder are not fed back individually. Instead, a codebook is designed for the precoder, and only the index of the codeword is fed back. This approach is referred to as limited-feedback precoding in the literature [44–48]. In the final part of this dissertation, we investigate the codebook design problem in X-structured precoding. Due to the quantization error, the channel matrix cannot be fully diagonalized and the X-structure cannot be maintained. Therefore, the subprecoders developed in [28–30] may not be applicable. We show that the proposed subprecoders can still be used in the limited-feedback system. Unlike the conventional precoding, X-structured precoding requires two codebooks, one for a unitary matrix diagonalizing the channel matrix and the other for the subprecoders. We propose using vector quantization (VQ) [49] to construct the codebook for unitary matrices. As for the subprecoder, the proposed methods only require a rotation angle and quantized angles can serve as the codebook. The other problem in the limited-feedback system is that the receiver cannot conduct ML detection on the 2×2 subsystems. We then propose interference-cancelation-based low-complexity detection schemes to solve the problem. This method combines 2×2 ML detection combined with SIC. Simulation results show that the proposed method can effectively reduce the computational complexity of the receiver and at the same time improve the system performance.

This dissertation is organized as follows. Chapter 2 considers the antenna selection scheme and proposes the basis-transformation method to achieve near-optimum performance. Chapter 3 details the proposed X-structured precoding for MIMO and MIMO relay systems. Chapter 4 extends the use of the proposed subprecoder to limited-feedback systems. Finally, Chapter 5

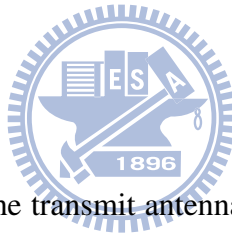
draws conclusions and outlines possible future works.





Chapter 2

Antenna Selection for ML Detectors in Spatial-Multiplexing MIMO and MIMO Relay Systems



In this chapter, we first consider the transmit antenna selection in spatial-multiplexing MIMO systems. For ML detection, it is well-known that optimum selection criterion is to choose the antenna subset giving the maximum free distance. However, the optimum solution is difficult to obtain since evaluating free distance requires an exhaustive search. To reduce the computational complexity, we resort to maximizing an lower bound of free distance, instead of free distance itself. In Section 2.1, we propose using a QRD-based lower bound as the selection criterion, and show that the lower bound yielded by QRD is tighter than that by SVD. However, the QRD-based lower bound may not be tight enough when the size of the MIMO system becomes large. In Section 2.2, we then propose a basis-transformation method to further tighten the QRD-based lower bound. In Section 2.3, we consider the issue of computational complexity and propose some low complexity methods for implementation. In Section 2.4, we show that the proposed methods can be easily extended to other applications. Finally, we evaluate the performance of the proposed methods in Section 2.5.

§ 2.1 Lower bounds for free distance

§ 2.1.1 System and Signal Models

Consider a spatial-multiplexing wireless MIMO system with N_t transmit antennas and N_r receive antennas, as described in Figure 2.1. Let $N_t > M$, $N_r \geq M$, and \mathbf{H} denote the $N_r \times N_t$ channel matrix. In transmit antenna selection, the receiver first selects M transmit antennas according to a selection criterion, where M is the number of transmitted bit streams. Let each transmit antenna subset be represented by an index p . Then, via a feedback channel, the receiver sends the index of the optimum antenna subset back to the transmitter. Finally, the transmitter uses the selected antennas for signal transmission. Note that there are $\binom{N_t}{M}$ antenna subsets, each of which corresponds to an $N_r \times M$ MIMO channel. Let x_i be the symbol transmitted at antenna i and $\mathbf{x} = [x_1, x_2, \dots, x_M]^T$ where $(\cdot)^T$ represents the transpose operation. The corresponding received signal vector can then be expressed as

$$\mathbf{y} = \mathbf{H}_p \mathbf{x} + \mathbf{n} \quad (2.1)$$

where \mathbf{H}_p is the channel matrix corresponding to the selected antenna subset and \mathbf{n} is the $N_r \times 1$ Gaussian noise vector. Assume that each entry of \mathbf{n} is identically and independently distributed (i.i.d.) with the covariance matrix of $\sigma^2 \mathbf{I}_{N_r}$, where σ^2 is the noise variance and \mathbf{I}_{N_r} is an $N_r \times N_r$ identity matrix. The ML detector searches all possible symbol vectors to obtain an estimate $\hat{\mathbf{x}}$ such that

$$\hat{\mathbf{x}} = \min_{\mathbf{x} \in \mathcal{X}^M} \|\mathbf{y} - \mathbf{H}_p \mathbf{x}\| \quad (2.2)$$

where \mathcal{X}^M is a set consisting of all possible transmitted symbol vectors. We also define \mathcal{X}^M as the symbol-vector constellation of \mathbf{x} .

It is well known that the performance of ML detection in high SNR depends on the free distance defined as

$$d_{\text{free}} = \min_{\mathbf{x}, \mathbf{x}' \in \mathcal{X}^M, \mathbf{x} \neq \mathbf{x}'} \|\mathbf{H}_p (\mathbf{x} - \mathbf{x}')\| \quad (2.3)$$

where $(\cdot)^H$ represents the Hermitian operation and $(\mathbf{x} - \mathbf{x}')$ is the difference vector. The free distance represents the minimum distance of the received signal constellation. Therefore, the optimum antenna selection criterion [18] for the ML receiver is equivalent to choosing the antenna subset whose \mathbf{H}_p gives the maximum free distance. We can compute the free distance of each candidate channel matrix using (2.3), and then choose the antenna subset with the largest d_{free} . This optimum solution can be found by an exhaustive search over all possible $\binom{N_t}{M}$ candidate channel matrices and all difference vectors. However, this exhaustive search requires very high computational complexity when considering a large number of transmitted bit-streams with a large-constellation modulation scheme. A suboptimum approach is considered to minimize a lower bound of the free distance, instead of the free distance itself.

§ 2.1.2 Lower Bound with SVD-Based Method

Let \mathbf{H}_p be an $N_r \times M$ full column-rank matrix with its SVD given as $\mathbf{H}_p = \mathbf{U}\mathbf{\Lambda}\mathbf{V}^H$, where \mathbf{U} is an $N_r \times N_r$ unitary matrix, \mathbf{V} is an $M \times M$ unitary matrix, and $\mathbf{\Lambda}$ is an $N_r \times M$ diagonal matrix. The non-zero entries of $\mathbf{\Lambda}$ are the singular values of \mathbf{H}_p . Define the symbol constellation of x_k as \mathcal{X}_k , and the minimum distance of \mathcal{X}_k as

$$d_{\min}(\mathcal{X}_k) = \min_{x_k, x'_k \in \mathcal{X}_k, x_k \neq x'_k} |x_k - x'_k|. \quad (2.4)$$

Also define the minimum distance of the symbol-vector constellation, \mathcal{X}^M , as

$$d_{\min}(\mathcal{X}^M) = \min_{\mathbf{x}, \mathbf{x}' \in \mathcal{X}^M, \mathbf{x} \neq \mathbf{x}'} \|\mathbf{x} - \mathbf{x}'\|. \quad (2.5)$$

In a spatial-multiplexing MIMO system, x_k 's are usually uncorrelated. Thus, we can have

$$d_{\min}(\mathcal{X}^M) = \min \{d_{\min}(\mathcal{X}_1), d_{\min}(\mathcal{X}_2), \dots, d_{\min}(\mathcal{X}_M)\}. \quad (2.6)$$

Note that if x_k 's are correlated, (2.6) is not valid in general. With (2.6), $d_{\min}(\mathcal{X}^M)$ can be easily computed for QAM constellations. Let a QAM symbol be represented by $a_I + ja_Q$ where $a_I \in \{\pm 1, \pm 3, \dots\}$ and $a_Q \in \{\pm 1, \pm 3, \dots\}$. We then have $d_{\min}(\mathcal{X}_1) = d_{\min}(\mathcal{X}_2) = \dots = d_{\min}(\mathcal{X}_M) = 2$ and $d_{\min}(\mathcal{X}^M) = \min \{2, 2, \dots, 2\} = 2$.

Using the Rayleigh-Ritz theorem, the SVD-based lower bound of the free distance was derived in [18] as

$$d_{\text{free}} \geq \lambda_M d_{\min}(\mathcal{X}^M) \quad (2.7)$$

where λ_M is the minimum singular value of the matrix \mathbf{H}_p . Note that (2.7) is different from that in [18] by a factor of M . The reason for this is that the free distance in our application is a relative not absolute value. Since all \mathbf{H}_p 's are of the same dimension, scaling the free distance will not change the selection result. Thus, the factor M is omitted for simplicity. The lower bound in (2.7) indicates that the free distance can be evaluated with λ_M and $d_{\min}(\mathcal{X}^M)$. It is simple to see that the value of $d_{\min}(\mathcal{X}^M)$ is the same for each \mathbf{H}_p . Thus, with the SVD-based method, only the minimum singular value of each \mathbf{H}_p is required to compute, and the computational complexity can be reduced dramatically. However, the main problem for the SVD-based method is that the lower bound (2.7) may not be tight enough. An alternative lower bound of the free distance derived from the QRD was developed in [10]. In this dissertation, we propose the use of this lower bound for solving the antenna selection problem.

§ 2.1.3 Lower Bound with QRD-Based Method

The matrix \mathbf{H}_p can be factorized in the form of $\mathbf{H}_p = \mathbf{Q}\mathbf{R}$, where \mathbf{Q} is an $N_r \times M$ column-wise orthonormal matrix and \mathbf{R} is an $M \times M$ upper-triangular matrix with positive real-valued diagonal entries as

$$\mathbf{R} = \begin{bmatrix} R_{1,1} & R_{1,2} & \dots & R_{1,M} \\ 0 & R_{2,2} & \dots & R_{2,M} \\ \vdots & \vdots & \ddots & \vdots \\ 0 & 0 & \dots & R_{M,M} \end{bmatrix}.$$

As mentioned, the matrix \mathbf{R} is also referred to as the R-factor [10] of \mathbf{H}_p . Let $[\mathbf{R}]_k$ denote the k th diagonal entry of \mathbf{R} . Via this decomposition, we can have another lower bound of the free

distance as

$$\begin{aligned} d_{\text{free}} &\geq \left(\min_{1 \leq k \leq M} [\mathbf{R}]_k \right) d_{\min}(\mathcal{X}^M) \\ &= [\mathbf{R}]_{\min} d_{\min}(\mathcal{X}^M) \end{aligned} \quad (2.8)$$

where $[\mathbf{R}]_{\min}$ represents the minimum diagonal entry in the matrix \mathbf{R} . Thus, we propose the use of (2.8) as a selection criterion, referred to as QRD-based method. In what follows, we show that the lower bound obtained with the QRD-based method is tighter than that with the SVD-based method.

For an arbitrary $M \times M$ positive-definite matrix $\mathbf{A} = \mathbf{H}_p^H \mathbf{H}_p$, we can have its eigenvalue decomposition expressed as $\mathbf{A} = \mathbf{V} \mathbf{\Sigma} \mathbf{V}^H$, where $\mathbf{\Sigma}$ is an $M \times M$ diagonal matrix whose nonzero entries are the eigenvalues of \mathbf{A} . It is known that a positive-definite matrix can also be decomposed by the Cholesky factorization in the form of $\mathbf{A} = \mathbf{B} \mathbf{D} \mathbf{B}^H$, where \mathbf{D} is an $M \times M$ diagonal matrix and \mathbf{B} is an $M \times M$ unit lower-triangular matrix expressed as

$$\mathbf{B} = \begin{bmatrix} 1 & 0 & \dots & 0 \\ B_{2,1} & 1 & \dots & 0 \\ \vdots & \vdots & \ddots & \vdots \\ B_{M,1} & B_{M,2} & \dots & 1 \end{bmatrix}.$$

The diagonal entries of \mathbf{D} are also referred to as Cholesky values [50]. Consider two sequences $\underline{\sigma} = (\sigma_1, \sigma_2, \dots, \sigma_M)$ and $\underline{d} = (d_1, d_2, \dots, d_M)$ consisting of the eigenvalues and Cholesky values of \mathbf{A} respectively. Note that the entries of both sequences $\underline{\sigma}$ and \underline{d} are arranged in the descending order so that $\sigma_1 \geq \sigma_2 \geq \dots \geq \sigma_M$ and $d_1 \geq d_2 \geq \dots \geq d_M$. With the above definitions, we can have the following proposition.

Proposition 2.1: For an $N_r \times M$ full column-rank matrix \mathbf{H}_p with its QRD and SVD expressed as $\mathbf{H}_p = \mathbf{Q} \mathbf{R}$ and $\mathbf{H}_p = \mathbf{U} \mathbf{\Lambda} \mathbf{V}^H$ respectively, the inequality $\lambda_M \leq [\mathbf{R}]_{\min}$ holds true for all channel realizations.

Proof: It is known that the Cholesky factorization of a positive-definite matrix $\mathbf{A} = \mathbf{H}_p^H \mathbf{H}_p$ is unique [51] and can be expressed as $\mathbf{A} = \mathbf{B} \mathbf{D} \mathbf{B}^H$. With the QRD $\mathbf{H}_p = \mathbf{Q} \mathbf{R}$, we can also

have

$$\mathbf{A} = \mathbf{R}^H \mathbf{R} = \mathbf{R}_u^H \mathbf{D}' \mathbf{R}_u \quad (2.9)$$

where \mathbf{R}_u is an $M \times M$ unit upper-triangular matrix and \mathbf{D}' is an $M \times M$ diagonal matrix. Let $\underline{r} = (r_1, r_2, \dots, r_M)$ and $\underline{d}' = (d'_1, d'_2, \dots, d'_M)$ denote the diagonal entries of \mathbf{R} and \mathbf{D}' respectively. From (2.9), we know that $r_k^2 = d'_k$ for all $k = 1, 2, \dots, M$. Furthermore, using the uniqueness property of the Cholesky factorization, it can be seen that the entries of the sequence \underline{d}' exactly represent the Cholesky values of \mathbf{A} .

Definition 2.1: Let $\underline{b} = (b_1, b_2, \dots, b_M)$ and $\underline{c} = (c_1, c_2, \dots, c_M)$ be two positive, real-valued sequences satisfying $b_1 \geq b_2 \geq \dots \geq b_M$ and $c_1 \geq c_2 \geq \dots \geq c_M$. We say that \underline{b} majorizes \underline{c} in the product sense [52] if

$$\prod_{k=1}^l b_k \geq \prod_{k=1}^l c_k \quad (2.10)$$

for all $l = 1, 2, \dots, M$, and with equality when $l = M$.

Lemma 2.1: For a positive-definite matrix $\mathbf{A} = \mathbf{H}_p^H \mathbf{H}_p$, the sequence $\underline{\sigma}$ majorizes the sequence \underline{d} in the product sense, i.e.,

$$\prod_{k=1}^l \sigma_k \geq \prod_{k=1}^l d_k \quad (2.11)$$

for all $l = 1, 2, \dots, M$, and with equality when $l = M$. This lemma and its proof can be found in [50, 52].

Assume that the entries of both \underline{r} and \underline{d}' are also with the descending order. Then, by Lemma 2.1, we can obtain

$$\prod_{k=1}^l \sigma_k \geq \prod_{k=1}^l d_k = \prod_{k=1}^l d'_k = \prod_{k=1}^l r_k^2 \quad (2.12)$$

for all $l = 1, 2, \dots, M$, and with equality when $l = M$. For a positive-definite matrix $\mathbf{A} = \mathbf{H}_p^H \mathbf{H}_p$, it is known that $\sigma_k = \lambda_k^2$, where λ_k is the k th largest singular value of \mathbf{H}_p . We thus

have

$$\prod_{k=1}^l \lambda_k^2 = \prod_{k=1}^l \sigma_k \geq \prod_{k=1}^l r_k^2 \quad (2.13)$$

for all $l = 1, 2, \dots, M$, and with equality when $l = M$. From (2.13), we arrive at that $\lambda_M^2 \leq r_M^2$. Note that $r_M = [\mathbf{R}]_{\min}$. We can have $\lambda_M \leq [\mathbf{R}]_{\min}$ since both λ_M and $[\mathbf{R}]_{\min}$ are positive values, which completes the proof.

§ 2.2 Proposed Basis-Transformation Method

In the previous section, we see that the lower bound obtained with the QRD-based method is tighter than that with the SVD-based method. In this section, we propose a method for further tightening the lower bound of the free distance. To do that, we first observe how the channel matrix affects the tightness of the bound in (2.8). From [10], it can be seen that when the diagonal entries of \mathbf{R} are all equal, the equality in (2.8) will hold. We then conjecture that the tightness of the lower bound is related to the spread of the diagonal entries in the R-factor, defined as the $[\mathbf{R}]$ -value spread. The $[\mathbf{R}]$ -value spread is the value of $[\mathbf{R}]_{\max}$ divided by that of $[\mathbf{R}]_{\min}$ where $[\mathbf{R}]_{\max}$ is the maximum diagonal entry in the R-factor. If the $[\mathbf{R}]$ -value spread is smaller, the bound in (2.8) is tighter. Now, considering the signal part in (2.1), we have

$$\begin{aligned} \mathbf{y}_s &= \mathbf{H}_p \mathbf{x} \\ &= x_1 \mathbf{h}_{p,1} + x_2 \mathbf{h}_{p,2} + \dots + x_M \mathbf{h}_{p,M} \end{aligned} \quad (2.14)$$

where $\mathbf{h}_{p,k}$ is the k th column of \mathbf{H}_p . Thus, \mathbf{y}_s can be seen as a vector expanded by a basis formed by the columns of \mathbf{H}_p , i.e., $[\mathbf{h}_{p,1}, \mathbf{h}_{p,2}, \dots, \mathbf{h}_{p,M}]$, and the corresponding coordinate is $[x_1, x_2, \dots, x_M]^T$. With an invertible matrix \mathbf{Z} , we can rewrite (2.14) as

$$\begin{aligned} \mathbf{y}_s &= \mathbf{H}_p \mathbf{Z} \mathbf{Z}^{-1} \mathbf{x} \\ &= \bar{\mathbf{H}}_p \bar{\mathbf{x}} \end{aligned} \quad (2.15)$$

where $\bar{\mathbf{H}}_p = \mathbf{H}_p \mathbf{Z}$ and $\bar{\mathbf{x}} = \mathbf{Z}^{-1} \mathbf{x}$. Thus, the basis is transformed to the columns of $\bar{\mathbf{H}}_p$, and the corresponding coordinate is $\bar{\mathbf{x}} = [\bar{x}_1, \bar{x}_2, \dots, \bar{x}_M]^T$. If a proper \mathbf{Z} can be chosen such that the $[\mathbf{R}]$ -value spread of the R-factor in $\bar{\mathbf{H}}_p$ is reduced, then the bound in (2.8) can be tightened. This is the basic concept of our basis-transformation method.

Using the idea described above, we rewrite the free distance as

$$\begin{aligned}
d_{\text{free}} &= \min_{\mathbf{x}, \mathbf{x}' \in \mathcal{X}^M, \mathbf{x} \neq \mathbf{x}'} \|\mathbf{H}_p (\mathbf{x} - \mathbf{x}')\| \\
&= \min_{\mathbf{x}, \mathbf{x}' \in \mathcal{X}^M, \mathbf{x} \neq \mathbf{x}'} \|\mathbf{H}_p \mathbf{Z} \mathbf{Z}^{-1} (\mathbf{x} - \mathbf{x}')\| \\
&= \min_{\bar{\mathbf{x}}, \bar{\mathbf{x}}' \in \bar{\mathcal{X}}^M, \bar{\mathbf{x}} \neq \bar{\mathbf{x}}'} \|\bar{\mathbf{H}}_p (\bar{\mathbf{x}} - \bar{\mathbf{x}}')\|
\end{aligned} \tag{2.16}$$

where $\bar{\mathcal{X}}^M$ is the symbol-vector constellation reshaped by \mathbf{Z}^{-1} . In Appendix A.1, we show that the lower bound yielded by the SVD in (2.7) is still valid. However, $d_{\min}(\bar{\mathcal{X}}_k)$ becomes difficult to find since in general $d_{\min}(\bar{\mathcal{X}}^M) \neq \min\{d_{\min}(\bar{\mathcal{X}}_1), \dots, d_{\min}(\bar{\mathcal{X}}_M)\}$ where $d_{\min}(\bar{\mathcal{X}}_k) = \min |\bar{x}_k - \bar{x}'_k|$. On the other hand, the lower bound yielded by the QRD in (2.8) is no longer valid. From [10], we see that the lower bound in (2.8) is derived with the assumption of (2.6). Thus, if let $d_{\min}(\bar{\mathcal{X}}^1) = \min\{d_{\min}(\bar{\mathcal{X}}_1), d_{\min}(\bar{\mathcal{X}}_2), \dots, d_{\min}(\bar{\mathcal{X}}_M)\}$, we can have a new lower bound from (2.8) as

$$d_{\text{free}} \geq [\bar{\mathbf{R}}]_{\min} d_{\min}(\bar{\mathcal{X}}^1). \tag{2.17}$$

As mentioned, $d_{\min}(\bar{\mathcal{X}}^1) \neq d_{\min}(\mathcal{X}^M)$ in general. We cannot conclude that (2.17) is tighter than (2.8) even when $[\bar{\mathbf{R}}]_{\min} \geq [\mathbf{R}]_{\min}$. The other problem with (2.17) is that the value of $d_{\min}(\bar{\mathcal{X}}^1)$ is no longer easy to obtain. This is because after the transformation, the signal constellation in each dimension is significantly expanded. The challenge in the basis-transformation method is to find \mathbf{Z} such that $d_{\min}(\bar{\mathcal{X}}^1)$ can be easily computed and at the same time $d_{\min}(\bar{\mathcal{X}}^1) = d_{\min}(\mathcal{X}^M)$. The constraints are stringent and cannot be satisfied by most of the transformations. Fortunately, we have found two matrices that can do the job.

§ 2.2.1 Permutation Matrix

The first transformation matrix we propose is the permutation matrix. For a given $N_r \times M$ candidate channel matrix \mathbf{H}_p , we can have $M!$ different column permutation patterns. Let $\mathbf{\Pi}_i$ denote the permutation matrix corresponding to the i th permutation pattern, where $1 \leq i \leq M!$.

We can rewrite the free distance as

$$\begin{aligned} d_{\text{free}} &= \min_{\mathbf{x}, \mathbf{x}' \in \mathcal{X}^M, \mathbf{x} \neq \mathbf{x}'} \|\mathbf{H}_p \mathbf{\Pi}_i \mathbf{\Pi}_i^{-1} (\mathbf{x} - \mathbf{x}')\| \\ &= \min_{\mathbf{x}, \mathbf{x}' \in \mathcal{X}^M, \mathbf{x} \neq \mathbf{x}'} \|\mathbf{H}_p \mathbf{\Pi}_i \mathbf{\Pi}_i^T (\mathbf{x} - \mathbf{x}')\| \end{aligned} \quad (2.18)$$

where $\mathbf{\Pi}_i^T = \mathbf{\Pi}_i^{-1}$ since $\mathbf{\Pi}_i$ is an orthogonal matrix. Note that the combinations of $\mathbf{\Pi}_i^T (\mathbf{x} - \mathbf{x}')$ are the same as those of $(\mathbf{x} - \mathbf{x}')$, which allows us to rewrite (2.18) as

$$d_{\text{free}} = \min_{\mathbf{x}, \mathbf{x}' \in \mathcal{X}^M, \mathbf{x} \neq \mathbf{x}'} \|\mathbf{H}_p \mathbf{\Pi}_i (\mathbf{x} - \mathbf{x}')\|. \quad (2.19)$$

Let \mathbf{R}_i denote the R-factor of $\mathbf{H}_p \mathbf{\Pi}_i$. The free distance can be bounded as

$$d_{\text{free}} \geq [\mathbf{R}_i]_{\min} d_{\min}(\mathcal{X}^M). \quad (2.20)$$

For a given \mathbf{H}_p , we can obtain $M!$ different R-factors with $M!$ permutations. Denote \mathbf{R}_{per} as the R-factor having the largest minimum diagonal entry. Then, the minimum diagonal entry of \mathbf{R}_{per} can be used in the lower bound in (2.8). Then, we have

$$d_{\text{free}} \geq [\mathbf{R}_{\text{per}}]_{\min} d_{\min}(\mathcal{X}^M) \quad (2.21)$$

where $[\mathbf{R}_{\text{per}}]_{\min} = \max([\mathbf{R}_1]_{\min}, [\mathbf{R}_2]_{\min}, \dots, [\mathbf{R}_{M!}]_{\min})$. In other words, we find the optimum permutation pattern such that the smallest [R]-value spread can be obtained. We summarize the proposed basis-transformation method with the permutation matrix (denoted as QRD-based BT-P) in Table 2.1. Assume that $\mathbf{\Pi}_1 = \mathbf{I}_M$. Then, $[\mathbf{R}_1]_{\min} = [\mathbf{R}]_{\min}$. Clearly, we can have the following inequality as

$$[\mathbf{R}_{\text{per}}]_{\min} \geq [\mathbf{R}]_{\min}. \quad (2.22)$$

The inequality in (2.22) indicates that this permutation method can improve the tightness of (2.8).

§ 2.2.2 Transformation Matrix in Lattice Reduction

The second transformation matrix we found is the basis-transformation matrix used in LR. The LR technique has been successfully applied to MIMO systems for enhancing the detection performance [19, 20]. The basic idea is to find a new basis for the transmitted symbol vector, and then signal detection is conducted in the basis-transformed domain. In this subsection, we propose using the transformation matrix used in LR to obtain tighter lower bound of the free distance. Note that the ML detection is still conducted in the original basis. With $\mathbf{H}_p = [\mathbf{h}_{p,1}, \mathbf{h}_{p,2}, \dots, \mathbf{h}_{p,M}]$, we can describe an M -dimensional lattice L as

$$L\{\mathbf{h}_{p,1}, \mathbf{h}_{p,2}, \dots, \mathbf{h}_{p,M}\} = \sum_{k=1}^M s_k \mathbf{h}_{p,k} \quad (2.23)$$

where s_k is a complex integer. The vector set $\{\mathbf{h}_{p,1}, \mathbf{h}_{p,2}, \dots, \mathbf{h}_{p,M}\}$ is a basis spanning L . Let \mathbf{P} be an invertible matrix whose entries are all complex integers, and we have

$$\begin{aligned} \mathbf{H}_{\text{LR},p} &= \mathbf{H}_p \mathbf{P} \\ &= [\mathbf{h}_{\text{LR},p,1}, \mathbf{h}_{\text{LR},p,2}, \dots, \mathbf{h}_{\text{LR},p,M}]. \end{aligned} \quad (2.24)$$

Note that all entries of \mathbf{P}^{-1} are also complex integers. Thus, the column vectors of the matrix $\mathbf{H}_{\text{LR},p}$ also form a basis for the same lattice. The LR method finds a basis whose elements are as orthogonal as possible, and at the same time the magnitudes of the basis elements are as short as possible. An example of LR with $M = 2$ is illustrated in Figure 2.2. As we can see, the reduced basis vectors will have shorter length, and the orthogonality of $\mathbf{H}_{\text{LR},p}$ is improved also. Several algorithms to implement LR have been proposed in the literature. Among them, the complex Lenstra-Lenstra-Lovász (CLLL) algorithm is most widely used since its computational complexity is lower. We then use CLLL as our LR algorithm. The operation of the CLLL algorithm is summarized in Table 2.2. As we can see in the table, a parameter $\delta \in (\frac{1}{2}, 1)$ is defined in CLLL. This parameter determines the orthogonality of the transformed channel matrix $\mathbf{H}_{\text{LR},p}$. A larger δ will make $\mathbf{H}_{\text{LR},p}$ closer to an orthogonal matrix. However, the CLLL algorithm will require more iterations to converge and its computational complexity is higher.

Now, we can conduct LR on \mathbf{H}_p to obtain \mathbf{P} . Rewrite the free distance in (2.3) as

$$\begin{aligned} d_{\text{free}} &= \min_{\mathbf{x}, \mathbf{x}' \in \mathcal{X}^M, \mathbf{x} \neq \mathbf{x}'} \|\mathbf{H}_p \mathbf{P} \mathbf{P}^{-1} (\mathbf{x} - \mathbf{x}')\| \\ &= \min_{\mathbf{x}_{\text{LR}}, \mathbf{x}'_{\text{LR}} \in \mathcal{X}_{\text{LR}}^M, \mathbf{x}_{\text{LR}} \neq \mathbf{x}'_{\text{LR}}} \|\mathbf{H}_{\text{LR}, p} (\mathbf{x}_{\text{LR}} - \mathbf{x}'_{\text{LR}})\| \end{aligned} \quad (2.25)$$

where $\mathbf{x}_{\text{LR}} - \mathbf{x}'_{\text{LR}} = \mathbf{P}^{-1} (\mathbf{x} - \mathbf{x}')$ and $\mathcal{X}_{\text{LR}}^M$ represents the symbol-vector constellation after the transformation. Thus, we can conduct the QRD on $\mathbf{H}_{\text{LR}, p}$ obtaining $\mathbf{H}_{\text{LR}, p} = \mathbf{Q}_{\text{LR}} \mathbf{R}_{\text{LR}}$. Using (2.17), we can have a lower bound of the free distance as

$$d_{\text{free}} \geq [\mathbf{R}_{\text{LR}}]_{\min} d_{\min} (\mathcal{X}_{\text{LR}}^1) \quad (2.26)$$

where $d_{\min} (\mathcal{X}_{\text{LR}}^1)$ is expressed as

$$d_{\min} (\mathcal{X}_{\text{LR}}^1) = \min\{d_{\min} (\mathcal{X}_{\text{LR},1}), d_{\min} (\mathcal{X}_{\text{LR},2}), \dots, d_{\min} (\mathcal{X}_{\text{LR},M})\}. \quad (2.27)$$

In Appendix A.2, we show that $d_{\min} (\mathcal{X}_{\text{LR}}^1)$ can be seen as equal to $d_{\min} (\mathcal{X}^M)$. As a result, only $[\mathbf{R}_{\text{LR}}]_{\min}$ needs to be evaluated in the comparison of (2.26) and (2.8).

Proposition 2.2: For an $N_r \times M$ full column-rank matrix \mathbf{H}_p , if LR is conducted with the CLLL algorithm, the following inequality is held;

$$[\mathbf{R}_{\text{LR}}]_{\min} \geq [\mathbf{R}]_{\min}. \quad (2.28)$$

Proof: See Appendix A.3.

Thus, for a candidate channel matrix, the lower bound obtained with (2.26) will be always tighter than or equal to the original QRD-based lower bound. We can then select the antenna subset whose corresponding channel matrix has the maximum $[\mathbf{R}_{\text{LR}}]_{\min}$. Note that the singular values of a matrix are invariant under the column permutation operation. Therefore, the tightness of the SVD-based lower bound cannot be improved by the transformation with permutation matrices. As for the transformation with the LR matrix \mathbf{P} , the minimum singular value may also be enlarged. However, as proved in Proposition 2.1, the resultant minimum singular value will be still smaller than $[\mathbf{R}_{\text{LR}}]_{\min}$.

§ 2.2.3 Cascade of Permutation and LR Matrices

To improve performance further, we can consider the cascade of a permutation and a LR matrix as another transformation matrix. Let $\mathbf{S}_i = \mathbf{P}\mathbf{\Pi}_i$. The free distance can then be expressed as

$$d_{\text{free}} = \min_{\mathbf{x}, \mathbf{x}' \in \mathcal{X}^M, \mathbf{x} \neq \mathbf{x}'} \left\| \mathbf{H}_p \mathbf{S}_i \mathbf{S}_i^{-1} (\mathbf{x} - \mathbf{x}') \right\| \quad (2.29)$$

$$= \min_{\mathbf{x}, \mathbf{x}' \in \mathcal{X}^M, \mathbf{x} \neq \mathbf{x}'} \left\| \mathbf{H}_p \mathbf{P} \mathbf{\Pi}_i \mathbf{\Pi}_i^T \mathbf{P}^{-1} (\mathbf{x} - \mathbf{x}') \right\|. \quad (2.30)$$

With the effective channel matrix $\mathbf{H}_p \mathbf{P} \mathbf{\Pi}_i$, the QRD-based lower bound of the free distance can be tightened even further. In this chapter, we denote QRD-based BT-C as the proposed QRD-based method with the basis transformation using the cascade of permutation and LR matrices. Table 2.3 summarizes the operations of the proposed QRD-based BT-C method. Denote $\mathbf{R}_{\text{LR},i}$ as the R-factor of $\mathbf{H}_p \mathbf{P} \mathbf{\Pi}_i$ and $[\mathbf{R}_{\text{cas}}]_{\min}$ as the R-factor having the largest minimum diagonal entry among all $\mathbf{R}_{\text{LR},i}$'s. In other words, $[\mathbf{R}_{\text{cas}}]_{\min} = \max([\mathbf{R}_{\text{LR},1}]_{\min}, [\mathbf{R}_{\text{LR},2}]_{\min}, \dots, [\mathbf{R}_{\text{LR},M!}]_{\min})$. Thus, we can have the following inequality:

$$[\mathbf{R}_{\text{cas}}]_{\min} \geq [\mathbf{R}_{\text{LR}}]_{\min}. \quad (2.31)$$

From (2.31) and (2.22), we see that the lower bound of $[\mathbf{R}_{\text{cas}}]_{\min}$ is larger than that of $[\mathbf{R}_{\text{per}}]_{\min}$ since $[\mathbf{R}_{\text{LR}}]_{\min} \geq [\mathbf{R}]_{\min}$. This, however, does not imply that $[\mathbf{R}_{\text{cas}}]_{\min} \geq [\mathbf{R}_{\text{per}}]_{\min}$. We can only say that the probability of $[\mathbf{R}_{\text{cas}}]_{\min} \geq [\mathbf{R}_{\text{per}}]_{\min}$ is larger. Furthermore, we can exchange the cascading order. In other words, we can let the transformation matrix be $\mathbf{S}_i = \mathbf{\Pi}_i \mathbf{P}_i$. In this case, however, we have to conduct LR for each $\mathbf{H}_p \mathbf{\Pi}_i$, and the resultant computational complexity is then higher. Finally, we can even use a transformation matrix by cascading a series of permutation and LR matrices. For example, we can have a transformation matrix in the form of $\mathbf{P}_1 \mathbf{\Pi}_i \mathbf{P}_2 \mathbf{\Pi}_{i'}$, where $1 \leq i \leq M!$ and $1 \leq i' \leq M!$. Simulations show that this may not be required. With only one-level cascading, the performance of the selection is very close to the optimum solution.

§ 2.3 Implementation Issues and Complexity Comparisons

The computational complexity of the basis-transformation method will be increased due to extra transformations and QRD operations. To reduce the computational complexity, we proposed several efficient methods for real-world implementations.

§ 2.3.1 Givens Rotations Method

To reduce the computational complexity of the QRDs, we propose using Givens rotations [53] to compute each $[\mathbf{R}_i]_{\min}$. Assume that $\mathbf{H}_{p,1} = \mathbf{Q}_1 \mathbf{R}_1$ is available via a complete QRD. Let $\mathbf{H}_{p,2}$ be another matrix obtained by exchanging two neighbor columns of $\mathbf{H}_{p,1}$. We seek to find \mathbf{R}_2 of $\mathbf{H}_{p,2}$ without using another complete QRD. Denote $\check{\mathbf{\Pi}}$ as a permutation matrix conducting a column-exchange operation on two neighbor columns, i.e.,

$$\mathbf{H}_{p,2} = \mathbf{Q}_1 \mathbf{R}_1 \check{\mathbf{\Pi}} = \mathbf{Q}_1 \check{\mathbf{R}}_1 \quad (2.32)$$

where $\check{\mathbf{R}}_1$ is a near upper-triangular matrix. Now, all we have to do is to transform $\check{\mathbf{R}}_1$ into a upper-triangular matrix again. Since $\check{\mathbf{\Pi}}$ only exchanges two neighbor columns of \mathbf{R}_1 , we can upper-triangularize $\check{\mathbf{R}}_1$ by a simple Givens rotation matrix \mathbf{G}_1 . Then, $\mathbf{G}_1 \check{\mathbf{R}}_1 = \mathbf{T}$, where \mathbf{T} is a upper-triangular matrix. Thus we can rewrite (2.32) as

$$\mathbf{H}_{p,2} = \mathbf{Q}_1 \mathbf{G}_1^H \mathbf{G}_1 \check{\mathbf{R}}_1 = \mathbf{Q}_2 \mathbf{T} \quad (2.33)$$

where $\mathbf{Q}_2 = \mathbf{Q}_1 \mathbf{G}_1^H$ is a unitary matrix. From (2.33), we know that $\mathbf{Q}_2 \mathbf{T}$ is the QRD of $\mathbf{H}_{p,2}$, and \mathbf{T} is equal to \mathbf{R}_2 . In other words, we obtain \mathbf{R}_2 by simply left-multiplying a Givens rotation matrix on $\check{\mathbf{R}}_1$ rather than by performing a complete QRD on $\mathbf{H}_{p,2}$. Therefore, we can dramatically reduce the computational complexity of the proposed basis-transformed method when conducting the permutation operations. Note that applying Givens rotations will not affect the performance of the proposed selection methods. Figure 2.3 illustrates an example (for $M = 3$) how each $[\mathbf{R}_i]_{\min}$ can be derived with Givens rotations.

§ 2.3.2 Efficient Permutations

Consider a Rayleigh flat-fading MIMO channel matrix \mathbf{H}_p . With the QRD, we have $\mathbf{H}_p = \mathbf{Q}\mathbf{R}$. It has been shown that the square value of each diagonal entry in \mathbf{R} is independently distributed with Gamma distribution [54]. That is, $[\mathbf{R}]_k^2 \sim G(M+1-k)$, where $G(M+1-k)$ denotes the Gamma distribution with mean $\mathbb{E}[[\mathbf{R}]_k^2] = (M+1-k)$. Thus, the expectation of $[\mathbf{R}]_M^2$, which is equal to one, is the smallest. As a result, $[\mathbf{R}]_M$ has the highest probability to be the minimum diagonal entry of \mathbf{R} . Also note that Givens rotations have to be conducted sequentially. Using these two properties, we propose an efficient permutation method to reduce the required computational complexity. The idea is to conduct permutations in a local rather than global manner. Define an integer \bar{M} and $\bar{M} < M$. With Givens rotations, permutating the first \bar{M} columns of \mathbf{H}_p will not change the resultant values of $([\mathbf{R}]_{\bar{M}+1}, [\mathbf{R}]_{\bar{M}+2}, \dots, [\mathbf{R}]_M)$. This is to say if $[\mathbf{R}]_M$ is the minimum value, these permutations are totally useless. Thus, we choose the last $M - \bar{M}$ columns of \mathbf{H}_p for local permutations. If \bar{M} is chosen to be much smaller than M , the computational complexity can be reduced significantly. Note that local permutations will result in some performance loss. In [54, 55], it has been theoretically shown that $\mathbb{E}[[\mathbf{R}]_M^2]$ tends to be larger when the columns of \mathbf{H}_p are exchanged according the norm-ascending order. This is referred to as pre-ordering. Thus, we can combine this pre-ordering with our efficient permutation method to compensate the performance loss.

The idea of efficient permutation can also be applied to the QRD-based BT-C scheme. As shown in Appendix A.3, the $[\mathbf{R}]$ -value spread of \mathbf{R}_{LR} will be effectively reduced with the CLLL algorithm. Thus, the values of the diagonal entries in \mathbf{R}_{LR} can become very close. Pre-ordering is then not required. From simulations, we found that due to some special properties of CLLL, using the first \bar{M} neighbor columns for local permutations can provide slightly better performance. For this reason, when conducting efficient permutations for the QRD-based BT-C scheme, we choose the first \bar{M} columns of $\mathbf{H}_p\mathbf{P}$. The operation of the QRD-based BT-C method implemented with efficient permutations (denoted as QRD-based BT-E) is shown in Table 2.4.

§ 2.3.3 Complexity Comparisons

In this dissertation, we use the number of floating operations (FLOPS) required in an algorithm as the measure for computational complexity. Many algorithms for conducting the QRD and SVD have been developed [53]. In general, the QRD requires less FLOPS than the SVD does [53]. Thus, the QRD-based selection scheme not only has better performance, but also requires lower computational complexity. In Table 2.5, we summarize the order of computational complexity in each proposed method.

As we can see, computing $[\mathbf{R}_i]_{\min}$ for $i = 2, \dots, M!$ in either the QRD-based BT-P or QRD-based BT-C method requires $\mathcal{O}(M^3 M!)$ FLOPS, which can be reduced to $\mathcal{O}(MM!)$ with Givens rotations. It has been shown that the computational complexity of the CLLL algorithm is $\mathcal{O}(M^4)$ [56]. Therefore, the total computational complexity of the QRD-based BT-C scheme with Given rotations is $\mathcal{O}(M^4 + MM!)$. The term $MM!$ may grow rapidly when M becomes very large, which dominates the total computational complexity. This problem can be solved with the efficient permutation method proposed in Section 2.3.2. In the QRD-based BT-E scheme, \bar{M} can be chosen much smaller than M , and the resultant computational complexity can be further reduced to $\mathcal{O}(M^4 + M\bar{M}!) \cong \mathcal{O}(M^4)$. Although the required complexity will be increased when LR is considered, the overall complexity is still much lower than that of the exhaustive search.

§ 2.4 Other Applications

§ 2.4.1 Receive and Joint Transmit/Receive Antenna Selection

Antenna selection can also be conducted at the receiver. As we did in transmit antenna selection, we can select a subset of receive antennas according to a performance criterion. Here, we select M out of N_r receive antenna elements. Note that the receiver does not have to feed the index of the selected antenna subset back to the transmitter, which is a significant advantage. However,

the performance of receive antenna selection may be inferior to transmit antenna selection for the same number of candidate channel matrices. We now give a simple example to illustrate this property. Consider a MIMO system with $N_t = 2$, $N_r = 3$, and $M = 2$, where the channel matrix can be expressed as

$$\mathbf{H} = \begin{bmatrix} h_{1,1} & h_{1,2} \\ h_{2,1} & h_{2,2} \\ h_{3,1} & h_{3,2} \end{bmatrix}.$$

From the diversity point of view, we can treat a 3×2 MIMO channel \mathbf{H} as two separate 3×1 sub-channels, each of which is obtained from a column of \mathbf{H} . The reason is that either x_1 or x_2 has the same diversity as the original 3×2 MIMO system since the ML detection is adopted at the receiver. This facilitates a simple performance analysis for the antenna selection problem. For receive antenna selection, x_1 have three candidate channel columns for selection, which are denoted as

$$\mathbf{h}_1 = \begin{bmatrix} h_{1,1} \\ h_{2,1} \end{bmatrix}, \mathbf{h}_2 = \begin{bmatrix} h_{1,1} \\ h_{3,1} \end{bmatrix}, \text{ and } \mathbf{h}_3 = \begin{bmatrix} h_{2,1} \\ h_{3,1} \end{bmatrix}.$$

It can be seen that there exists correlation between any two columns since those candidate channel columns have the common entries. This correlation will degrade the performance of receive antenna selection.

Now, consider transmit antenna selection in a MIMO system with $N_t = 3$, $N_r = 2$, and $M = 2$, where the channel matrix can be expressed as

$$\mathbf{H} = \begin{bmatrix} h_{1,1} & h_{1,2} & h_{1,3} \\ h_{2,1} & h_{2,2} & h_{2,3} \end{bmatrix}.$$

For transmit antenna selection, x_1 also has three candidate channel columns given by

$$\mathbf{h}_1 = \begin{bmatrix} h_{1,1} \\ h_{2,1} \end{bmatrix}, \mathbf{h}_2 = \begin{bmatrix} h_{1,2} \\ h_{2,2} \end{bmatrix}, \text{ and } \mathbf{h}_3 = \begin{bmatrix} h_{1,3} \\ h_{2,3} \end{bmatrix}.$$

Note here that three independent columns are available for selection, which is different from receive antenna selection. This clearly indicates that transmit antenna selection can outperform

receive antenna selection for the same number of candidate channel matrices. However, as mentioned, conducting antenna selection at the transmitter side requires feedback overhead. Thus, there is a trade-off between the feedback requirement and diversity performance. Also note that increasing the number of receive antennas may not be always possible due to the receiver size constraint. Therefore, we can then consider joint transmit/receive antenna selection, conducting antenna selection at both the transmitter and the receiver side simultaneously, to achieve the optimum tradeoff.

Consider an $N_r \times N_t$ MIMO channel \mathbf{H} , where $N_r > M$ and $N_t > M$. We have $\binom{N_t}{M} \times \binom{N_r}{M}$ possible candidate channel matrices. It is worth noting that we only need $\lceil \log_2 \binom{N_t}{M} \rceil$ bits for feedback, where $\lceil t \rceil$ denotes the smallest integer larger than t . Besides, joint selection scheme may provide more candidate channel matrices for a fixed number of total antennas. For example, if $N_t = 4$, $N_r = 4$, and $M = 3$, we have sixteen candidate channel matrices, and only two bits are required for feedback. If we conduct pure transmit antenna selection with $N_t = 5$, $N_r = 3$, and $M = 3$, the number of the candidates is reduced to ten. Furthermore, the required bits for feedback will be increased to four. Note that the total numbers of antenna elements are the same for these two cases, i.e., $N_t + N_r = 8$.

§ 2.4.2 Antenna Selection in MIMO Relay Systems

Recently, cooperative communications have drawn a great deal of attention in wireless transmission. With the additional relay nodes, spatial diversity can be effectively enhanced. Multiple antennas can be placed at the source, the relays, and the destination. Such a cooperative system is referred to as a MIMO relay system. We now extend the proposed methods to antenna selection in MIMO relay systems. In this dissertation, we only consider a two-hop amplify-and-forward (AF) system, as illustrated in Figure 2.4.

As mentioned, we can consider antenna selection at each node for performance improvement. Assume that the relay node is equipped with N_{re} antennas. Let \mathbf{H}_{SR} be the $N_{re} \times N_t$ source-to-relay channel matrix and \mathbf{H}_{RD} be the $N_r \times N_{re}$ relay-to-destination channel matrix.

In the AF relay scheme, signal transmission is divided into two phases. Denote p_1 and p_2 as the indices of the candidate channel matrices in Phase I and Phase II, respectively. With antenna selection at both source and relay nodes, the source transmits the signal \mathbf{x} to the relay through an $M \times M$ channel $\mathbf{H}_{\text{SR},p_1}$ during Phase I. Note that in a two-hop system, the destination cannot receive the transmitted signal from the source in Phase I. Thus, the received signal at the relay can be expressed as $\mathbf{y}_1 = \mathbf{H}_{\text{SR},p_1} \mathbf{x} + \mathbf{n}_{\text{SR}}$, where \mathbf{n}_{SR} is a white Gaussian noise vector. In Phase II, the relay amplifies and retransmits \mathbf{y}_1 through an $M \times M$ channel $\mathbf{H}_{\text{RD},p_2}$. The corresponding received signal at the destination, denoted by \mathbf{y}_2 , can then be expressed as

$$\mathbf{y}_2 = \mathbf{H}_{\text{RD},p_2} (\mathbf{H}_{\text{SR},p_1} \mathbf{x} + \mathbf{n}_{\text{SR}}) + \mathbf{n}_{\text{RD}} \quad (2.34)$$

where \mathbf{n}_{RD} is also a white Gaussian noise vector. Equivalently, (2.34) can be written as

$$\mathbf{y}_2 = \mathbf{H}_{\text{eq},p} \mathbf{x} + \mathbf{n}_{\text{eq}} \quad (2.35)$$

where $\mathbf{H}_{\text{eq},p} = \mathbf{H}_{\text{RD},p_2} \mathbf{H}_{\text{SR},p_1}$, $\mathbf{n}_{\text{eq}} = \mathbf{H}_{\text{RD},p_2} \mathbf{n}_{\text{SR}} + \mathbf{n}_{\text{RD}}$, and p depends on p_1 and p_2 . Note that the equivalent noise vector \mathbf{n}_{eq} is colored with the covariance matrix of

$$\mathbf{K}_p = \sigma_{\text{SR}}^2 \left(\mathbf{H}_{\text{RD},p_2} \mathbf{H}_{\text{RD},p_2}^H + \frac{\sigma_{\text{RD}}^2}{\sigma_{\text{SR}}^2} \mathbf{I}_M \right) \quad (2.36)$$

where σ_{SR}^2 and σ_{RD}^2 are the variances of \mathbf{n}_{SR} and \mathbf{n}_{RD} , respectively. To conduct ML detection, the equivalent noise vector must be whitened and this can be achieved by left-multiplying a matrix \mathbf{W}_p on \mathbf{y}_2 , where

$$\mathbf{W}_p = \left(\mathbf{H}_{\text{RD},p_2} \mathbf{H}_{\text{RD},p_2}^H + \frac{\sigma_{\text{RD}}^2}{\sigma_{\text{SR}}^2} \mathbf{I}_M \right)^{-\frac{1}{2}}. \quad (2.37)$$

After the whitening process, the resultant received signal can be expressed as

$$\mathbf{y}'_2 = \mathbf{W}_p \mathbf{H}_{\text{eq},p} \mathbf{x} + \mathbf{W}_p \mathbf{n}_{\text{eq}} \quad (2.38)$$

where $\mathbf{y}'_2 = \mathbf{W}_p \mathbf{y}_2$. Since the covariance of $\mathbf{W}_p \mathbf{n}_{\text{eq}}$ becomes a scaled identity matrix $\sigma_{\text{SR}}^2 \mathbf{I}_M$, the selection schemes described in Section 2.1 and 2.2 can be directly used to enhance the system performance.

§ 2.4.3 Sphere Decoding Algorithm

The sphere decoding algorithm (SDA) is an efficient method to realize the ML detection in MIMO systems. In this subsection, we demonstrate the use of our proposed selection methods for SDA. Considering the signal model in (2.1), the idea of SDA is to search a subset of \mathcal{X}^M such that

$$\|\mathbf{y} - \mathbf{H}_p \mathbf{x}\| \leq \gamma \quad (2.39)$$

where γ is the radius of the searching sphere. First, we conduct the QRD on \mathbf{H}_p yielding $\mathbf{H}_p = \mathbf{Q}\mathbf{R}$. Since \mathbf{Q} is a unitary matrix, (2.39) can be rewritten as

$$\begin{aligned} \|\mathbf{y} - \mathbf{H}_p \mathbf{x}\| &= \|\mathbf{y} - \mathbf{Q}\mathbf{R}\mathbf{x}\| \\ &= \|\mathbf{y}' - \mathbf{R}\mathbf{x}\| \end{aligned} \quad (2.40)$$

where $\mathbf{y}' = \mathbf{Q}^H \mathbf{y}$. Let y'_i denote the i th entry of \mathbf{y}' . With the upper-triangular structure of \mathbf{R} , we can further rewrite (2.40) as

$$\begin{aligned} \|\mathbf{y} - \mathbf{H}_p \mathbf{x}\|^2 &= |y'_M - R_{M,M}x_M|^2 + |y'_{M-1} - R_{M-1,M}x_M - R_{M-1,M-1}x_{M-1}|^2 + \cdots \\ &\leq \gamma^2 \end{aligned} \quad (2.41)$$

The expression of (2.41) allows a tree search operation, starting with x_M , for finding the solution candidates. Then, the candidate with the minimum distance is chosen as the output.

As we can see, the QRD operation is required in the SDA. Thus, the QRD processing unit can be shared with proposed antenna selection methods. However, if we adopt other selection methods such as the SVD-based or capacity-based method [18], extra circuits are required to conduct the SVD or calculate the channel capacity. Thus, with the proposed methods, the implementation complexity of the receiver can be effectively reduced. The capacity-based method, maximizing the capacity of the channel matrix, is described as follows. For a given candidate

channel matrix \mathbf{H}_p , the channel capacity is expressed as

$$C = \log_2 \det \left(\mathbf{I}_M + \frac{\varepsilon}{M} \mathbf{H}_p^H \mathbf{H}_p \right) \quad (2.42)$$

where ε is the average SNR. The method then evaluates (2.42) for each candidate channel matrix, and selects the antenna subset having the maximum channel capacity. The computational complexity of the capacity-based method is $\mathcal{O}(M^3)$, mainly arising from the matrix multiplication and the determinant computation in (2.42). One additional overhead for the method is that the estimation of the noise variance is required.

§ 2.5 Simulations and Discussions

In this section, we report simulations evaluating the performance of our proposed selection methods. The simulation setup is described as follows. A flat-fading MIMO channel \mathbf{H} is used; its entries are assumed to be i.i.d. complex Gaussian random variables with zero mean and unit variance. The modulation scheme is QPSK, and the detection method is ML. Besides, the parameter δ in the CLLL algorithm is set as 0.99. In our simulations, several selection methods are compared, including 1) the SVD-based method, 2) the capacity-based method, 3) the QRD-based method, 4) the QRD-based BT-P method, 5) the QRD-based BT-C method, 6) the QRD-based BT-E method, and 7) the optimum method realized with an exhaustive search.

Figure 2.5 shows the bit error rate (BER) performance of transmit antenna selection in the MIMO system. Here, $N_t = 6$, $N_r = 3$, and $M = 3$. As we can see, the QRD-based method indeed outperforms the SVD-based method. The performance of the capacity-based method is comparable to that of the QRD-based scheme. However, the capacity-based method requires additional information of the noise variance. The QRD-based BT-C method can outperform the SVD-based by 1.8 dB at the BER of 10^{-4} . We also observe that the QRD-based BT-C method provides the near-optimum performance. These results indicate that the $[\mathbf{R}]$ -value spread can be reduced effectively with the QRD-based BT-C method. The performance of CLLL depends on the parameter δ . As mentioned, if δ is smaller (close to 0.5), the computational complexity will

be lower. However, the performance will be poorer. As the value of δ we use is close to one, the columns of the channel matrix will be approximately orthogonal after the transformation. Thus, the number of the channel columns to be permuted can be chosen as a smaller value for the reduction of the computational complexity. Here, we let $\bar{M} = 2$. In other words, only two permutation patterns are considered. As we can see, the performance of the QRD-based BT-E method is almost the same as that of the QRD-based BT-C method. Note that the computational complexity of the QRD-based BT-E method is much lower.

Figure 2.6 shows the BER comparison for receive antenna selection. We assume $N_t = 3$, $N_r = 6$, and $M = 3$. The results show that the proposed QRD-based BT-C method can also achieve near-optimum performance. As for other methods, the similar behavior can be observed. Note that we also let the number of candidate channel matrices is equal to that in Figure 2.5. This allows us to verify the analysis shown in Section 2.4.1. From the figure, we can see that receive antenna selection indeed suffers from performance loss compared to transmit antenna selection, which is consistent with our analysis. Furthermore, another observation is that the performance gaps between various methods are slightly reduced in Figure 2.6. This result can also be attributed to the correlation between candidate channel matrices.

Figure 2.7 compares the performance of various selection schemes for joint transmit/receive antenna selection. Similarly, we let $N_t = 5$, $N_r = 4$, and $M = 3$ such that the number of the total antennas remains the same. Distributing the extra antennas at both the transmitter and the receiver side, we can have $\binom{5}{3} \times \binom{4}{3}$ candidate channel matrices to choose from. Note that receive antenna selection is involved, indicating that its performance may be worse than the pure transmit antenna selection with the same total number of antennas. However, the number of the candidate channel matrices becomes larger in this case, and the selection performance can then be enhanced. Overall, the performance is improved in all methods.

Next, we consider the performance comparison for a two-hop AF MIMO relay system. Figure 2.8 shows the simulation results. In the figure, the performance is evaluated as a function of the average SNR per antenna at the relay, denoted as SNR_R . Besides, the average SNR per

antenna at the destination, denoted by SNR_D , is assumed to be 25 dB. Here, we let $N_t = 4$, $N_r = 4$, $N_{re} = 4$, and $M = 3$. In this case, we require two bits for sending the optimum indices of antenna subsets back to the source and the relay node, respectively. With the system model described in Section 2.4.2, the relay node can receive and retransmit signal with different antenna subsets, which means we have $\binom{4}{3} \times \binom{4}{3} \times \binom{4}{3} \times \binom{4}{3}$ candidate channel matrices to be evaluated and the computational complexity can be very high. Thus, we can consider an simplified scheme where the same antenna subset is used for signal reception and retransmission at the relay. With this simplification, the number of candidate channel matrices is reduced to 64. Similar to the previous results, the proposed QRD-based BT-C method can still achieve near-optimum performance. In this scenario, it outperforms the SVD-based method by 2 dB at the BER of 10^{-4} . Note that all the schemes will exhibit an error floor when SNR_R is close to SNR_D . The reason is that as σ_{SR}^2 is small, the system performance is dominated by σ_{RD}^2 .

Finally, we provide the BER performance comparison when the ML detection is implemented with the SDA. Transmit antenna selection is considered and the result is shown in Figure 2.9. The search radius γ is determined according to $\gamma^2 = \tau \times \det(\mathbf{H}_p \mathbf{H}_p^H)^{\frac{1}{2M}}$ [57]. We set $\tau = 5$ so that the SDA can provide good performance and at the same time its computational complexity remains reasonably low. From Figure 2.9, we can observe that the behavior of each scheme is very similar to that in Figure 2.5. The performance of the QRD-based BT-C scheme with the SDA is still comparable to that of the optimum method.

Table 2.1: Algorithm of proposed QRD-based BT-P method

Algorithm 2.1: QRD-based BT-P Design

- (1) For each candidate channel matrix \mathbf{H}_p , compute $\mathbf{H}_{p,i} = \mathbf{H}_p \mathbf{\Pi}_i$ where $i = 1, 2, \dots, M!$;
 - (2) for $i = 1 : M!$
 - (3) $[\mathbf{Q}_i, \mathbf{R}_i] = \text{QR Decomposition}(\mathbf{H}_{p,i})$;
 - (4) $[\mathbf{R}_i]_{\min} = \text{minimum diagonal entry of } \mathbf{R}_i$;
 - (5) end
 - (6) $[\mathbf{R}_{\text{per}}]_{\min} = \max([\mathbf{R}_1]_{\min}, [\mathbf{R}_2]_{\min}, \dots, [\mathbf{R}_{M!}]_{\min})$;
 - (7) Let $[\mathbf{R}_{\text{per}}]_{\min}$ be the minimum diagonal entry of the R-factor for \mathbf{H}_p ;
 - (8) Choose the antenna subset whose \mathbf{H}_p has the largest $[\mathbf{R}_{\text{per}}]_{\min}$;
-

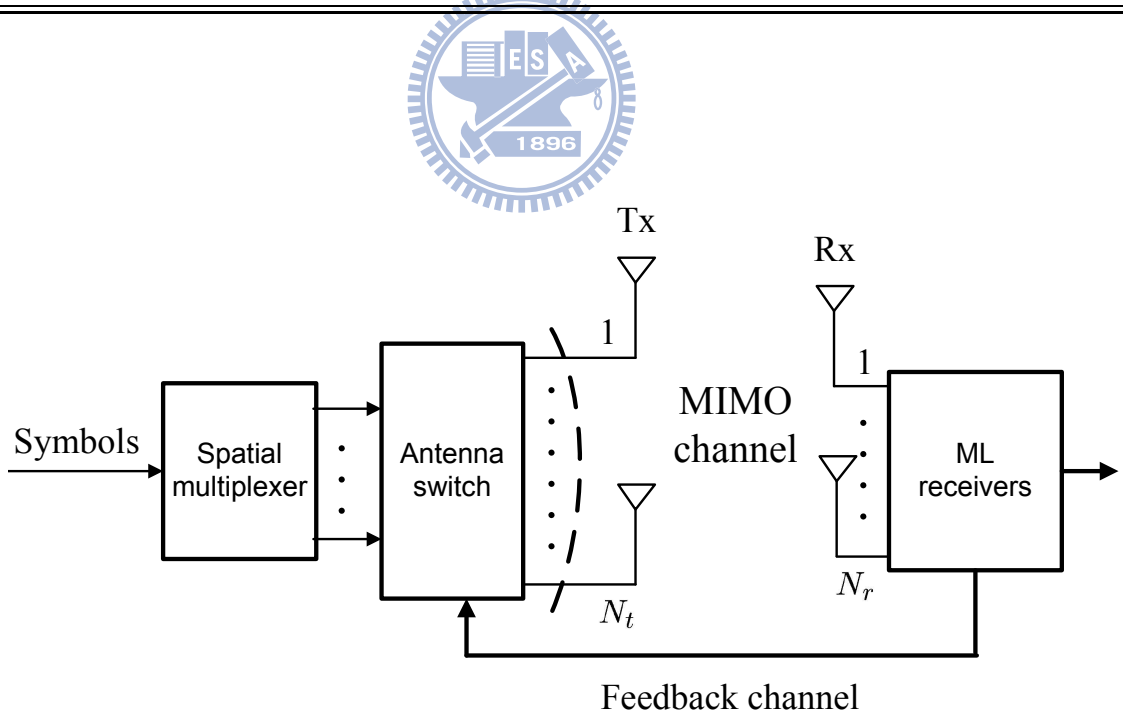
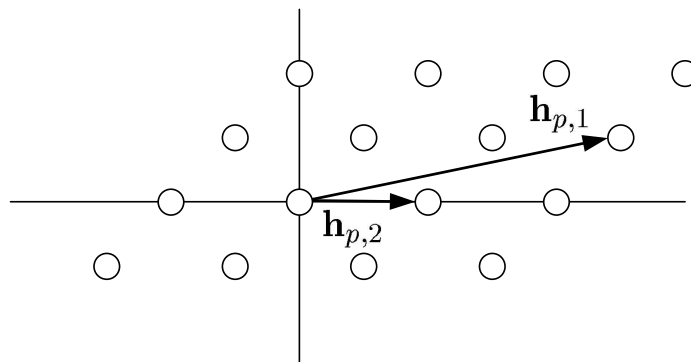
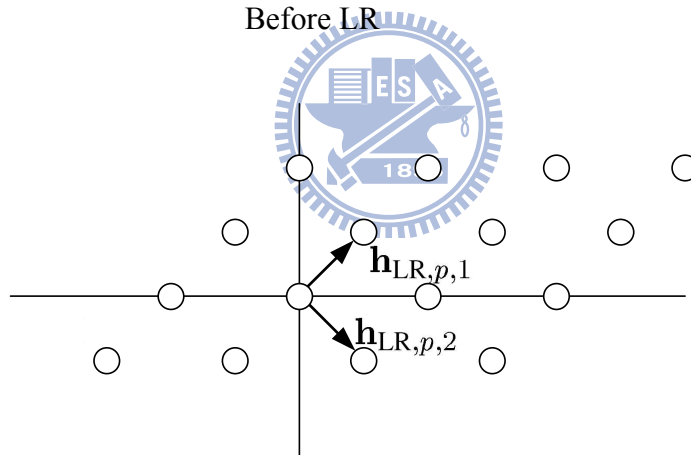


Figure 2.1: System model for transmit antenna selection in a spatial-multiplexing MIMO system.



Before LR



After LR

Figure 2.2: LR for $M = 2$.

Table 2.2: Operations of CLLL algorithm

Input: \mathbf{H}_p ; Output: \mathbf{Q} , \mathbf{R} , and \mathbf{T} ;

- (1) $[\mathbf{Q}, \mathbf{R}] = \text{QR Decomposition}(\mathbf{H}_p)$;
- (2) $\delta \in (\frac{1}{2}, 1)$;
- (3) $M = \text{size}(\mathbf{H}_p, 2)$;
- (4) $\mathbf{T} = \mathbf{I}_M$;
- (5) $m = 2$;
- (6) while $m \leq M$
 - (7) for $q = (m - 1) : -1 : 1$
 - (8) $u = \text{round}(R_{q,m}/R_{q,q})$;
 - (9) if $u \sim 0$
 - (10) $\mathbf{R}_{(1:q,m)} = \mathbf{R}_{(1:q,m)} - u\mathbf{R}_{(1:q,q)}$;
 - (11) $\mathbf{T}_{(:,m)} = \mathbf{T}_{(:,m)} - u\mathbf{T}_{(:,q)}$;
 - (12) end
 - (13) end
 - (14) if $\delta |R_{m-1,m-1}|^2 > |R_{m,m}|^2 + |R_{m-1,m}|^2$
 - (15) Swap the $(m - 1)$ th and m th columns in \mathbf{R} and \mathbf{T} ;
 - (16) Set $\Theta = \begin{bmatrix} \alpha^H & \beta \\ -\beta & \alpha \end{bmatrix}$, where $\alpha = \frac{R_{m-1,m-1}}{\|\mathbf{R}_{(m-1:m,m-1)}\|}$ and $\beta = \frac{R_{m,m-1}}{\|\mathbf{R}_{(m-1:m,m-1)}\|}$;
 - (17) $\mathbf{R}_{(m-1:m,m-1:M)} = \Theta\mathbf{R}_{(m-1:m,m-1:M)}$;
 - (18) $\mathbf{Q}_{(:,m-1:m)} = \mathbf{Q}_{(:,m-1:m)}\Theta^H$;
 - (19) $m = \max(m - 1, 2)$;
 - (20) else
 - (21) $m = m + 1$;
 - (22) end
- (23) end

Table 2.3: Algorithm of proposed QRD-based BT-C method

Algorithm 2.2: QRD-based BT-C Design

- (1) For each candidate channel matrix \mathbf{H}_p , $\mathbf{P} = \text{CLLL}(\mathbf{H}_p)$;
 - (2) for $i = 1 : M!$
 - (3) $[\mathbf{Q}_{\text{LR},i}, \mathbf{R}_{\text{LR},i}] = \text{QR Decomposition}(\mathbf{H}_p \mathbf{P} \Pi_i)$;
 - (4) $[\mathbf{R}_{\text{LR},i}]_{\min} = \text{minimum diagonal entry of } \mathbf{R}_{\text{LR},i}$;
 - (5) end
 - (6) $[\mathbf{R}_{\text{cas}}]_{\min} = \max([\mathbf{R}_{\text{LR},1}]_{\min}, [\mathbf{R}_{\text{LR},2}]_{\min}, \dots, [\mathbf{R}_{\text{LR},M!}]_{\min})$;
 - (7) Let $[\mathbf{R}_{\text{cas}}]_{\min}$ be the minimum diagonal entry of the R-factor for \mathbf{H}_p ;
 - (8) Choose the antenna subset whose \mathbf{H}_p has the largest $[\mathbf{R}_{\text{cas}}]_{\min}$;
-

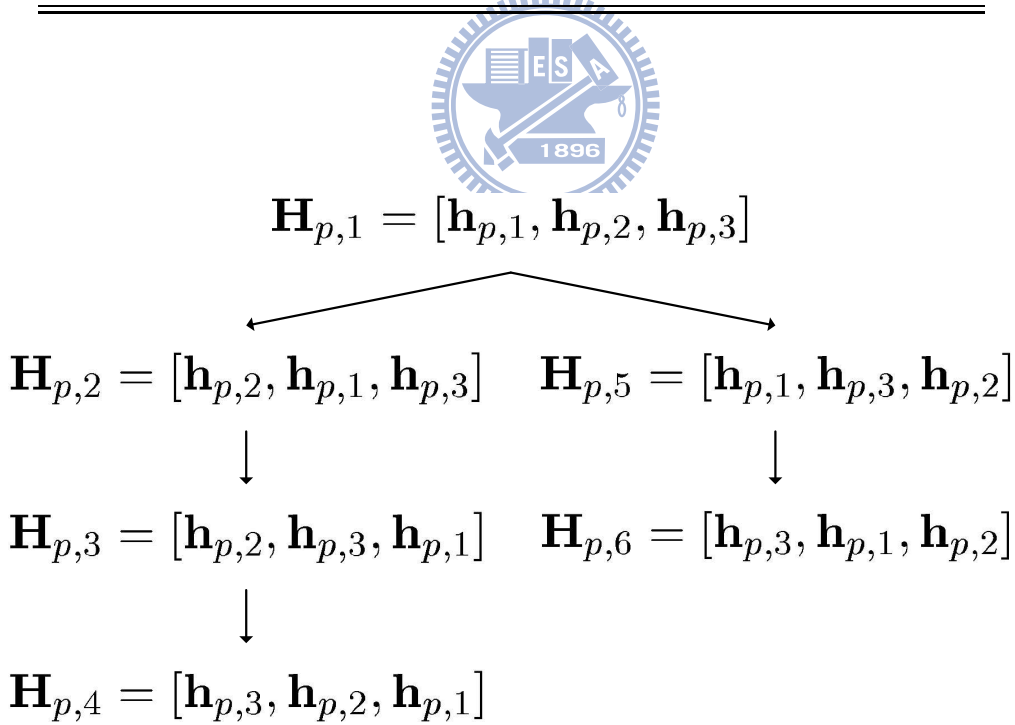


Figure 2.3: $[\mathbf{R}_i]_{\min}$ computations for $M = 3$.

Table 2.4: Algorithm of proposed QRD-based BT-E method

Algorithm 2.3: QRD-based BT-E Design

- (1) For each candidate channel matrix \mathbf{H}_p , $\mathbf{P} = \text{CLLL}(\mathbf{H}_p)$;
 - (2) Choose $\bar{M} < M$;
 - (3) for $i = 1 : \bar{M}$!
 - (4) $[\mathbf{Q}_{\text{LR},i}, \mathbf{R}_{\text{LR},i}] = \text{QR Decomposition}(\mathbf{H}_p \mathbf{P} \Pi_i)$;
 - (5) $[\mathbf{R}_{\text{LR},i}]_{\min} = \text{minimum diagonal entry of } \mathbf{R}_{\text{LR},i}$;
 - (6) end
 - (7) $[\mathbf{R}_{\text{cas}}^{\text{eff}}]_{\min} = \max([\mathbf{R}_{\text{LR},1}]_{\min}, [\mathbf{R}_{\text{LR},2}]_{\min}, \dots, [\mathbf{R}_{\text{LR},\bar{M}}]_{\min})$;
 - (8) Let $[\mathbf{R}_{\text{cas}}^{\text{eff}}]_{\min}$ be the minimum diagonal entry of the R-factor for \mathbf{H}_p ;
 - (9) Choose the antenna subset whose \mathbf{H}_p has the largest $[\mathbf{R}_{\text{cas}}^{\text{eff}}]_{\min}$;
-

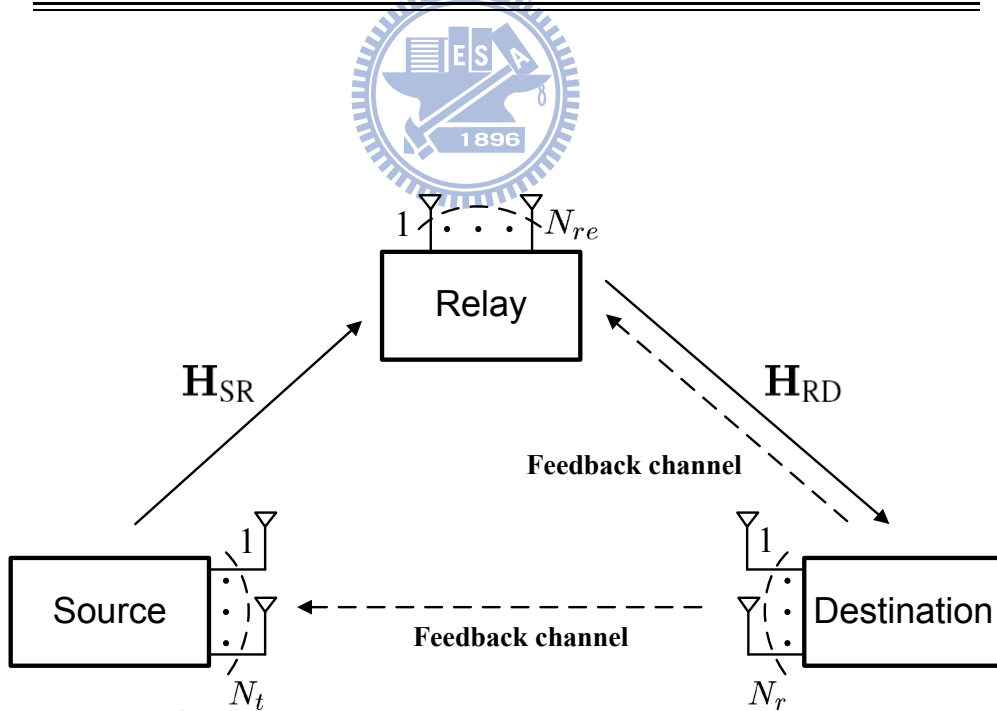


Figure 2.4: System model of a two-hop AF MIMO relay system.

Table 2.5: Complexity comparisons for different antenna selection methods

	\mathbf{P}	$[\mathbf{R}_1]_{\min}$	$[\mathbf{R}_i]_{\min}$ for $i = 2, \dots, M!$	Total
QRD-based	\setminus	$\mathcal{O}(M^3)$	\setminus	$\mathcal{O}(M^3)$
QRD-based BT-P	\setminus	$\mathcal{O}(M^3)$	$\mathcal{O}(M^3 M!)$	$\mathcal{O}(M^3 M!)$
QRD-based BT-P with Givens rotations	\setminus	$\mathcal{O}(M^3)$	$\mathcal{O}(MM!)$	$\mathcal{O}(M^3 + MM!)$
	\mathbf{P}	$[\mathbf{R}_{LR,1}]_{\min}$	$[\mathbf{R}_{LR,i}]_{\min}$ for $i = 2, \dots, M!$	Total
QRD-based BT-C	$\mathcal{O}(M^4)$	$\mathcal{O}(M^3)$	$\mathcal{O}(M^3 M!)$	$\mathcal{O}(M^4 + M^3 M!)$
QRD-based BT-C with Givens rotations	$\mathcal{O}(M^4)$	$\mathcal{O}(M^3)$	$\mathcal{O}(MM!)$	$\mathcal{O}(M^4 + MM!)$
	\mathbf{P}	$[\mathbf{R}_{LR,1}]_{\min}$	$[\mathbf{R}_{LR,i}]_{\min}$ for $i = 2, \dots, \bar{M}!$	Total
QRD-based BT-E	$\mathcal{O}(M^4)$	$\mathcal{O}(M^3)$	$\mathcal{O}(M^3 \bar{M}!)$	$\mathcal{O}(M^4 + M^3 \bar{M}!)$
QRD-based BT-E with Givens rotations	$\mathcal{O}(M^4)$	$\mathcal{O}(M^3)$	$\mathcal{O}(M \bar{M}!)$	$\mathcal{O}(M^4 + M \bar{M}!)$

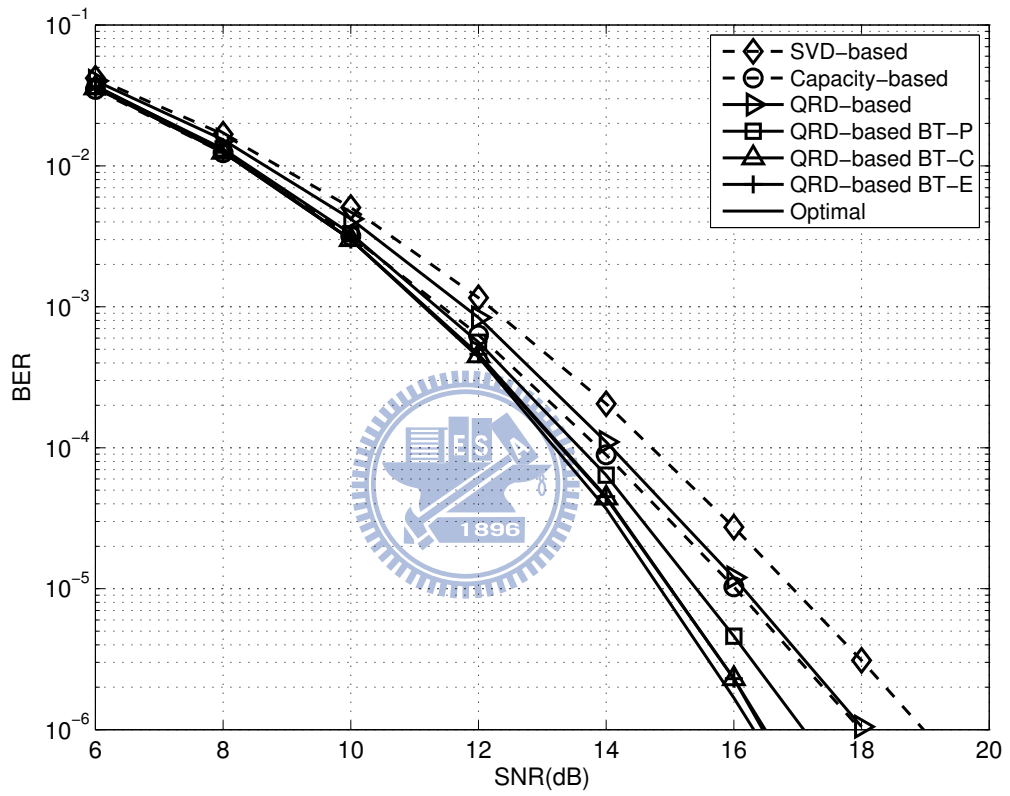


Figure 2.5: BER performance comparison for transmit antenna selection ($N_t = 6$, $N_r = 3$, and $M = 3$).

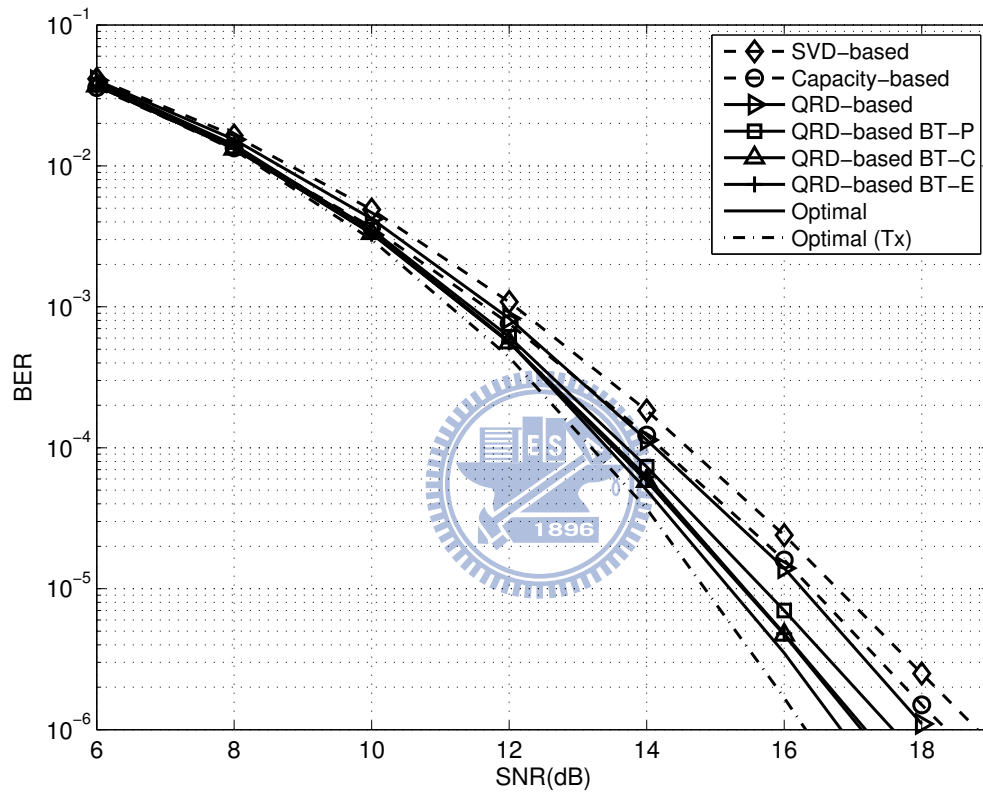


Figure 2.6: BER performance comparison for receive antenna selection ($N_t = 3$, $N_r = 6$, and $M = 3$).

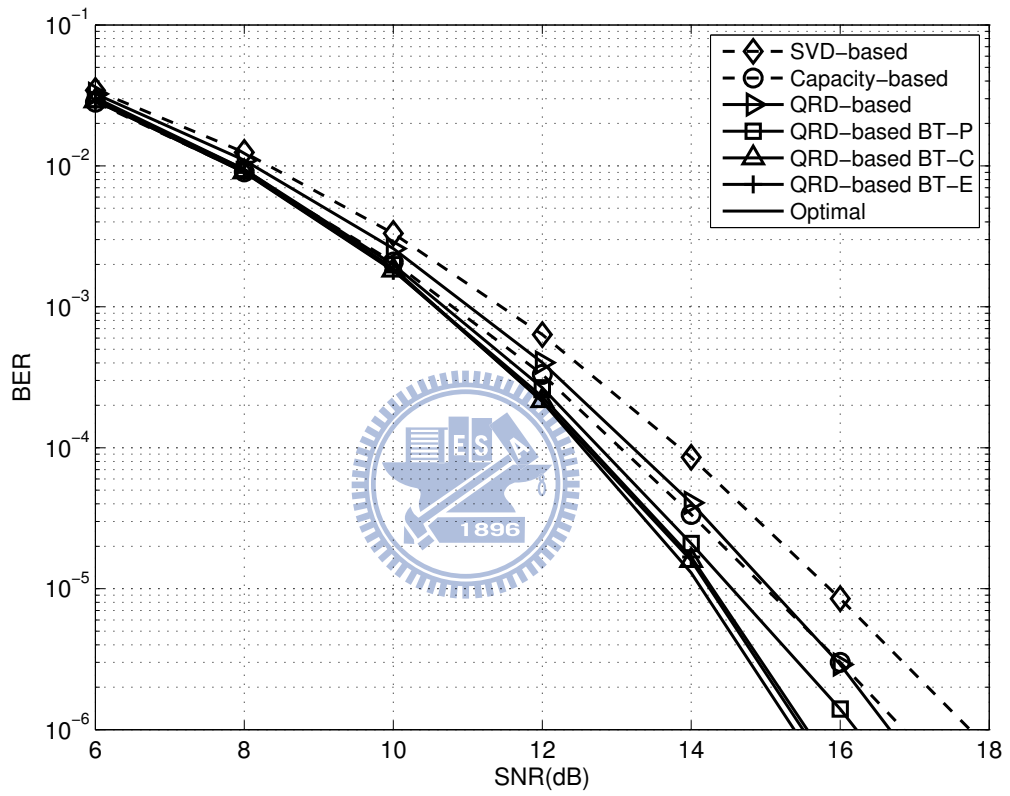


Figure 2.7: BER performance comparison for joint transmit/receive antenna selection ($N_t = 5$, $N_r = 4$, and $M = 3$).

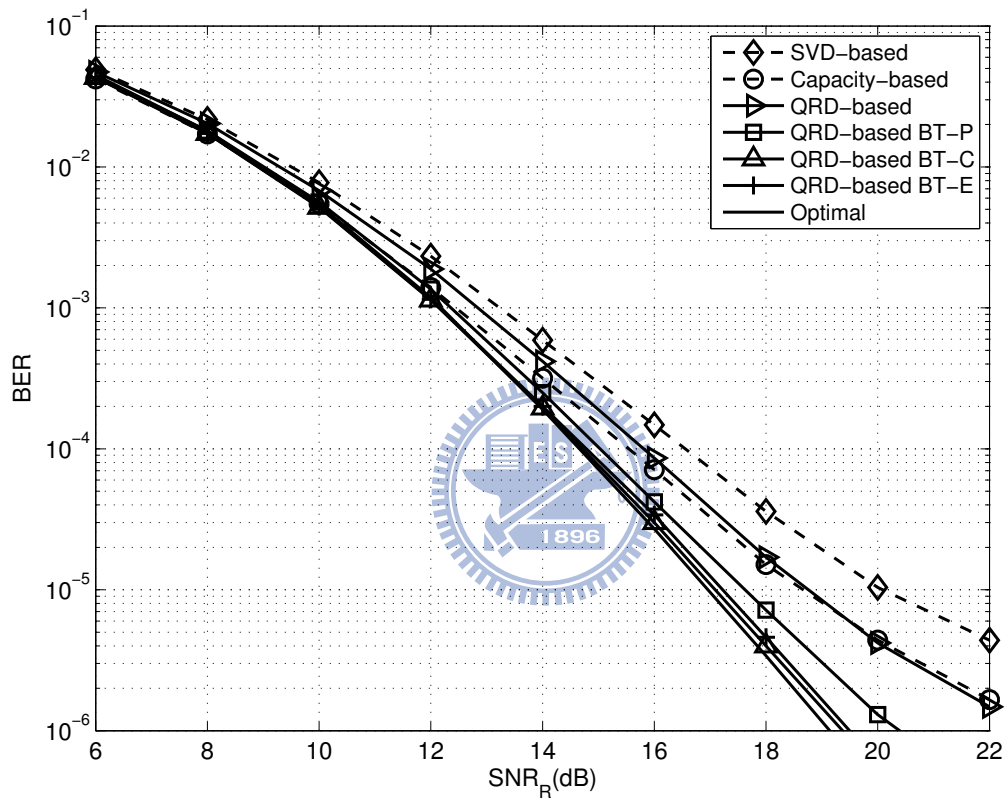


Figure 2.8: BER performance comparison for antenna selection in a two-hop MIMO relay system ($N_t = 4$, $N_{re} = 4$, $N_r = 4$, and $M = 3$).

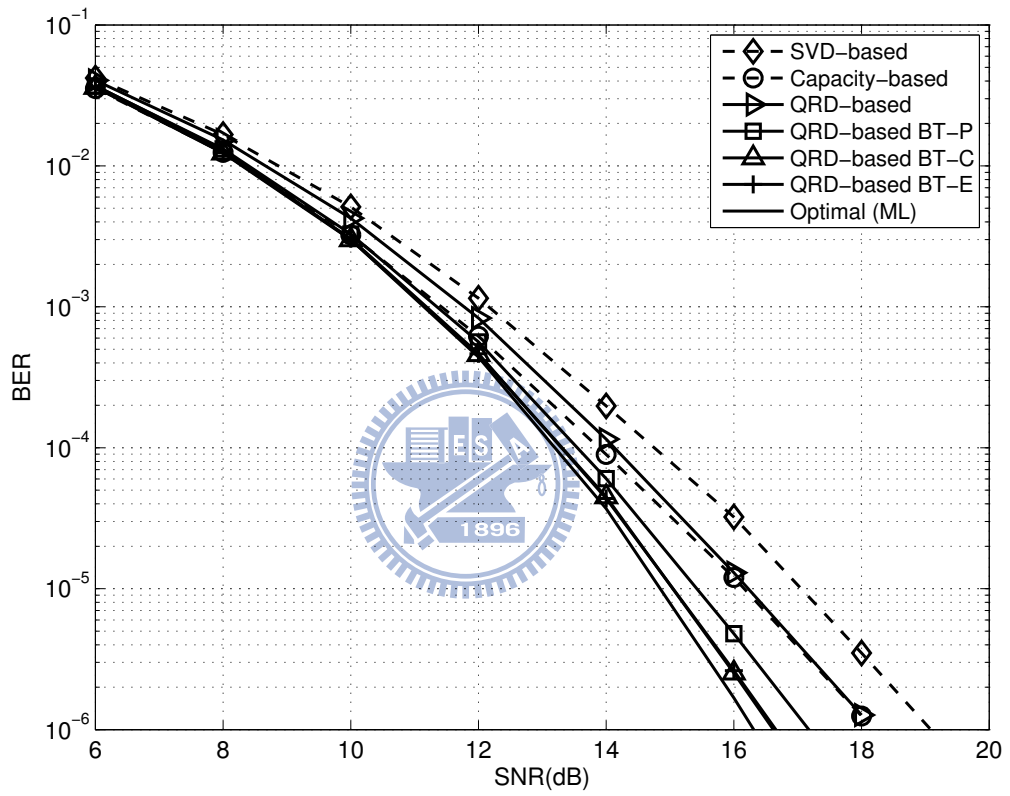
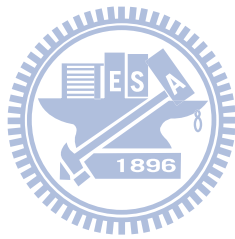


Figure 2.9: BER performance comparison for transmit antenna selection with SDA ($N_t = 6$, $N_r = 3$, and $M = 3$).



Chapter 3

X-Structured Precoding for ML Detectors in Spatial-Multiplexing MIMO and MIMO Relay Systems



In this chapter, we will study the design of the X-structured precoder. In Section 3.1, we give the system model and formulate the problem. In Section 3.2, we review the existing design methods for X-structured precoding. As mentioned, the design of the X-structured precoder is equivalent to the design of a 2×2 subprecoder, and most existing subprecoder designs require either numerical searches or table look-up operations. In Section 3.3, we propose a simple but effective method to solve these problems. We also consider joint source/relay precoders design for a two-hop AF MIMO relay system in Section 3.4. However, it is much more difficult to derive the optimum source and relay precoders, simultaneously. To overcome this problem, we propose using an iterative method deriving the source and relay precoders, individually and repeatedly. With some mild assumptions, the problem can be transformed to a scalar-valued optimization problem, and the solution can be solved by using Karash-Kuhn-Tucker (KKT) conditions. Finally, we evaluate the performance of the proposed methods in Section 3.5.

§ 3.1 System Models and Problem Formulation

Consider a precoded spatial-multiplexing MIMO system with N_t transmit antennas and N_r receive antennas, as described in Figure 3.1. Let $\mathbf{x} = [x_1, x_2, \dots, x_M]^T$ denote the $M \times 1$ symbol vector. In spatial multiplexing, each entry of \mathbf{x} is independently chosen from a finite-set constellation \mathcal{X} . For L -QAM, \mathcal{X} is given by

$$\mathcal{X} = \frac{1}{\sqrt{K}} \{ \pm a \pm bj \mid a, b \in (1, 3, \dots, \sqrt{L} - 1) \} \quad (3.1)$$

where $K = \frac{2}{3}(L - 1)$. Let \mathbf{H} denote the $N_r \times N_t$ channel matrix, which is assumed to be known at both the transmitter and receiver. Using the CSI at the transmitter, we can design a $N_t \times M$ precoding matrix \mathbf{M} and conduct precoding by left-multiplying \mathbf{M} on \mathbf{x} . In general, the power of \mathbf{M} has to be constrained, i.e., $\text{tr} \{ \mathbf{M}^H \mathbf{M} \} = P_T$ where P_T is a constant. The received symbol vector can then be expressed as

$$\mathbf{y} = \mathbf{H}\mathbf{M}\mathbf{x} + \mathbf{n} \quad (3.2)$$

where \mathbf{n} is the Gaussian noise vector. Assume that each entry of \mathbf{n} is i.i.d. with the covariance matrix of $\sigma_n^2 \mathbf{I}_{N_r}$, where σ_n^2 is the noise variance. At the receiver, the ML detector searches all possible symbol vectors to obtain an estimate $\hat{\mathbf{x}}$ such that

$$\hat{\mathbf{x}} = \min_{\mathbf{x} \in \mathcal{X}^M} \|\mathbf{y} - \mathbf{H}\mathbf{M}\mathbf{x}\|. \quad (3.3)$$

The error probability of the detection can then be represented as

$$P_e = \frac{1}{L^M} \sum_{i=1}^{L^M} \sum_{j=1, j \neq i}^{L^M} P_{ij} \quad (3.4)$$

where P_{ij} is the pair-wise error probability (PEP) that a transmitted symbol vector \mathbf{x}_i is falsely detected to some other \mathbf{x}_j . Let $d_{i,j}$ denote the distance between two distinct received symbol vectors $\mathbf{H}\mathbf{M}\mathbf{x}_i$ and $\mathbf{H}\mathbf{M}\mathbf{x}_j$. Similarly, the free distance of the MIMO system is then defined as:

$$d_{\text{free}} \triangleq \min d_{i,j} = \min_{\mathbf{x}_i, \mathbf{x}_j \in \mathcal{X}^M, \mathbf{x}_i \neq \mathbf{x}_j} \|\mathbf{H}\mathbf{M}(\mathbf{x}_i - \mathbf{x}_j)\|. \quad (3.5)$$

Thus, the worst-case PEP, denoted by P_w , can be expressed as $P_w = Q\left(\sqrt{\frac{d_{\text{free}}^2}{2\sigma_n^2}}\right)$ where $Q(\cdot)$ denotes the Q-function defined as $Q(x) = \frac{1}{\sqrt{2\pi}} \int_x^\infty e^{-\frac{t^2}{2}} dt$. It is simple to see that if d_{free} is much smaller than other $d_{i,j}$'s, P_e will be dominated by P_w and the precoder design by minimizing P_e is the same as that by minimizing P_w . As a result, the design criterion for \mathbf{M} is equivalent to maximizing the free distance of a MIMO system. The problem now is to find \mathbf{M} such that the free distance is maximized. This problem is known to be difficult since d_{free} depends on the discrete set \mathcal{X}^M . Note that the error probability P_e is also referred to as block error rate (BLER).

A recently developed method to overcome the problem is the application of the X-structured precoder [28]. To do that, \mathbf{H} is first transformed into parallel subchannels and precoding is applied on the subchannels. Using SVD, we can have $\mathbf{H} = \mathbf{U}\mathbf{\Sigma}\mathbf{V}^H$, where \mathbf{U} is an $N_r \times M$ matrix, $\mathbf{\Sigma}$ is an $M \times M$ real-valued diagonal matrix, and \mathbf{V}^H is an $M \times N_t$ matrix. Note that $\mathbf{U}^H\mathbf{U} = \mathbf{V}^H\mathbf{V} = \mathbf{I}_M$ and $\mathbf{\Sigma} = \text{diag}(\lambda_1, \lambda_2, \dots, \lambda_M)$ where λ_i 's are the singular values of \mathbf{H} . Let λ_i 's be arranged in a descending order, i.e., $\lambda_1 \geq \lambda_2 \geq \dots \geq \lambda_M > 0$ and $\mathbf{M} = \mathbf{V}\mathbf{F}$, where \mathbf{F} is an $M \times M$ matrix. Left-multiplying \mathbf{U}^H on \mathbf{y} , we can have the equivalent received signal model as

$$\mathbf{r} = \mathbf{\Sigma}\mathbf{F}\mathbf{x} + \mathbf{n}' \quad (3.6)$$

where $\mathbf{r} = \mathbf{U}^H\mathbf{y}$ and $\mathbf{n}' = \mathbf{U}^H\mathbf{n}$ is the noise vector with the same covariance matrix as \mathbf{n} . In what follows, we will refer \mathbf{F} as the precoder since \mathbf{M} can be derived if \mathbf{F} is obtained. Note that the power constraint of the precoder still holds, i.e., $\text{tr}\{\mathbf{M}^H\mathbf{M}\} = \text{tr}\{\mathbf{F}^H\mathbf{F}\}$. Therefore, we can have the problem reformulated as:

$$\begin{aligned} \max_{\mathbf{F}} \quad & \min_{\mathbf{x}, \mathbf{x}' \in \mathcal{X}^M, \mathbf{x} \neq \mathbf{x}'} \|\mathbf{\Sigma}\mathbf{F}(\mathbf{x} - \mathbf{x}')\| \\ \text{s.t.} \quad & \text{tr}\{\mathbf{F}^H\mathbf{F}\} = P_T. \end{aligned} \quad (3.7)$$

The diagonal structure of $\mathbf{\Sigma}$ in (3.7) greatly facilitates the derivation of the solution. The key idea is to apply an X-structure on \mathbf{F} meaning that subchannels ordered according to their singu-

lar values are paired to obtain a set of 2×2 subsystems, and 2×2 subprecoders are designed to maximize the free distances of the subsystems.

§ 3.2 Existing Subprecoders for MIMO Systems

We first focus on the design of a 2×2 precoder in (3.7). For $M = 2$, Σ can be expressed as:

$$\Sigma = \begin{bmatrix} \lambda_1 & 0 \\ 0 & \lambda_2 \end{bmatrix} = \rho \begin{bmatrix} \cos \gamma & 0 \\ 0 & \sin \gamma \end{bmatrix} \quad (3.8)$$

where $\rho = \sqrt{\lambda_1^2 + \lambda_2^2}$ is the channel gain, and $\gamma = \tan^{-1} \left(\frac{\lambda_2}{\lambda_1} \right)$ is an angle related to the channel. Clearly, $0 < \gamma \leq \frac{\pi}{4}$ so that $\lambda_1 \geq \lambda_2$ is satisfied. With the SVD, an \mathbf{F} can be written as $\mathbf{F} = \mathbf{U}_F \Sigma_F \mathbf{V}_F^H$, where both \mathbf{U}_F and \mathbf{V}_F are 2×2 unitary matrices and Σ_F is a 2×2 diagonal matrix. It has been shown in [31] that \mathbf{U}_F can be an identity matrix without affecting the system performance for symmetric QAM modulations. Then \mathbf{V}_F and Σ_F can be parameterized as follows:

$$\begin{cases} \Sigma_F = \sqrt{P_T} \begin{bmatrix} \cos \psi & 0 \\ 0 & \sin \psi \end{bmatrix} \\ \mathbf{V}_F^H = \begin{bmatrix} \cos \theta & \sin \theta \\ -\sin \theta & \cos \theta \end{bmatrix} \begin{bmatrix} 1 & 0 \\ 0 & e^{i\varphi} \end{bmatrix} \end{cases} \quad (3.9)$$

where $0 \leq \psi \leq \frac{\pi}{2}$, $0 \leq \varphi \leq \frac{\pi}{2}$, and $0 \leq \theta \leq \frac{\pi}{4}$. Given a set of difference vectors, the optimum precoder can then be found by a numerical search over all possible values of ψ , φ , and θ .

§ 3.2.1 Complex-Valued Subprecoder Design

With (3.8) and (3.9), the complex-valued subprecoder, \mathbf{F}_c , was found in [32]. The solution of \mathbf{F}_c is derived by using a numerical search method. Let $N = 2^{\frac{1}{2} \log_2 L} - 1$. The expression of

optimum \mathbf{F}_c is given by

$$\mathbf{F}_c = \begin{cases} \mathbf{F}_{c,1} = \sqrt{P_T} \begin{bmatrix} \cos \theta_{c,1} & \sin \theta_{c,1} e^{j\varphi_{c,1}} \\ 0 & 0 \end{bmatrix} & \text{for } \gamma \leq \gamma_c \\ \mathbf{F}_{c,2} = \frac{\sqrt{P_T}}{2} \begin{bmatrix} \cos \psi_{c,2} & 0 \\ 0 & \sin \psi_{c,2} \end{bmatrix} \begin{bmatrix} \sqrt{2} & 1+j \\ -\sqrt{2} & 1+j \end{bmatrix} & \text{for } \gamma > \gamma_c \end{cases} \quad (3.10)$$

where $\theta_{c,1}$, $\varphi_{c,1}$, and $\psi_{c,2}$ are given by

$$\begin{cases} \varphi_{c,1} = \tan^{-1} \left(\frac{1}{2N+\sqrt{3}} \right) \\ \theta_{c,1} = \tan^{-1} (2 \sin \varphi_{c,1}) \\ \psi_{c,2} = \tan^{-1} \frac{\sqrt{2}-1}{\tan \gamma} \end{cases} \quad (3.11)$$

and the threshold γ_c in (3.10) is expressed as

$$\gamma_c = \tan^{-1} \left(\sqrt{\frac{\sqrt{2}-1}{\sqrt{2N^2 + \sqrt{6}N + \sqrt{2}-1}}} \right). \quad (3.12)$$

It can be seen that two operation modes are used in \mathbf{F}_c . When $\gamma \leq \gamma_c$, $\mathbf{F}_{c,1}$ pours all the transmit power on the strongest subchannel λ_1 and maps the two bit-streams into a scalar symbol for transmission. We refer this subprecoder as a rank-deficient subprecoder. When $\gamma > \gamma_c$, $\mathbf{F}_{c,2}$ utilizes both subchannels with a power allocation scheme. The resultant free distance is given by:

$$d_{\text{free}, \mathbf{F}_c} = \begin{cases} \sqrt{P_T \rho^2 \frac{4}{K} \frac{\cos^2 \gamma}{N^2 + \sqrt{3}N + 2}} & \text{for } \gamma \leq \gamma_c \\ \sqrt{P_T \rho^2 \frac{4}{K} \frac{(2-\sqrt{2}) \cos^2 \gamma \sin^2 \gamma}{1 + (2-2\sqrt{2}) \cos^2 \gamma}} & \text{for } \gamma > \gamma_c. \end{cases} \quad (3.13)$$

It has been shown [31] that \mathbf{F}_c is optimal for 4-QAM (QPSK). However, it is suboptimal for higher QAM constellations [32].

§ 3.2.2 Real-Valued Subprecoder Design

Obtaining the optimum complex-valued subprecoders for higher QAM constellations is difficult since the computational complexity of the numerical search is high. To overcome this problem, the real-valued subprecoder, denoted by \mathbf{F}_r , was proposed in [30]. The main idea of \mathbf{F}_r is to simplify the subprecoder structure as

$$\mathbf{F}_r = \sqrt{P_T} \begin{bmatrix} \cos \psi_r & 0 \\ 0 & \sin \psi_r \end{bmatrix} \begin{bmatrix} \cos \theta_r & -\sin \theta_r \\ \sin \theta_r & \cos \theta_r \end{bmatrix}. \quad (3.14)$$

Comparing (3.14) with (3.9), we can see that the number of the parameters to be searched is reduced. Similar to \mathbf{F}_c , it was shown that \mathbf{F}_r can be operated in two modes, denoted by $\mathbf{F}_{r,1}$ and $\mathbf{F}_{r,2}$. Let $l = \frac{1}{2} \log_2(L)$ and $\theta_{r,1} = \tan^{-1} \frac{1}{2^l}$. For $l \in \{1, 2, \dots, 5\}$, \mathbf{F}_r can be expressed as:

$$\mathbf{F}_r = \begin{cases} \mathbf{F}_{r,1} = \sqrt{P_T} \begin{bmatrix} \cos \theta_{r,1} & -\sin \theta_{r,1} \\ 0 & 0 \end{bmatrix} & \text{for } \gamma \leq \gamma_r \\ \mathbf{F}_{r,2} & \text{for } \gamma > \gamma_r. \end{cases} \quad (3.15)$$

It is worth noting that a different channel angle γ will require a different $\mathbf{F}_{r,2}$. Therefore, we need to store the values of the precoders and conduct table look-up operations in real-time applications. The free distance provided by $\mathbf{F}_{r,1}$ is given by:

$$d_{\text{free}, \mathbf{F}_{r,1}} = \sqrt{P_T \rho^2 \frac{4}{K} \cos^2 \gamma \sin^2 \theta_{r,1}}. \quad (3.16)$$

On the other hand, obtaining the corresponding free distance for $\mathbf{F}_{r,2}$ requires table look-ups since $\mathbf{F}_{r,2}$ in (3.15) does not have a closed-form expression.

§ 3.2.3 Orthogonal Subprecoder Design

The rotation matrix, which is an orthogonal matrix, can be used as the subprecoder also [29].

Let \mathbf{F}_o denote the subprecoder. Then,

$$\mathbf{F}_o = \sqrt{\frac{P_T}{2}} \begin{bmatrix} \cos \theta_o & \sin \theta_o \\ -\sin \theta_o & \cos \theta_o \end{bmatrix}. \quad (3.17)$$

It is simple to see that \mathbf{F}_o is derived by further simplifying the structure of \mathbf{F}_r in (3.14). Let $\beta = \frac{1}{\tan \gamma}$. The optimum θ_o for 4-QAM was found with a closed-form as [29]:

$$\theta_o = \begin{cases} \tan^{-1} ((\beta^2 - 1) - \sqrt{1 - 2\beta}) & \text{for } \beta > \sqrt{3} \\ \frac{\pi}{4} & \text{for } \beta \leq \sqrt{3}. \end{cases} \quad (3.18)$$

From (3.18), we can observe that the orthogonal subprecoder always uses both subchannels since \mathbf{F}_o is a full-rank matrix. This structure constraint will lead to performance loss when γ is small. Besides, the closed-form solution in (3.18) exists only for 4-QAM. In other words, finding the optimum rotation angle for $L > 4$ requires a numerical search too.

§ 3.3 Proposed Subprecoders for MIMO Systems

As discussed, existing subprecoder designs require either numerical searches or look-up tables stored. In this section, we propose a design giving simple closed-form expressions for any QAM sizes. To do that, we consider an alternative design criterion in (3.7). Instead of maximizing the free distance itself, we propose maximizing a lower bound.

Considering the QRD of a full column-rank matrix \mathbf{H} , we can have $\mathbf{H} = \mathbf{Q}\mathbf{R}$, where \mathbf{Q} is an $N_r \times N_t$ column-wise orthonormal matrix and \mathbf{R} is an $N_t \times N_t$ upper-triangular matrix with positive real-valued diagonal entries. As mentioned in Chapter 2, the free distance can be lower bounded by

$$d_{\text{free}} \geq \left(\min_{1 \leq i \leq N_t} \mathbf{R}(i, i) \right) d_{\min}(\mathcal{X}^M) \quad (3.19)$$

where $\mathbf{R}(i, j)$ denotes the (i, j) th entry of \mathbf{R} . Note that \mathbf{R} is also known as the R-factor of \mathbf{H} . Clearly, the lower bound in (3.19) is maximized when the R-factor has equal diagonal entries. This problem can be solved by GMD. From [9, 10], we can have the following decomposition of \mathbf{H} as

$$\mathbf{H} = \tilde{\mathbf{Q}}\tilde{\mathbf{R}}\mathbf{P}^H \quad (3.20)$$

where $\tilde{\mathbf{Q}}$ is an $N_r \times N_t$ column-wise orthonormal matrix, \mathbf{P} is an $N_t \times N_t$ unitary matrix, and $\tilde{\mathbf{R}}$ is an $N_t \times N_t$ upper-triangular matrix having equal diagonal entries given by

$$\tilde{\mathbf{R}}(i, i) = \left(\prod_{k=1}^{N_t} \tilde{\mathbf{R}}(k, k) \right)^{\frac{1}{N_t}} = \left(\prod_{n=1}^{N_t} \lambda_n \right)^{\frac{1}{N_t}} \quad \text{for } i = 1, 2, \dots, N_t. \quad (3.21)$$

It can be seen that \mathbf{P} can be used as a precoder and $\tilde{\mathbf{Q}}^H \mathbf{H} \mathbf{P}$ will have equal diagonal entries. Note that \mathbf{P} is independent of the QAM constellation, which is a great advantage when designing the precoder for ML detection. Although the GMD method is analytically tractable, its corresponding free distance will be significantly degraded for ill-conditioned channels. To enhance the performance, we can replace \mathbf{P} with the rank-deficient precoder when the value of γ is small.

§ 3.3.1 GMD-Based Subprecoder with Rank-Deficiency

From (3.20), we can have the subprecoder \mathbf{F}_{GMD} expressed as $\mathbf{F}_{\text{GMD}} = \sqrt{\frac{P_T}{2}} \mathbf{P}$. Note that for $M = 2$, \mathbf{F}_{GMD} has a simple expression as

$$\mathbf{F}_{\text{GMD}} = \sqrt{\frac{P_T}{2}} \begin{bmatrix} \sqrt{\frac{\lambda_2}{\lambda_1 + \lambda_2}} & -\sqrt{\frac{\lambda_1}{\lambda_1 + \lambda_2}} \\ \sqrt{\frac{\lambda_1}{\lambda_1 + \lambda_2}} & \sqrt{\frac{\lambda_2}{\lambda_1 + \lambda_2}} \end{bmatrix}. \quad (3.22)$$

Furthermore, the resultant free distance can also be easily obtained by

$$d_{\text{free,GMD}} = \sqrt{P_T \rho^2 \frac{4 \cos \gamma \sin \gamma}{K}}. \quad (3.23)$$

From (3.23), we can see that $d_{\text{free,GMD}} \approx 0$ as γ approaches zero. Note that γ is associated with the condition number of the channel matrix. In other words, the performance of \mathbf{F}_{GMD}

can be significantly degraded for ill-conditioned channels. This degradation can be mitigated by replacing \mathbf{F}_{GMD} with the rank-deficient subprecoder when the value of γ is small. Thus, we propose a subprecoder combining \mathbf{F}_{GMD} with the rank-deficient subprecoder in (3.10), i.e., $\mathbf{F}_{c,1}$, expressed as:

$$\mathbf{F}_{p,1} = \begin{cases} \sqrt{P_T} \begin{bmatrix} \cos \theta_{c,1} & \sin \theta_{c,1} e^{j\varphi_{c,1}} \\ 0 & 0 \end{bmatrix} & \text{for } \gamma \leq \gamma_1 \\ \sqrt{\frac{P_T}{2}} \begin{bmatrix} \sqrt{\frac{\lambda_2}{\lambda_1 + \lambda_2}} & -\sqrt{\frac{\lambda_1}{\lambda_1 + \lambda_2}} \\ \sqrt{\frac{\lambda_1}{\lambda_1 + \lambda_2}} & \sqrt{\frac{\lambda_2}{\lambda_1 + \lambda_2}} \end{bmatrix} & \text{for } \gamma > \gamma_1. \end{cases} \quad (3.24)$$

The threshold γ_1 can be derived by the channel angle satisfying the following equation:

$$\sqrt{P_T \rho^2 \frac{4 \cos \gamma \sin \gamma}{K}} = \sqrt{P_T \rho^2 \frac{4 \cos^2 \gamma}{N^2 + \sqrt{3}N + 2}}. \quad (3.25)$$

We can then have γ_1 as

$$\gamma_1 = \tan^{-1} \left(\frac{2}{N^2 + \sqrt{3}N + 2} \right). \quad (3.26)$$

Besides, we can also combine \mathbf{F}_{GMD} with the rank-deficient subprecoder in (3.15), i.e., $\mathbf{F}_{r,1}$, yielding an alternative subprecoder as:

$$\mathbf{F}_{p,2} = \begin{cases} \sqrt{P_T} \begin{bmatrix} \cos \theta_{r,1} & -\sin \theta_{r,1} \\ 0 & 0 \end{bmatrix} & \text{for } \gamma \leq \gamma_2 \\ \sqrt{\frac{P_T}{2}} \begin{bmatrix} \sqrt{\frac{\lambda_2}{\lambda_1 + \lambda_2}} & -\sqrt{\frac{\lambda_1}{\lambda_1 + \lambda_2}} \\ \sqrt{\frac{\lambda_1}{\lambda_1 + \lambda_2}} & \sqrt{\frac{\lambda_2}{\lambda_1 + \lambda_2}} \end{bmatrix} & \text{for } \gamma > \gamma_2. \end{cases} \quad (3.27)$$

Using the same method as that in (3.25), we can derive the threshold γ_2 as

$$\gamma_2 = \tan^{-1} \left(2 \sin^2 \left(\tan^{-1} \frac{1}{2^l} \right) \right). \quad (3.28)$$

From (3.24) and (3.27), we can see that both $\mathbf{F}_{p,1}$ and $\mathbf{F}_{p,2}$ give closed-form expressions. Thus, no look-up tables are required.

§ 3.3.2 Extension to MIMO Systems for $M > 2$

For a MIMO system with $M > 2$, the X-structured precoder allows a simple solution for the ML receiver. Assuming M is even, then every two subchannels can be paired to yield $\frac{M}{2}$ subsystems. Therefore, the 2×2 subprecoders discussed in the previous subsections can be directly applied. Let the subchannels be ordered with respect to their singular values. Then, the X-structured precoder pairs the i th and $(M - i + 1)$ th subchannels, and the corresponding channel gain and channel angle can be expressed as

$$\begin{cases} \rho_i &= \sqrt{\lambda_i^2 + \lambda_{M-i+1}^2} \\ \gamma_i &= \tan^{-1} \left(\frac{\lambda_{M-i+1}}{\lambda_i} \right). \end{cases} \quad (3.29)$$

Using γ_i , we can construct the resultant subprecoder $\mathbf{F}_{p,(i)}$ for the i th subsystem. Let each subprecoder be under unit-power constraint, i.e., $\text{tr} \left\{ \mathbf{F}_{p,(i)}^H \mathbf{F}_{p,(i)} \right\} = 1$. Also let $d_{\text{free},i}$ denote the free distance provided by the i th subsystem. Clearly, the overall system performance is dominated by the subsystem with $d_{\text{free},\min}$, where $d_{\text{free},\min}$ is the minimum value among all $d_{\text{free},i}$'s. Hence, we can adopt a power allocation scheme aiming to maximize $d_{\text{free},\min}$ so that the performance can be further enhanced. Let Υ_i denote the power allocated on the i th subsystem, and M' denote number of subsystems. Similar to the method used in [28], the problem of finding the optimum power allocation matrix, denoted by Υ , can be formulated as:

$$\begin{aligned} & \max_{\Upsilon} \min_i \Upsilon_i d_{\text{free},i} \\ & s.t. \quad \sum_{i=1}^{M'} \Upsilon_i^2 = P_T. \end{aligned} \quad (3.30)$$

The solution of (3.30) is given by [28]:

$$\Upsilon_i^2 = P_T \left(d_{\text{free},i}^2 \sum_{k=1}^{M'} \frac{1}{d_{\text{free},k}^2} \right)^{-1} \quad \text{for } i = 1, 2, \dots, M'. \quad (3.31)$$

Using (3.31), we can find the resultant free distance of the each subsystem is equal to $\Upsilon_i d_{\text{free},i}$ expressed as:

$$\Upsilon_i d_{\text{free},i} = \sqrt{P_T \left(\sum_{k=1}^{M'} \frac{1}{d_{\text{free},k}^2} \right)^{-1}}. \quad (3.32)$$

As we can see, the optimum Υ is to equalize the free distance among all subsystems. That means the subsystem with smaller free distance will be allocated higher transmit power. It can be easily verified that $\Upsilon_i d_{\text{free},i} \geq d_{\text{free},\min}$, and hence the performance is improved. With Υ_i , the resultant precoder is still of X-structure. For example, the X-structured precoder \mathbf{F} with proposed subprecoder $\mathbf{F}_{p,1,(i)}$ and Υ for $M = 4$ can be expressed as

$$\mathbf{F} = \begin{bmatrix} \Upsilon_1 \mathbf{F}_{p,1,(1)}(1,1) & 0 & 0 & \Upsilon_1 \mathbf{F}_{p,1,(1)}(1,2) \\ 0 & \Upsilon_2 \mathbf{F}_{p,1,(2)}(1,1) & \Upsilon_2 \mathbf{F}_{p,1,(2)}(1,2) & 0 \\ 0 & \Upsilon_2 \mathbf{F}_{p,1,(2)}(2,1) & \Upsilon_2 \mathbf{F}_{p,1,(2)}(2,2) & 0 \\ \Upsilon_1 \mathbf{F}_{p,1,(1)}(2,1) & 0 & 0 & \Upsilon_1 \mathbf{F}_{p,1,(1)}(2,2) \end{bmatrix}. \quad (3.33)$$

If M is odd, the $(\frac{M+1}{2})$ th symbol is then independently precoded and detected without coupling another symbol. Note that computing Υ_i requires the information of $d_{\text{free},i}$. For this regard, the proposed precoders are more efficient since the free distance can be easily calculated.

§ 3.3.3 Complexity Comparisons

Similar to Chapter 2, we use the number of floating operations (FLOPS) required in a precoding scheme as the measure for computational complexity. The complexity for conducting the SVD of \mathbf{H} is $\mathcal{O}(N_r^2 N_t + N_t^2 N_r)$, that for calculating \mathbf{M} is $\mathcal{O}(N_t M)$ FLOPS, and that of calculating \mathbf{r} is $\mathcal{O}(N_r^2)$ FLOPS. The above operations are involved in all the methods. Note that both the orthogonal and real-valued precoders need look-up tables in their applications. This is an additional overhead which is not required for proposed precoders. The precoding complexity comparison is summarized in Table 3.1.

Next, we compare the ML-detection complexity in each method. It has been shown in [30] that the ML-detection complexity in any subsystem with the complex-valued precoder is a function of $\mathcal{O}(L\sqrt{L})$. The detection complexity can be reduced to $\mathcal{O}(\sqrt{L})$ when the precoder consists of real values [30]. Thus, the ML-detection complexity associated with $\mathbf{F}_{p,1}$ is higher than that with $\mathbf{F}_{p,2}$. Fortunately, the probability of $\gamma \leq \gamma_1$ decreases for large values of L . Therefore, the detection complexity corresponding to $\mathbf{F}_{p,1}$ can also be $\mathcal{O}(\sqrt{L})$ for higher QAM constellations. The detection complexity comparisons for all precoders is summarized in Table 3.2.

§ 3.4 Joint Precoders Design for MIMO Relay Systems

In this section, we will consider the precoder design in two-hop AF MIMO relay systems. Similar to the conventional MIMO system, we can conduct precoding at both the source and relay nodes. These two precoders can be jointly optimized for further performance enhancement. Note that the ML receiver is used at the destination.

§ 3.4.1 Problem Formulation and Source Precoder Design

The system model we consider is shown in Figure 3.2. Let \mathbf{H}_{SR} denote the $N_{re} \times N_s$ source-to-relay channel matrix and \mathbf{H}_{RD} denote the $N_d \times N_{re}$ relay-to-destination channel matrix. In the AF MIMO relay scheme, the signal transmission is divided into two phases. In Phase I, \mathbf{x} is transmitted from the source and then received at the relay. Note that in a two-hop system, the destination cannot receive the signal from the source in Phase I. Let \mathbf{F}_S denote the $N_s \times M$ source precoding matrix. The received signal at the relay can then be expressed as

$$\mathbf{y}_R = \mathbf{H}_{SR}\mathbf{F}_S \mathbf{x} + \mathbf{n}_R. \quad (3.34)$$

where \mathbf{n}_R is the Gaussian noise vector with the covariance matrix $\sigma_{n,r}^2 \mathbf{I}_{N_{re}}$. In Phase II, \mathbf{y}_R is first left-multiplied by the $N_{re} \times N_{re}$ relay precoding matrix \mathbf{F}_R and then retransmitted to the

destination through \mathbf{H}_{RD} . The received signal at the destination can be expressed as

$$\mathbf{y}_D = \mathbf{H}_{RD} \mathbf{F}_R \mathbf{H}_{SR} \mathbf{F}_S \mathbf{x} + \mathbf{H}_{RD} \mathbf{F}_R \mathbf{n}_R + \mathbf{n}_D. \quad (3.35)$$

where \mathbf{n}_D is the Gaussian noise vector with the covariance matrix $\sigma_{n,d}^2 \mathbf{I}_{N_d}$. The received signal can be rewritten as

$$\mathbf{y}_D = \mathbf{H} \mathbf{F}_S \mathbf{x} + \mathbf{n} \quad (3.36)$$

where $\mathbf{H} = \mathbf{H}_{RD} \mathbf{F}_R \mathbf{H}_{SR}$ and $\mathbf{n} = \mathbf{H}_{RD} \mathbf{F}_R \mathbf{n}_R + \mathbf{n}_D$. It is simple to see that \mathbf{n} is not white and the covariance matrix of \mathbf{n} can be found as

$$\begin{aligned} \mathbf{R}_n &= \mathbb{E}[\mathbf{n}\mathbf{n}^H] \\ &= \sigma_{n,r}^2 \mathbf{H}_{RD} \mathbf{F}_R \mathbf{F}_R^H \mathbf{H}_{RD}^H + \sigma_{n,d}^2 \mathbf{I}_{N_d}. \end{aligned} \quad (3.37)$$

To facilitate our derivation, we first conduct a whitening processing on \mathbf{y}_D . From (3.37), we can have the whitening matrix, denoted by \mathbf{W} , as

$$\mathbf{W} = (\sigma_{n,r}^2 \mathbf{H}_{RD} \mathbf{F}_R \mathbf{F}_R^H \mathbf{H}_{RD}^H + \sigma_{n,d}^2 \mathbf{I}_{N_d})^{-\frac{1}{2}}. \quad (3.38)$$

After whitening, the received signal can be rewritten as

$$\tilde{\mathbf{y}}_D \triangleq \mathbf{W} \mathbf{y}_D = \tilde{\mathbf{H}} \mathbf{F}_S \mathbf{x} + \tilde{\mathbf{n}} \quad (3.39)$$

where $\tilde{\mathbf{H}} = \mathbf{W} \mathbf{H}$ is the $N_d \times N_s$ equivalent channel matrix expressed as

$$\tilde{\mathbf{H}} = (\sigma_{n,r}^2 \mathbf{H}_{RD} \mathbf{F}_R \mathbf{F}_R^H \mathbf{H}_{RD}^H + \sigma_{n,d}^2 \mathbf{I}_{N_d})^{-\frac{1}{2}} \mathbf{H}_{RD} \mathbf{F}_R \mathbf{H}_{SR}. \quad (3.40)$$

The free distance corresponding to $\tilde{\mathbf{H}}$ can be defined as

$$d_{\text{free}} = \min_{\mathbf{x}_i, \mathbf{x}_j \in \mathcal{X}^M, \mathbf{x}_i \neq \mathbf{x}_j} \left\| \tilde{\mathbf{H}} \mathbf{F}_S (\mathbf{x}_i - \mathbf{x}_j) \right\|. \quad (3.41)$$

Therefore, the objective now is to find the precoders, \mathbf{F}_S and \mathbf{F}_R , so that the free distance can be maximized. The optimization problem can be formulated as:

$$\begin{aligned}
& \max_{\mathbf{F}_S, \mathbf{F}_R} d_{\text{free}} \\
& s.t. \\
& \mathbf{C}_1 : \text{tr} \{ \mathbf{F}_S \mathbf{F}_S^H \} = P_{S,T} \\
& \mathbf{C}_2 : \text{tr} \{ \mathbf{F}_R (\sigma_{n,r}^2 \mathbf{I}_{N_{r_e}} + \mathbf{H}_{SR} \mathbf{F}_S \mathbf{F}_S^H \mathbf{H}_{SR}^H) \mathbf{F}_R^H \} = P_{R,T}
\end{aligned} \tag{3.42}$$

where \mathbf{C}_1 and \mathbf{C}_2 represent the transmit power constraints at the source and relay respectively. As we can see, solving the problem in (3.42) is complicated since d_{free} is a nonlinear and complicated function of \mathbf{F}_S and \mathbf{F}_R . Also, both precoders are coupled in the constraint \mathbf{C}_2 . As a result, the optimum solution is difficult to find. To solve the problem, we propose an iterative method solving \mathbf{F}_S and \mathbf{F}_R alternatively. Using the approach, we can first rewrite the original problem in (3.42) as:

$$\begin{aligned}
& \max_{\mathbf{F}_S, \mathbf{F}_R} d_{\text{free}} = \max_{\mathbf{F}_R} \max_{\mathbf{F}_S} d_{\text{free}} \\
& s.t. \quad \mathbf{C}_1 \text{ and } \mathbf{C}_2.
\end{aligned} \tag{3.43}$$

Let \mathbf{F}_R be given and we have the optimization as:

$$\begin{aligned}
& \max_{\mathbf{F}_S} \min_{\mathbf{x}_i, \mathbf{x}_j \in \mathcal{X}^M, \mathbf{x}_i \neq \mathbf{x}_j} \left\| \tilde{\mathbf{H}} \mathbf{F}_S (\mathbf{x}_i - \mathbf{x}_j) \right\| \\
& s.t. \quad \text{tr} \{ \mathbf{F}_S \mathbf{F}_S^H \} = P_{S,T}.
\end{aligned} \tag{3.44}$$

It is easy to see that (3.44) is similar to a MIMO precoder design problem. Consider the following SVDs:

$$\mathbf{H}_{RD} = \mathbf{U}_{RD} \mathbf{\Sigma}_{RD} \mathbf{V}_{RD}^H \tag{3.45}$$

$$\mathbf{H}_{SR} = \mathbf{U}_{SR} \mathbf{\Sigma}_{SR} \mathbf{V}_{RD}^H \tag{3.46}$$

where \mathbf{U}_{RD} , \mathbf{V}_{RD}^H , \mathbf{U}_{SR} , and \mathbf{V}_{SR}^H are column-wise orthonormal matrices, both $\mathbf{\Sigma}_{SR}$ and $\mathbf{\Sigma}_{RD}$ are $M \times M$ diagonal matrices, and $\mathbf{U}_{RD}^H \mathbf{U}_{RD} = \mathbf{U}_{SR}^H \mathbf{U}_{SR} = \mathbf{V}_{RD}^H \mathbf{V}_{RD} = \mathbf{V}_{SR}^H \mathbf{V}_{SR} = \mathbf{I}_M$.

We can let \mathbf{F}_S have the form as:

$$\mathbf{F}_S = \mathbf{V}_{SR}\mathbf{F}'_S. \quad (3.47)$$

With (3.47), we can further rewrite the received signal $\tilde{\mathbf{y}}_D$ as

$$\tilde{\mathbf{y}}_D = \tilde{\mathbf{H}}\mathbf{V}_{SR}\mathbf{F}'_S\mathbf{x} + \tilde{\mathbf{n}} = \tilde{\mathbf{H}}'\mathbf{F}'_S\mathbf{x} + \tilde{\mathbf{n}} \quad (3.48)$$

where $\tilde{\mathbf{H}}' = \tilde{\mathbf{H}}\mathbf{V}_{SR}$ expressed by

$$\tilde{\mathbf{H}}' = (\sigma_{n,r}^2 \mathbf{H}_{RD}\mathbf{F}_R\mathbf{F}_R^H\mathbf{H}_{RD}^H + \sigma_{n,d}^2 \mathbf{I}_{N_d})^{-1/2} \mathbf{H}_{RD}\mathbf{F}_R\mathbf{U}_{SR}\boldsymbol{\Sigma}_{SR}. \quad (3.49)$$

Let $\tilde{\boldsymbol{\Sigma}}'$ denote the matrix with the singular values of $\tilde{\mathbf{H}}'$. With $\tilde{\boldsymbol{\Sigma}}'$, we can solve \mathbf{F}'_S by applying the methods proposed in Section 3.3. For a given \mathbf{F}_S , however, the solution of \mathbf{F}_R is much more involved. This problem is investigated in the next subsection.

§ 3.4.2 Relay Precoder Design

From (3.49), we first observe that $\tilde{\mathbf{H}}'$ is still a nonlinear and complicated function of \mathbf{F}_R and finding the optimum \mathbf{F}_R is a difficult work. Even the optimum solution can be found, we have to conduct a new SVD and matrix inversion when solving \mathbf{F}_S at each iteration. This will greatly increase the computational complexity of the problem. To overcome these problems, we propose imposing a special structure on \mathbf{F}_R such that the X-structure of \mathbf{F}_S can be maintained and at the same time \mathbf{F}_R can be solved with a closed-form solution. The main idea is to let \mathbf{F}_R diagonalize the equivalent channel $\tilde{\mathbf{H}}'$. This can be easily accomplished by choosing \mathbf{F}_R as

$$\mathbf{F}_R = \mathbf{V}_{RD}\boldsymbol{\Sigma}_R\mathbf{U}_{SR}^H \quad (3.50)$$

where $\boldsymbol{\Sigma}_R$ is an $M \times M$ diagonal matrix needs to be designed. With (3.50), we can rewrite $\mathbf{R}_{\tilde{\mathbf{n}}}$ as

$$\mathbf{R}_{\tilde{\mathbf{n}}} = \sigma_{n,r}^2 \mathbf{U}_{RD}\boldsymbol{\Sigma}_{RD}\boldsymbol{\Sigma}_R\boldsymbol{\Sigma}_R^H\boldsymbol{\Sigma}_{RD}^H\mathbf{U}_{RD}^H + \sigma_{n,d}^2 \mathbf{I}_{N_d}. \quad (3.51)$$

Hence, we can rewrite the whitening matrix \mathbf{W} as follows:

$$\begin{aligned}
\mathbf{W} &= \mathbf{R}_{\tilde{n}}^{-\frac{1}{2}} \\
&= \left(\mathbf{U}_{RD} \left(\sigma_{n,r}^2 \boldsymbol{\Sigma}_{RD} \boldsymbol{\Sigma}_R \boldsymbol{\Sigma}_R^H \boldsymbol{\Sigma}_{RD}^H + \sigma_{n,d}^2 \mathbf{I}_M \right) \mathbf{U}_{RD}^H \right)^{-\frac{1}{2}} \\
&= \left(\sigma_{n,r}^2 \boldsymbol{\Sigma}_{RD} \boldsymbol{\Sigma}_R \boldsymbol{\Sigma}_R^H \boldsymbol{\Sigma}_{RD}^H + \sigma_{n,d}^2 \mathbf{I}_M \right)^{-\frac{1}{2}} \mathbf{U}_{RD}^H.
\end{aligned} \tag{3.52}$$

With (3.50) and (3.52), the resultant $\tilde{\mathbf{H}}'$ is an $M \times M$ diagonal matrix expressed as

$$\tilde{\mathbf{H}}' = \left(\sigma_{n,r}^2 \boldsymbol{\Sigma}_{RD} \boldsymbol{\Sigma}_R \boldsymbol{\Sigma}_R^H \boldsymbol{\Sigma}_{RD}^H + \sigma_{n,d}^2 \mathbf{I}_M \right)^{-1/2} \boldsymbol{\Sigma}_{RD} \boldsymbol{\Sigma}_R \boldsymbol{\Sigma}_{SR}. \tag{3.53}$$

Thus, $\tilde{\mathbf{H}}'$ in (3.53) is diagonal and can be directly used for constructing \mathbf{F}'_S without extra SVD and matrix inversion operations. In addition, the relay precoder to be determined is reduced to a diagonal matrix $\boldsymbol{\Sigma}_R$. This can significantly reduce the computational complexity of the joint design.

Let $P_{e,i}$ denote the BLER of the i th subsystem. We can have the overall P_e expressed as

$$P_e = 1 - \prod_{i=1}^{M'} (1 - P_{e,i}) \approx \sum_{i=1}^{M'} P_{e,i} \tag{3.54}$$

where M' is the number of subsystems. As discussed, $P_{e,i}$ is dominated by $P_{w,i}$, where $P_{w,i}$ denotes the worst-case PEP of the i th subsystem. Note that $P_{w,i} = Q \left(\sqrt{\frac{d_{\text{free},i}^2}{2}} \right)$ since $\sigma_{\tilde{n}}^2 = 1$ due to the whitening matrix in (3.52). Then, we define P_w as

$$P_w = \sum_{i=1}^{M'} Q \left(\sqrt{\frac{d_{\text{free},i}^2}{2}} \right). \tag{3.55}$$

As seen from (3.54) and (3.55), minimizing P_e can be equivalent to minimizing P_w . Hence, the design criterion for $\boldsymbol{\Sigma}_R$ is equivalent to minimizing (3.55). Based on the Chernoff bound, we can have an approximate of $Q(x)$ as $Q(x) \approx \frac{1}{a} \exp^{-\frac{x^2}{2}}$, where a is a positive value. Consequently, P_w can be approximately expressed as

$$P_w \approx \frac{1}{a} \sum_{i=1}^{M'} \exp^{-\frac{d_{\text{free},i}^2}{4}}. \tag{3.56}$$

Since directly minimizing P_w is difficult, we then seek a lower bound from which our optimization can be conducted.

Proposition 3.1: Given the full-rank \mathbf{F}'_S , the relay precoder in (3.50), and the channel matrix in (3.53), maximizing $\det(\tilde{\mathbf{H}}'\tilde{\mathbf{H}}'^H)$ is equivalent to minimizing a lower bound of P_w . The lower bound is equal to $M' \exp^{-\frac{1}{4}(\prod_{i=1}^{M'} d_{\text{free},i}^2)^{\frac{1}{M'}}$, where M' is the number of the subsystems.

Proof: To prove the proposition, we need following lemmas.

Lemma 3.1: Let w_1 and w_2 be two positive values satisfying $w_1 + w_2 = 1$ and consider two positive values x and y . If $y \geq x \geq 1$, then the following inequality is held:

$$\exp^{-x^{w_1}y^{w_2}} \leq w_1 \exp^{-x} + w_2 \exp^{-y}. \quad (3.57)$$

Proof: The proof of the lemma is provided in Appendix B.1.

With Lemma 3.1, we can then derive another lemma.

Lemma 3.2: Assume that \mathbf{F}'_S , Σ_{SR} and Σ_{RD} are given. Then, $\sum_{i=1}^{M'} \exp^{-\frac{d_{\text{free},i}^2}{4}}$ in (3.56) is lower bounded as:

$$\sum_{i=1}^{M'} \exp^{-\frac{d_{\text{free},i}^2}{4}} \geq M' \exp^{-\frac{1}{4}(\prod_{i=1}^{M'} d_{\text{free},i}^2)^{\frac{1}{M'}}}. \quad (3.58)$$

Proof: The proof of the lemma is provided in Appendix B.2.

Note that the equality in (3.58) is held when $d_{\text{free},i}^2$'s are equal for all $i = 1, 2, \dots, M'$. In X-structured \mathbf{F}'_S , the i th and $(M - i + 1)$ th subchannels are paired together. Therefore, all $d_{\text{free},i}^2$'s will be close. This property further demonstrates the tightness of the lower bound in (3.58). To proceed, without loss of generality, we can first consider the system with a full-rank \mathbf{F}'_S . In this case, $d_{\text{free},i}^2$ can be expressed by $d_{\text{free},i}^2 = \epsilon \tilde{\mathbf{H}}'(i, i) \tilde{\mathbf{H}}'(M - i + 1, M - i + 1)$ for all $i = 1, 2, \dots, M'$. Then, we have

$$\prod_{i=1}^{M'} d_{\text{free},i}^2 = \epsilon^{M'} \sqrt{\det(\tilde{\mathbf{H}}'\tilde{\mathbf{H}}'^H)}. \quad (3.59)$$

Since ϵ is a constant, we then come to the conclusion that minimizing the lower bound in (3.58) is equivalent to maximizing $\det(\tilde{\mathbf{H}}'\tilde{\mathbf{H}}'^H)$.

Using the fact that the arithmetic mean is greater than or equal to the geometric mean, we can easily derive another lower bound for the left-hand side of (3.58) as:

$$\sum_{i=1}^{M'} \exp^{-\frac{d_{\text{free},i}^2}{4}} \geq M' \exp^{-\frac{1}{4} \left(\frac{1}{M'} \sum_{i=1}^{M'} d_{\text{free},i}^2 \right)}. \quad (3.60)$$

The following lemma compares the lower bound in (3.58) and that in (3.60).

Lemma 3.3: The lower bound in (3.58) is tighter than that in (3.60).

Proof: First, using the fact that the arithmetic mean is greater than or equal to the geometric mean, we can prove (3.60) as follows:

$$\begin{aligned} \sum_{i=1}^{M'} \exp^{-\frac{d_{\text{free},i}^2}{4}} &\geq M' \left(\prod_{i=1}^{M'} \exp^{-\frac{d_{\text{free},i}^2}{4}} \right)^{\frac{1}{M'}} \\ &= M' \left(\exp^{-\frac{1}{4} \sum_{i=1}^{M'} d_{\text{free},i}^2} \right)^{\frac{1}{M'}} \\ &= M' \exp^{-\frac{1}{4} \left(\frac{1}{M'} \sum_{i=1}^{M'} d_{\text{free},i}^2 \right)}. \end{aligned} \quad (3.61)$$

Second, using the fact again, we can obtain

$$\left(\prod_{i=1}^{M'} d_{\text{free},i}^2 \right)^{\frac{1}{M'}} \leq \frac{1}{M'} \sum_{i=1}^{M'} d_{\text{free},i}^2. \quad (3.62)$$

From (3.61) and (3.62), we then have

$$\begin{aligned} \sum_{i=1}^{M'} \exp^{-\frac{d_{\text{free},i}^2}{4}} &\geq M' \exp^{-\frac{1}{4} \left(\prod_{i=1}^{M'} d_{\text{free},i}^2 \right)^{\frac{1}{M'}}} \\ &\geq M' \exp^{-\frac{1}{4} \left(\frac{1}{M'} \sum_{i=1}^{M'} d_{\text{free},i}^2 \right)}. \end{aligned} \quad (3.63)$$

Note that the result in Proposition 3.1 is valid only for the proposed subprecoders with which the properties of the GMD solution in Proposition 3.1 can be applied. For other subprecoders, (3.59) may not be held and finding a solution for the precoders will become much more complicated. For Lemma 3.2 to apply, both x and y have to be greater than one. This translates to the BLER of the subsystem (in Proposition 3.1) must be less than 10^{-1} which is usually satisfied

in real-world applications. It is worth noting that $\left(\prod_{i=1}^{M'} d_{\text{free},i}^2\right)^{\frac{1}{M'}}$ in (3.58) can be seen as a geometric free distance of the MIMO relay system, and it can be used to evaluate P_w . It is interesting to note that this is similar to the geometric SNR in multicarrier systems [58]. However, the geometric SNR is derived from the maximization of the channel capacity. Instead, the geometric free distance we derived here is to minimize the BLER. To proceed, let r denote the rank of \mathbf{F}'_S . We first solve Σ_R by assuming $r = M$. From (3.53), we have

$$\tilde{\mathbf{H}}\tilde{\mathbf{H}}'^H = \Sigma_{SR}^H \Sigma_R^H \Sigma_{RD}^H (\sigma_{n,r}^2 \Sigma_{RD} \Sigma_R \Sigma_{SR}^H \Sigma_{RD}^H + \sigma_{n,d}^2 \mathbf{I}_M)^{-1} \Sigma_{RD} \Sigma_R \Sigma_{SR}. \quad (3.64)$$

Defining $\mathbf{A} = \Sigma_{RD} \Sigma_R \Sigma_{SR}^H \Sigma_{RD}^H$, we can rewrite $\det(\tilde{\mathbf{H}}\tilde{\mathbf{H}}'^H)$ as:

$$\begin{aligned} \det(\tilde{\mathbf{H}}\tilde{\mathbf{H}}'^H) &= \det\left(\Sigma_{SR} \Sigma_{SR}^H \mathbf{A} (\sigma_{n,r}^2 \mathbf{A} + \sigma_{n,d}^2 \mathbf{I}_M)^{-1}\right) \\ &= \det(\Sigma_{SR} \Sigma_{SR}^H) \det\left(\mathbf{A} (\sigma_{n,r}^2 \mathbf{A} + \sigma_{n,d}^2 \mathbf{I}_M)^{-1}\right). \end{aligned} \quad (3.65)$$

Since $\det(\Sigma_{SR} \Sigma_{SR}^H)$ in (3.65) is independent of the relay precoder, the relay precoder can then be solved through the following optimization:

$$\begin{aligned} &\max_{\Sigma_R} \det\left(\mathbf{A} (\sigma_{n,r}^2 \mathbf{A} + \sigma_{n,d}^2 \mathbf{I}_M)^{-1}\right) \\ &s.t. \\ &tr\left\{\sigma_{n,r}^2 \Sigma_R \Sigma_R^H + \Sigma_R \Sigma_{SR} \mathbf{F}'_S \mathbf{F}'_S{}^H \Sigma_{SR}^H \Sigma_R^H\right\} = P_{R,T}. \end{aligned} \quad (3.66)$$

Let $\mathbf{B} = \mathbf{F}'_S \mathbf{F}'_S{}^H$. Also let $\sigma_{R,i}$, $\sigma_{sr,i}$, and $\sigma_{rd,i}$ be the i th diagonal entry of Σ_R , Σ_{SR} , and Σ_{RD} respectively. Taking \ln operation, we can reformulate (3.66) as:

$$\begin{aligned} &\min_{\sigma_{R,i}^2} - \sum_{i=1}^M \ln\left(\frac{\sigma_{R,i}^2 \sigma_{rd,i}^2}{\sigma_{R,i}^2 \sigma_{rd,i}^2 \sigma_{n,r}^2 + \sigma_{n,d}^2}\right) \\ &s.t. \\ &\sum_{i=1}^M \sigma_{R,i}^2 (\sigma_{n,r}^2 + \mathbf{B}(i,i) \sigma_{sr,i}^2) = P_{R,T}. \end{aligned} \quad (3.67)$$

We can see that the relay precoder design problem has been transformed into a scalar-valued optimization problem. The reformulated problem in (3.67) can be solved by using the KKT

conditions [45]. The solution is then expressed in the closed-form as

$$\sigma_{R,i}^2 = \sqrt{\frac{\mu\sigma_{n,d}^2}{\sigma_{rd,i}^2\sigma_{n,r}^2 (\sigma_{n,r}^2 + \mathbf{B}(i,i)\sigma_{sr,i}^2)} + \left(\frac{\sigma_{n,d}^2}{2\sigma_{rd,i}^2\sigma_{n,r}^2}\right)^2} - \frac{\sigma_{n,d}^2}{2\sigma_{rd,i}^2\sigma_{n,r}^2} \quad (3.68)$$

where μ is chosen to satisfy the relay power constraint. The derivation of (3.68) can be found in Appendix B.3. As we can see, the proposed subprecoder does lead to a simple expression of Σ_R .

As seen from (3.68), we have to know \mathbf{B} to solve the relay precoder. To simplify the problem, we first do not consider the source power allocation. Thus, \mathbf{B} can be expressed as

$$\mathbf{B}(i,i) = \frac{P_{S,T}}{M} \quad \text{for } i = 1, 2, \dots, M. \quad (3.69)$$

Using the resultant Σ_R and $\tilde{\mathbf{H}}'$, the next step is to construct \mathbf{F}'_S with the methods proposed in Section 3.3. If the channel angles of all subsystems are larger than the angle threshold, r is still equal to M . From the structure of \mathbf{B} , we can see that its diagonals are unchanged. In other words, Σ_R will not be changed by the updated \mathbf{F}'_S . Then, the iteration stops in just one iteration. On the other hand, if at least one subprecoder is of rank-deficiency, (3.69) is not held. Then, the iteration cannot stop in just one iteration. Note that the order of the diagonal entries of $\tilde{\mathbf{H}}'$ can be changed during the iteration. In such case, we have to re-solve $\sigma_{R,i}^2$, which is not desirable. The following proposition states that this problem can be avoided.

Proposition 3.2: With the relay precoder given in (3.50) and (3.68), the diagonal entries of resultant $\tilde{\mathbf{H}}'$ is with descending order when the SNR of relay-to-destination path is much higher than that of source-to-relay path.

Proof: Without loss of generality, we can let $\sigma_{n,r}^2 = \sigma_{n,d}^2 = 1$. Therefore, the SNRs of source-to-relay and relay-to-destination channels are defined via the variances of \mathbf{H}_{SR} and \mathbf{H}_{RD} . Using (3.68), we can have

$$\sigma_{R,i}^2\sigma_{rd,i}^2 = \sqrt{\frac{\mu\sigma_{rd,i}^2}{(1 + \mathbf{B}(i,i)\sigma_{sr,i}^2)} + \frac{1}{4}} - \frac{1}{2}. \quad (3.70)$$

Without Υ at the source node, we can have $\mathbf{B} = \alpha \mathbf{I}_M$ where $\alpha = \frac{P_{S,T}}{M}$. Assume that the SNR of relay-to-destination path is higher than that of source-to-relay path so that $\mu\sigma_{rd,i}^2 \gg 1 + \alpha\sigma_{sr,i}^2$. Then, $\sigma_{R,i}^2\sigma_{rd,i}^2$ can be approximately expressed as:

$$\sigma_{R,i}^2\sigma_{rd,i}^2 \approx \sqrt{\frac{\mu\sigma_{rd,i}^2}{1 + \alpha\sigma_{sr,i}^2}}. \quad (3.71)$$

Hence, $\tilde{\mathbf{H}}'$ can be expressed as:

$$\begin{aligned} \tilde{\mathbf{H}}'(i, i) &= (\sigma_{R,i}^2\sigma_{rd,i}^2 + 1)^{-\frac{1}{2}} \sigma_{R,i}\sigma_{rd,i}\sigma_{sr,i} \\ &= \left(\sqrt{\frac{\mu\sigma_{rd,i}^2}{1 + \alpha\sigma_{sr,i}^2}} + 1 \right)^{-\frac{1}{2}} \left(\sqrt{\frac{\mu\sigma_{rd,i}^2}{1 + \alpha\sigma_{sr,i}^2}} \right)^{\frac{1}{2}} \sigma_{sr,i} \\ &= \left(1 + \frac{1 + \alpha\sigma_{sr,i}^2}{\mu\sigma_{rd,i}^2} \right)^{-\frac{1}{2}} \sigma_{sr,i} \\ &\approx \sigma_{sr,i}. \end{aligned} \quad (3.72)$$

Then, the diagonal entries of $\tilde{\mathbf{H}}'$ are with descending order since $\sigma_{sr,i}$ decreases with i .

Proposition 3.2 shows that the ordering of $\tilde{\mathbf{H}}'(i, i)$ will not be changed and thus the new pairing operations are not necessary during the iterations. We now investigate the case of rank-deficiency. When at least a subsystem is rank-deficient, r becomes smaller than M . From Proposition 3.2, it is simple to see that the γ values of the paired subsystems have an ascending order, i.e.,

$$\begin{aligned} \tan^{-1} \left(\frac{\tilde{\mathbf{H}}'(M, M)}{\tilde{\mathbf{H}}'(1, 1)} \right) &\leq \tan^{-1} \left(\frac{\tilde{\mathbf{H}}'(M-1, M-1)}{\tilde{\mathbf{H}}'(2, 2)} \right) \\ &\leq \dots \\ &\leq \tan^{-1} \left(\frac{\tilde{\mathbf{H}}'(\frac{M}{2} + 1, \frac{M}{2} + 1)}{\tilde{\mathbf{H}}'(\frac{M}{2}, \frac{M}{2})} \right). \end{aligned} \quad (3.73)$$

This property indicates that when $r < M$, the corresponding \mathbf{B} will be of the following structure:

$$\mathbf{B} = \text{diag}(\underbrace{2\alpha, 2\alpha, \dots, 2\alpha}_{M-r}, \underbrace{\alpha, \alpha, \dots, \alpha}_{2r-M}, \underbrace{0, 0, \dots, 0}_{M-r}). \quad (3.74)$$

In the following proposition, we will demonstrate how to solve Σ_R when \mathbf{B} is of the structure in (3.74).

Proposition 3.3: Consider a rank-deficient \mathbf{F}'_S with rank r , where $\frac{M}{2} \leq r < M$. Let $\tilde{\mathbf{H}}'_{1:m}$ denote a square matrix consisting of the first m columns and rows of $\tilde{\mathbf{H}}'$. The objective function for the design of Σ_R can be chosen as $\det \left(\tilde{\mathbf{H}}'_{1:M-r} \tilde{\mathbf{H}}'^H_{1:M-r} \right) \det \left(\tilde{\mathbf{H}}'_{1:r} \tilde{\mathbf{H}}'^H_{1:r} \right)$ such that the lower bound in (3.58) can be minimized.

Proof: From (3.74), it is clear that the rank-deficient subprecoder is used in the first $M - r$ subsystems while the full-rank subprecoder is adopted in the last $r - \frac{M}{2}$ subsystems. According to the channel angle, the free distance of the i th subsystem can be expressed as:

$$d_{\text{free},i}^2 = \begin{cases} \tilde{\mathbf{H}}'(i, i) \tilde{\mathbf{H}}'(M - i + 1, M - i + 1) \epsilon_{1,i} \\ \tilde{\mathbf{H}}'(i, i) \tilde{\mathbf{H}}'(i, i) \epsilon_{2,i} \end{cases} \quad (3.75)$$

where both $\epsilon_{1,i}$ and $\epsilon_{2,i}$ depend on the QAM constellation. Hence, we can rewrite $\prod_{i=1}^{M'} d_{\text{free},i}^2$ as:

$$\begin{aligned} \prod_{i=1}^{M'} d_{\text{free},i}^2 &= \prod_{j=1}^{M-r} \tilde{\mathbf{H}}'(j, j) \tilde{\mathbf{H}}'(j, j) \epsilon_{2,j} \\ &\times \prod_{l=M-r+1, l \leq M'}^{M'} \tilde{\mathbf{H}}'(l, l) \tilde{\mathbf{H}}'(M - l + 1, M - l + 1) \epsilon_{1,l} \\ &= \underbrace{\prod_{j=1}^{M-r} \epsilon_{2,j} \prod_{k=M-r+1}^{M'} \epsilon_{1,k}}_{\epsilon} \prod_{l=1}^{M-r} \tilde{\mathbf{H}}'(l, l) \prod_{p=1}^r \tilde{\mathbf{H}}'(p, p) \\ &= \epsilon \sqrt{\det \left(\tilde{\mathbf{H}}'_{1:M-r} \tilde{\mathbf{H}}'^H_{1:M-r} \right) \det \left(\tilde{\mathbf{H}}'_{1:r} \tilde{\mathbf{H}}'^H_{1:r} \right)}. \end{aligned} \quad (3.76)$$

Obviously, ϵ only depends on the QAM constellation. Hence, the objective function is equivalent to maximizing $\det \left(\tilde{\mathbf{H}}'_{1:M-r} \tilde{\mathbf{H}}'^H_{1:M-r} \right) \det \left(\tilde{\mathbf{H}}'_{1:r} \tilde{\mathbf{H}}'^H_{1:r} \right)$ when $\frac{M}{2} \leq r < M$.

When $\frac{M}{2} \leq r < M$, we can conduct the rank-deficiency operations for $M - r$ subsystems at one time, equivalently switching off $M - r$ subchannels. However, this approach may not be efficient. This is because the relay precoder will re-allocate its power and some of the rank-deficient subsystems may become non-deficient in the next iteration. For this reason, we only

let one subchannel be switched off at one time. Starting from the first subsystem, if we find $\tan^{-1} \left(\frac{\tilde{\mathbf{H}}'(M,M)}{\tilde{\mathbf{H}}'(1,1)} \right)$ is smaller than the angle threshold, then let $r = M - 1$ and reformulate \mathbf{B} as

$$\mathbf{B} = \text{diag}\{2\alpha, \alpha, \alpha, \dots, \alpha, 0\}. \quad (3.77)$$

Let κ_i be defined as:

$$\kappa_i = \begin{cases} 2 & \text{for } i = 1, 2, \dots, M - r \\ 1 & \text{for } i = M - r + 1, M - r + 2, \dots, r. \end{cases} \quad (3.78)$$

From the results in Proposition 3.3, the optimization of $\sigma_{R,i}^2$ for $\frac{M}{2} \leq r < M$ can then be reformulated as:

$$\begin{aligned} \min_{\sigma_{R,i}^2} & - \sum_{i=1}^r \ln \left(\frac{\kappa_i \sigma_{R,i}^2 \sigma_{rd,i}^2}{\sigma_{R,i}^2 \sigma_{rd,i}^2 \sigma_{n,r}^2 + \sigma_{n,d}^2} \right) \\ \text{s.t.} & \\ & \sum_{i=1}^r \sigma_{R,i}^2 (\sigma_{n,r}^2 + \mathbf{B}(i,i) \sigma_{sr,i}^2) = P_{R,T}. \end{aligned} \quad (3.79)$$

Then, the solution of the problem in (3.79) can be expressed as

$$\sigma_{R,i}^2 = \sqrt{\frac{\bar{\mu}_i \sigma_{n,d}^2}{\sigma_{rd,i}^2 \sigma_{n,r}^2 (\sigma_{n,r}^2 + \mathbf{B}(i,i) \sigma_{sr,i}^2)} + \left(\frac{\sigma_{n,d}^2}{2\sigma_{rd,i}^2 \sigma_{n,r}^2} \right)^2} - \frac{\sigma_{n,d}^2}{2\sigma_{rd,i}^2 \sigma_{n,r}^2} \quad (3.80)$$

where $\bar{\mu}_i = \mu \kappa_i$. The derivation of (3.80) is given in Appendix B.4. Note that for the rank-deficient case, the right-hand side of (3.70) can be expressed as

$$\sigma_{R,i}^2 \sigma_{rd,i}^2 = \sqrt{\frac{\bar{\mu}_i \sigma_{rd,i}^2}{1 + \mathbf{B}(i,i) \sigma_{sr,i}^2}}. \quad (3.81)$$

From (3.77) and (3.78), we see that $\bar{\mu}_i$ and $\mathbf{B}(i,i)$ are equally affected by κ_i . As a result, the statement in Proposition 3.2 is still valid here. The above procedure is then repeatedly conducted until all non-zero channels angles are larger than the angle threshold or r has been equal to $\frac{M}{2}$. When $r = \frac{M}{2}$, $\bar{\mu}_i$ becomes a constant for all $i = 1, 2, \dots, r$. In this case, the structure of $\sigma_{R,i}^2$ in (3.80) will be reduced to that in (3.68). Figure 3.7 summarizes the complete operations of the proposed algorithm, referred to as Algorithm 3.1.

In previous discussions, we do not conduct the source power allocation among all subsystems. This simplification may result in performance loss since error rate performance can be affected by the subsystem with the minimum free distance. Exploiting Υ will complicate the optimization of Σ_R since the behavior of $\mathbf{B}(i, i)$ is no longer easy to follow. To overcome, we propose another iterative method to further improve system performance. Let \mathbf{F}_S'' denote the source precoder with power allocation. Then, \mathbf{F}_S'' can be expressed as

$$\mathbf{F}_S'' = \Upsilon \mathbf{F}_S'. \quad (3.82)$$

We assume that the initial $\mathbf{F}_S^{(0)}$ is of full-rank, and choose an identity matrix as the initial $\Upsilon^{(0)}$. Using (3.53) and (3.68), we can solve $\Sigma_R^{(1)}$ and then obtain the resultant $\tilde{\mathbf{H}}^{(1)}$. Consequently, both $\mathbf{F}_S^{(1)}$ and $\Upsilon^{(1)}$ are to be updated with the information of $\tilde{\mathbf{H}}^{(1)}$ in the next iteration. This method is conducted iteratively till no further improvement can be exploited. The detailed algorithm, denoted by Algorithm 3.2, is summarized in Table 3.3.

§ 3.5 Simulations and Discussions

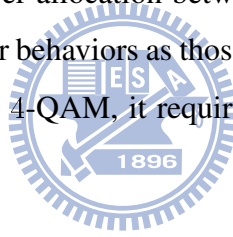
In this section, we report simulation results demonstrating the effectiveness of the proposed algorithms. In simulations, we consider a flat-fading MIMO channel. The entries of the channel matrix are assumed to be identically and independently distributed complex Gaussian random variables with zero mean and unit variance.

§ 3.5.1 Performance Comparisons for MIMO Systems

First, we evaluate the performance of each X-structured precoder in MIMO systems. Five schemes are compared. That is, 1) existing subprecoder \mathbf{F}_c , 2) existing subprecoder \mathbf{F}_r , 3) existing subprecoder \mathbf{F}_o , 4) proposed subprecoder $\mathbf{F}_{p,1}$, 5) proposed subprecoder $\mathbf{F}_{p,2}$. Figure 3.3 compares the precoding performance for the MIMO system with $N_t = 2$, $N_r = 2$, and $M = 2$, showing the results of 4- and 16-QAM schemes, simultaneously. As we can see, the proposed

subprecoders outperform \mathbf{F}_o and give the comparable performance to that of \mathbf{F}_r . Note that \mathbf{F}_r requires table look-ups in run time. Furthermore, \mathbf{F}_c slightly outperforms other subprecoders in 4-QAM, but suffers from performance loss in 16-QAM. The performance of \mathbf{F}_o is not shown for 16-QAM since it is worse than that of \mathbf{F}_r [30]. Note that the proposed method adopts the GMD solution for well-conditioned channels. Although \mathbf{F}_{GMD} provides the suboptimum solution, the performance loss of either $\mathbf{F}_{p,1}$ or $\mathbf{F}_{p,2}$ is limited. This can be explained by the facts follows. The corresponding free distance for each subprecoder decreases as γ is decreased. As a result, the error rate performance is dominated by ill-conditioned channels. Instead of using \mathbf{F}_{GMD} , the proposed method will use a rank-deficient subprecoder for a small value of γ and the performance loss can be mitigated.

Figure 3.4 shows the precoding performance for a MIMO system with $N_t = 4$, $N_r = 4$, and $M = 4$. In this scenario, the power allocation between subsystems is conducted with (3.31). From the figure, we observe similar behaviors as those in Figure 3.3. Note that although \mathbf{F}_c can provide optimum performance for 4-QAM, it requires higher detection complexity compared with the other methods.



§ 3.5.2 Performance Comparisons for MIMO Relay Systems

Next, we evaluate the performance of various precoding methods in a two-hop AF MIMO relay system. Seven systems are considered; the first five systems use the ML detection in the receiver while the last two use the QR-SIC detection. They are: 1) jointly precoded system with $\mathbf{F}_{p,1}$ and \mathbf{F}_R (JP- $\mathbf{F}_{p,1}$ - \mathbf{F}_R -ML-PA), 2) jointly precoded system with $\mathbf{F}_{p,2}$ and \mathbf{F}_R (JP- $\mathbf{F}_{p,2}$ - \mathbf{F}_R -ML-PA), 3) jointly precoded system with $\mathbf{F}_{p,2}$ and \mathbf{F}_R without source power allocation (JP- $\mathbf{F}_{p,2}$ - \mathbf{F}_R -ML-WPA), 4) source precoded system with $\mathbf{F}_{p,1}$ (SP- $\mathbf{F}_{p,1}$ -ML-PA), 5) unprecoded system with ML detection (UP-ML), 6) jointly precoded system (JP-QR-SIC), and 7) source precoded system (SP-QR-SIC). Both the JP-QR-SIC and SP-QR-SIC are obtained from [59] without considering the source-to-destination link. Let SNR_{sr} and SNR_{rd} denote the received SNR at each relay antenna and destination antenna, respectively.

Figure 3.5 shows the performance comparison for 4-QAM. Here, we let $N_t = 4$, $N_{r_e} = 4$, $N_d = 4$, $\text{SNR}_{r_d} = 25\text{dB}$ and SNR_{s_r} be varied. Also let $I = 3$ in Algorithm 3.2 for reasonable precoding complexity. As seen, the proposed JP- $\mathbf{F}_{p,1}$ - \mathbf{F}_R -ML-PA and JP- $\mathbf{F}_{p,2}$ - \mathbf{F}_R -ML-PA schemes indeed outperform other precoding methods. It is also observed that about 1dB performance loss (at $\text{BLER} = 10^{-4}$) will be induced when the source power allocation matrix Υ is not included. Compared with the UP-ML scheme, the proposed methods can provide more than 4dB performance improvement when BLER is 10^{-3} . Note that the detection complexity of the UP-ML scheme can be much higher than the other methods due to the requirement for 4×4 ML detection. The SP- $\mathbf{F}_{p,1}$ -ML-PA scheme suffers from performance loss since only the source precoding is considered in the system. As for the JP-QR-SIC and SP-QR-SIC schemes, their performances degrade significantly for high SNR. Note that in QR-SIC detection, the detection complexity at each receive antenna is $\mathcal{O}(L)$. Besides, a complete GMD operation is required for finding the source precoder in either the JP-QR-SIC or SP-QR-SIC scheme. It is clear that the proposed precoding methods are more efficient.

Figure 3.6 shows the performance comparison for 16-QAM. We let $N_t = 4$, $N_{r_e} = 4$, $N_d = 4$, $I = 5$, $\text{SNR}_{r_d} = 35\text{dB}$ and SNR_{s_r} be varied. It can be observed that the proposed methods still provide the significant performance improvement. Compared to the results in Figure 3.5, we can see that the improvements of the proposed methods are slightly reduced. This result can be explained by the fact that the free distances yielded by the proposed subprecoders will be rapidly decreased for ill-conditioned channels when a large QAM modulation is considered. In other words, the improvement obtained from the rank-deficiency subprecoders is reduced.

Table 3.1: Complexity comparisons for X-structured precoding

X-structured precoding			
Subprecoder	SVD of \mathbf{H}	\mathbf{M}	Look-up tables
\mathbf{F}_c	$\mathcal{O}(N_r^2 N_t + N_t^2 N_r)$	$\mathcal{O}(N_t M)$	\times
\mathbf{F}_r	$\mathcal{O}(N_r^2 N_t + N_t^2 N_r)$	$\mathcal{O}(N_t M)$	required for $L > 4$
\mathbf{F}_o	$\mathcal{O}(N_r^2 N_t + N_t^2 N_r)$	$\mathcal{O}(N_t M)$	required for $L > 4$
Proposed $\mathbf{F}_{p,1}$	$\mathcal{O}(N_r^2 N_t + N_t^2 N_r)$	$\mathcal{O}(N_t M)$	\times
Proposed $\mathbf{F}_{p,2}$	$\mathcal{O}(N_r^2 N_t + N_t^2 N_r)$	$\mathcal{O}(N_t M)$	\times

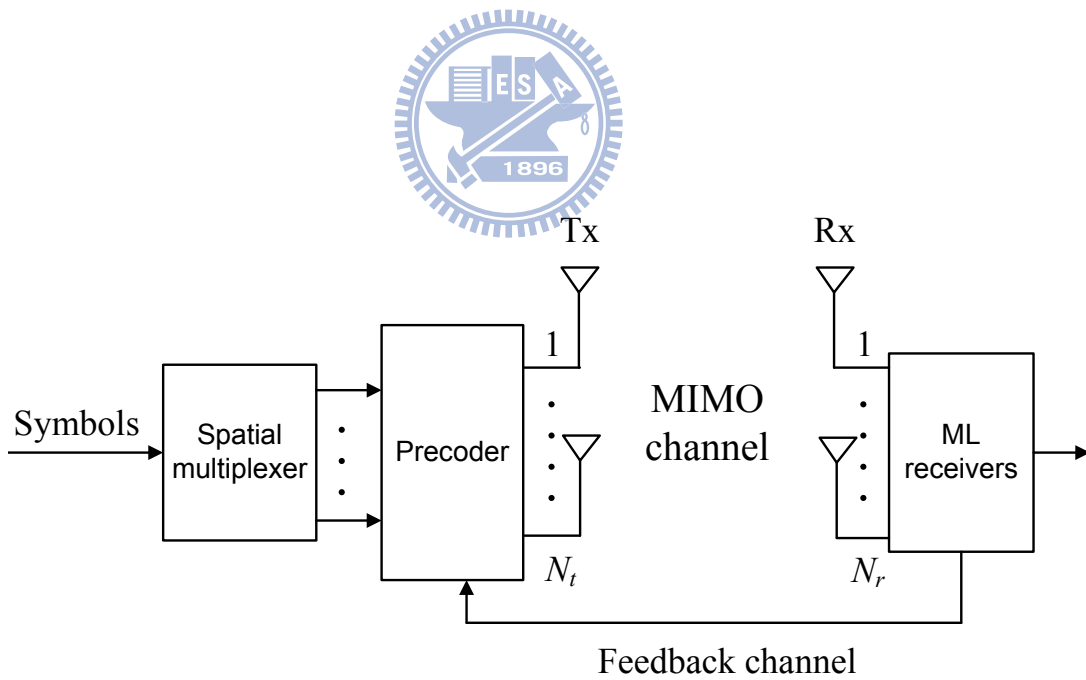


Figure 3.1: System model for a precoded spatial-multiplexing MIMO system.

Table 3.2: Detection complexity comparisons for X-structured precoding

Detection complexity		
Subprecoder	\mathbf{r}	ML detection
\mathbf{F}_c	$\mathcal{O}(N_r^2)$	$\approx \mathcal{O}(M'L\sqrt{L})$ for large values of L
\mathbf{F}_r	$\mathcal{O}(N_r^2)$	$\mathcal{O}(M'\sqrt{L})$
\mathbf{F}_o	$\mathcal{O}(N_r^2)$	$\mathcal{O}(M'\sqrt{L})$
Proposed $\mathbf{F}_{p,1}$	$\mathcal{O}(N_r^2)$	$\approx \mathcal{O}(M'\sqrt{L})$ for large values of L
Proposed $\mathbf{F}_{p,2}$	$\mathcal{O}(N_r^2)$	$\mathcal{O}(M'\sqrt{L})$

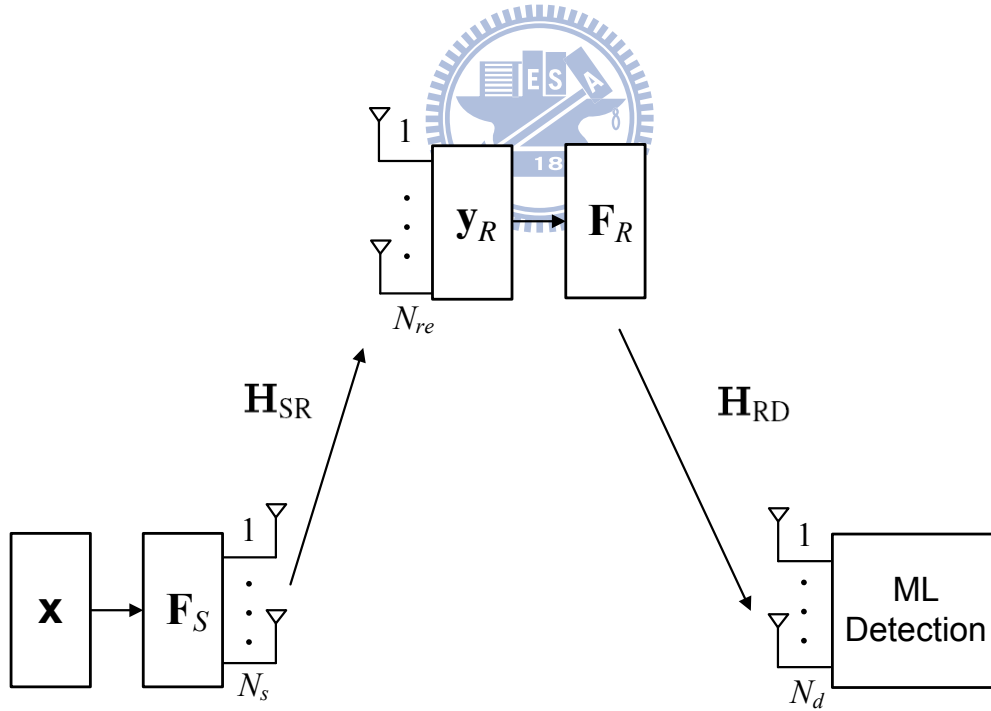


Figure 3.2: System model for a precoded spatial-multiplexing MIMO relay system.

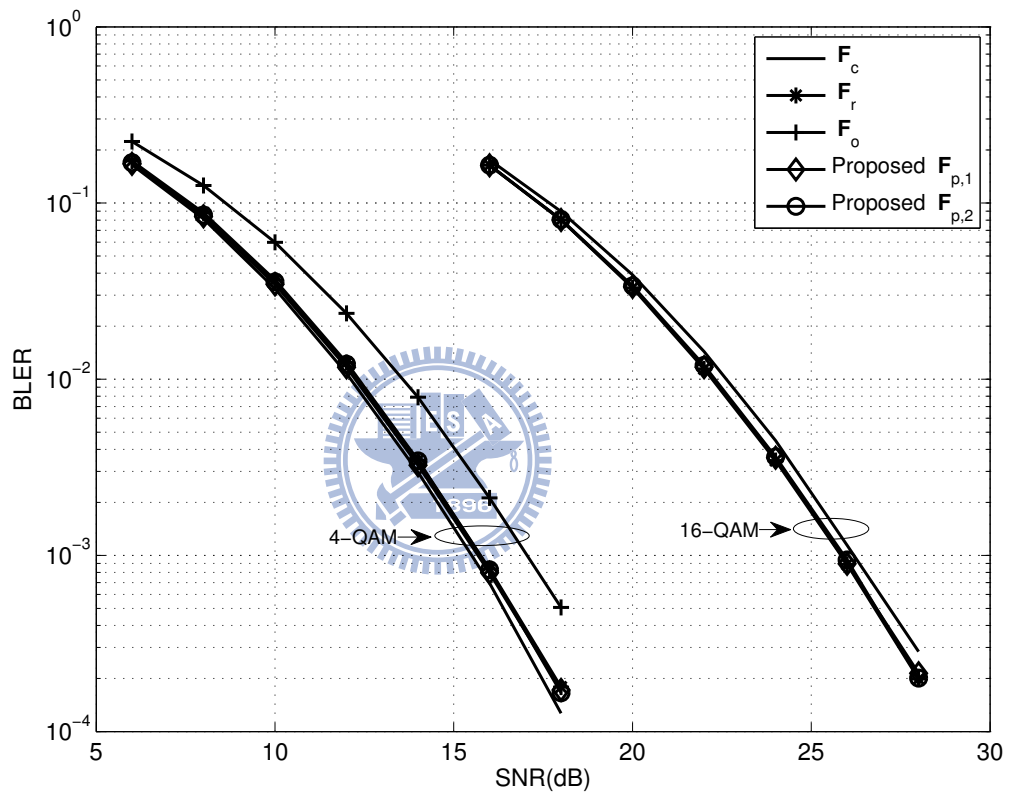


Figure 3.3: BLER performance comparisons for MIMO systems with $N_t = 2$, $N_r = 2$, and $M = 2$.

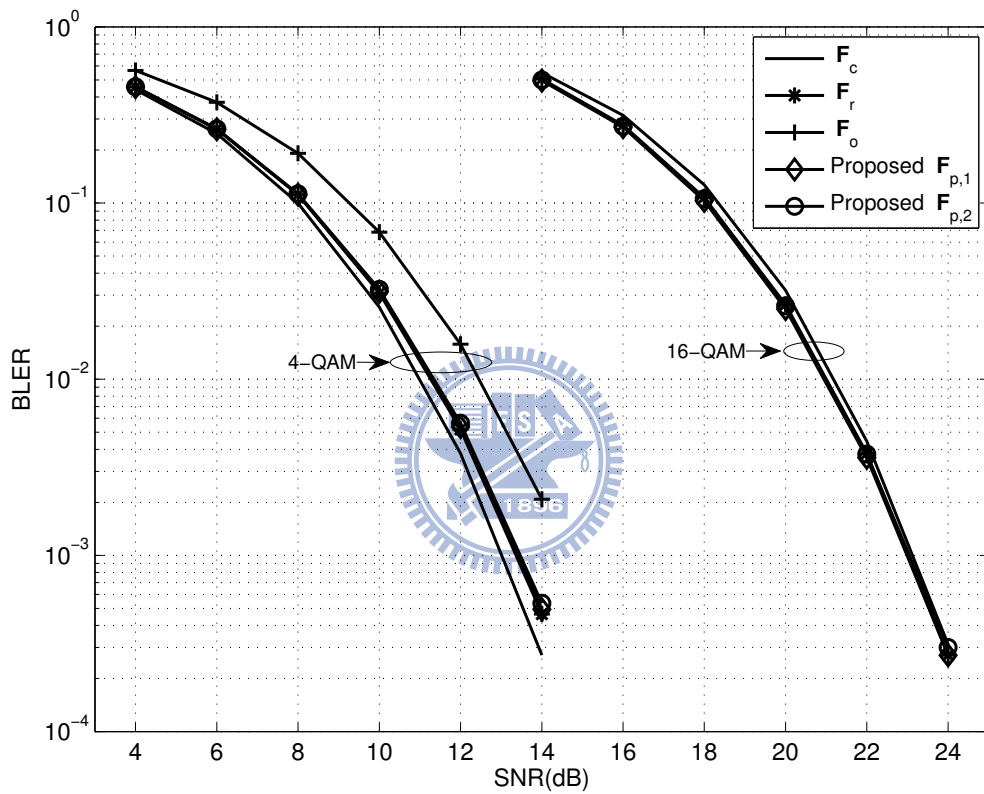


Figure 3.4: BLER performance comparisons for MIMO systems with $N_t = 4$, $N_r = 4$, and $M = 4$.

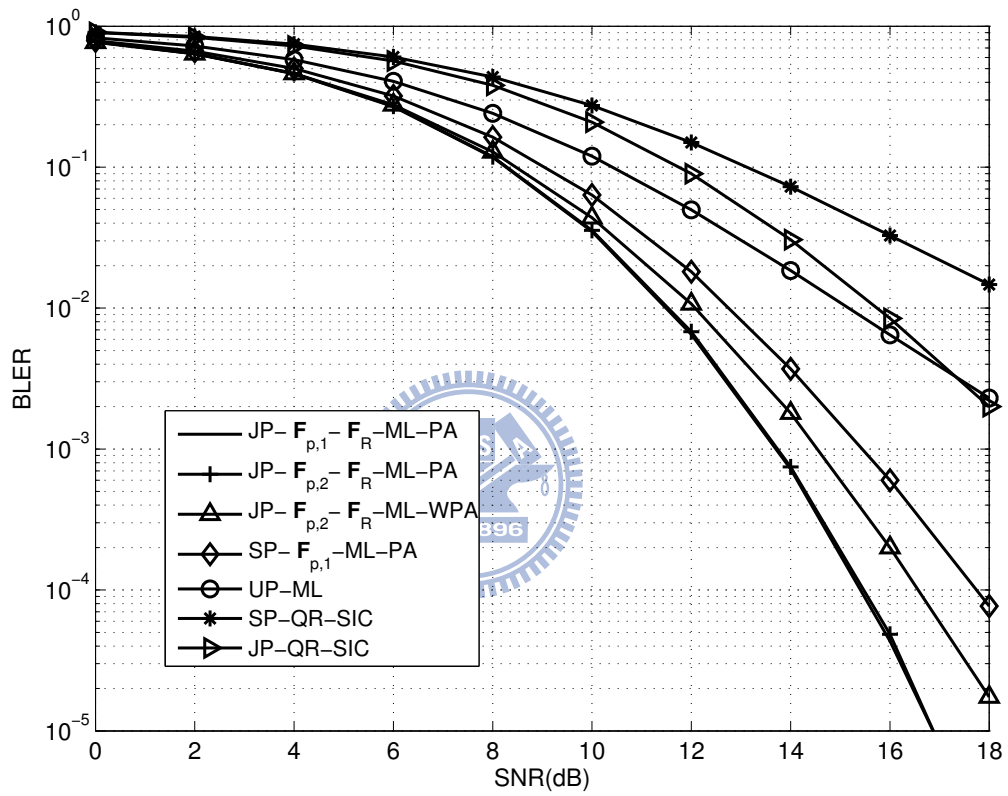


Figure 3.5: BLER performance comparisons for MIMO relay systems with 4-QAM ($N_t = 4$, $N_r = 4$, $N_d = 4$, and $M = 4$).

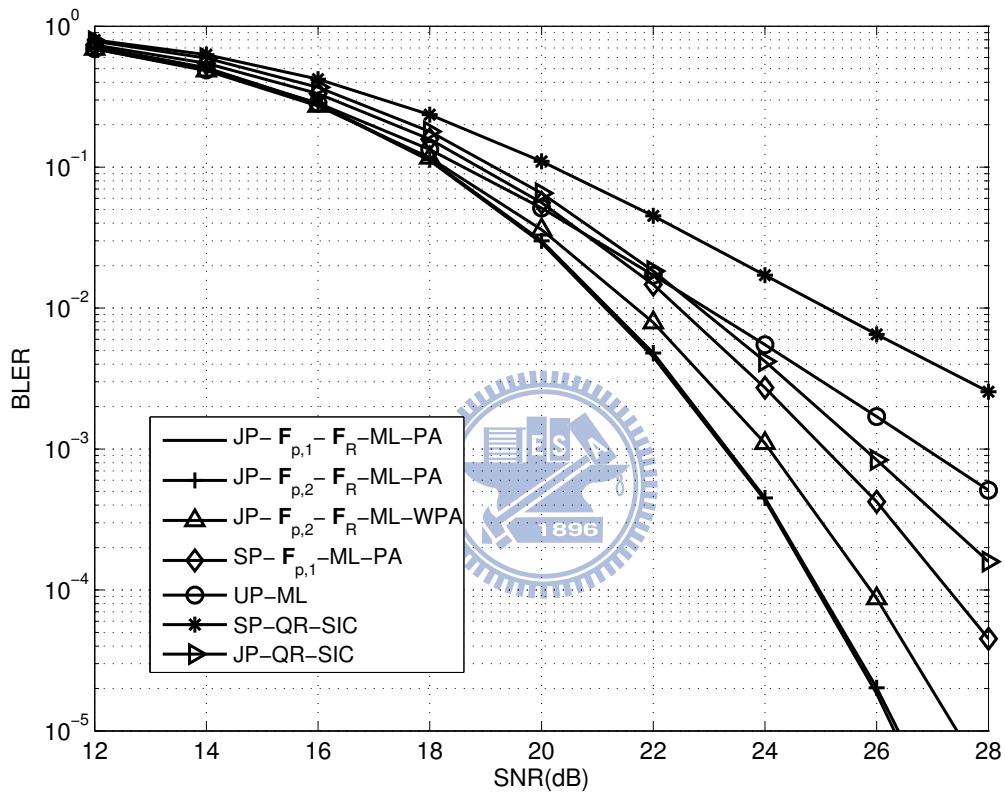


Figure 3.6: BLER performance comparisons for MIMO relay systems with 16-QAM ($N_t = 4$, $N_r = 4$, $N_d = 4$, and $M = 4$).

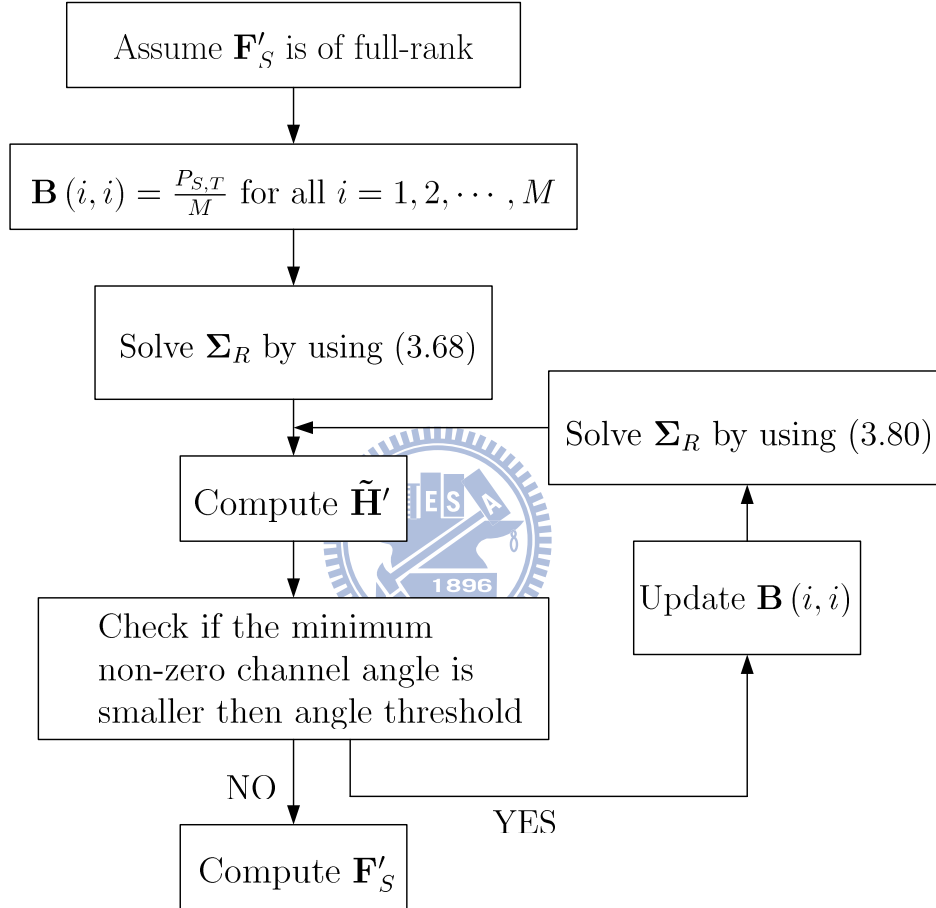


Figure 3.7: **Algorithm 3.1:** Joint source/relay precoders design without source power allocation Υ .

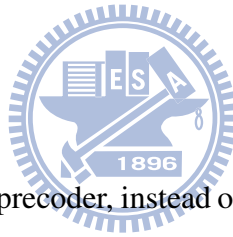
Table 3.3: Joint source/relay precoders design with source power allocation

Algorithm 3.2: Algorithm of Joint Precoders Design with Υ

- (1) Set $r = M$, and choose the initial $\Upsilon^{(0)} = \sqrt{\frac{1}{M'}} \mathbf{I}_M$
 - (2) Let the initial $\mathbf{B}^{(0)}$ be $\mathbf{B}^{(0)} = \alpha \mathbf{I}_M$;
 - (3) Set I as the number of iterations;
 - (3) for $i = 1 : I$;
 - (5) Use **Algorithm 3.1** to obtain $\Sigma_R^{(i)}$ and $\mathbf{F}_S'^{(i)}$;
 - (6) Compute $\Upsilon^{(i)}$ with (3.31);
 - (7) Update $\mathbf{B}^{(i)}$ with $\Upsilon^{(i)} \mathbf{F}_S'^{(i)}$;
 - (8) end;
-

Chapter 4

Limited-Feedback for X-Structured Precoding in Spatial-Multiplexing MIMO Systems



As mentioned, the feedback of the precoder, instead of CSI, is generally preferable in real-world applications. Then, a codebook is designed for the precoder, and only the index of the codeword is fed back. To search a codeword for a channel matrix, also known as codeword selection, two methods have been proposed. The first one calculates the optimum precoder and then selects the codeword having the shortest distance to the optimum precoder [46]. In this case, we need to know the optimum precoder. The second method simply evaluates all the codewords and then chooses one minimize a certain criterion (e.g., the free distance) [60]. Note that limited feedback of X-structured precoding is different to other kinds of precoding in the sense that two types of precoding matrices are required, the right unitary matrix of SVD, referred to as right singular matrix, and the subprecoder. There are several challenges in this limited feedback problem. First, the channel matrix cannot be completely diagonalized since the right singular matrix is quantized and the X-structure cannot be maintained anymore. Second, the diagonal entries of the SVD-transformed channel are not real numbers, and the subprecoders developed

in Chapter 3 are not directly applicable. Finally, the decoupled 2×2 ML detectors cannot be applied in the receiver since the X-structure is lost. In this chapter, we will investigate how to solve these problems.

§ 4.1 System Models and Problem Formulation

Consider a precoded spatial-multiplexing MIMO system with limited feedback, as described in Figure 4.1. The operation of the system is described as follows. A codebook \mathcal{F} is pre-constructed and known at both the transmitter and receiver. According to some selection criterion, the optimum codeword is chosen from \mathcal{F} at the receiver. Next, the corresponding index is fed back to the transmitter via a low-rate feedback channel. Finally, the precoding can be conducted with the chosen codeword.

As mentioned, in X-structured precoding, two codebooks are required; one is for \mathbf{V} which is of full column-rank and the other is for \mathbf{F} which can be rank-deficient. The equivalent precoding matrix is $\mathbf{M} = \mathbf{V}\mathbf{F}$. Let \mathcal{F}_1 and \mathcal{F}_2 denote the codebook designed for \mathbf{V} and \mathbf{F} respectively. Then, we have

$$\mathcal{F}_1 = \{\mathbf{F}_{1,1}, \mathbf{F}_{1,2}, \dots, \mathbf{F}_{1,B_1}\} \quad (4.1)$$

$$\mathcal{F}_2 = \{\mathbf{F}_{2,1}, \mathbf{F}_{2,2}, \dots, \mathbf{F}_{2,B_2}\} \quad (4.2)$$

where $\mathbf{F}_{i,j}$'s are the codewords, i.e., quantized precoding matrices, and B_1 and B_2 are the size of the two codebooks, respectively. Note here that \mathbf{F} consists of subprecoders, and thus the codewords of \mathcal{F}_2 can be 2×2 matrices. The received signal can then be expressed as

$$\mathbf{y} = \mathbf{H}\mathbf{V}_p\mathbf{F}_q\mathbf{x} + \mathbf{n} \quad (4.3)$$

where $\mathbf{V}_p \in \mathcal{F}_1$ and \mathbf{F}_q is constructed from the codewords in \mathcal{F}_2 . Using the SVD of \mathbf{H} , i.e., $\mathbf{H} = \mathbf{U}\mathbf{\Sigma}\mathbf{V}^H$, we can have the transformed received signal, \mathbf{r} , expressed as

$$\mathbf{r} = \mathbf{U}^H\mathbf{y} = \mathbf{\Sigma}\mathbf{V}^H\mathbf{V}_p\mathbf{F}_q\mathbf{x} + \mathbf{U}^H\mathbf{n}. \quad (4.4)$$

In general, \mathbf{V} will not be equal to \mathbf{V}_p , a quantized \mathbf{V} . As a result, $\Sigma \mathbf{V}^H \mathbf{V}_p$ is no longer a real-valued diagonal matrix. Note that the subprecoders proposed in Chapter 3 are derived based on Σ , a real-valued diagonal matrix. Thus, the subprecoders need to be redesigned. In what follows, we will first consider the design of \mathcal{F}_1 . Then, we will investigate how to design the subprecoders when the equivalent channel is not a real-valued diagonal matrix. Besides, we demonstrate that the construction of \mathcal{F}_2 can be simplified to the quantization of a single angle. Finally, we propose a low-complexity detection method which combines 2×2 ML detectors with SIC.

§ 4.2 Quantization for X-Structured Precoding

In this section, we first consider the quantization of \mathbf{V} . As mentioned, \mathbf{V} is quantized with a codebook. Hence, the first task is to construct the codebook \mathcal{F}_1 . Several methods have been proposed to construct a codebook consisting of unitary matrices. Hereby, we use vector quantization (VQ) [49] to construct \mathcal{F}_1 since it is simple and effective. VQ first generates a training set $\{\mathbf{V}_i\}_{i=1}^{N_c}$ where N_c is the size of the samples, and then updates the codebook iteratively. Let the codebook obtained in the $j - 1$ iteration be denoted by $\{\tilde{\mathbf{V}}_i(j - 1)\}_{i=1}^{B_1}$. The operation of VQ can be summarized as follows:

1. Partition the training set into B_1 clusters by the nearest neighbor rule:

$$\mathcal{S}_i = \{\mathbf{V}_n : \|\mathbf{V}_n - \tilde{\mathbf{V}}_i(j - 1)\| \leq \|\mathbf{V}_n - \tilde{\mathbf{V}}_m(j - 1)\|, \forall m \neq i\}. \quad (4.5)$$

where \mathcal{S}_i is the i th cluster.

2. Update the codebook with the centroid rule:

$$\tilde{\mathbf{V}}_i(j) = \frac{1}{N_{\mathcal{S}_i}} \sum_{\mathbf{V}_n \in \mathcal{S}_i} \mathbf{V}_n, \quad i = 1, 2, \dots, B_1. \quad (4.6)$$

where $N_{\mathcal{S}_i}$ is the number of samples in the i th cluster.

3. Normalize the codewords such that $\tilde{\mathbf{V}}_i(j)\tilde{\mathbf{V}}_i^H(j) = \tilde{\mathbf{V}}_i^H(j)\tilde{\mathbf{V}}_i(j) = \mathbf{I}_M$.
4. If the difference of $\tilde{\mathbf{V}}_i(j)$ and $\tilde{\mathbf{V}}_i(j-1)$, $i = 1, 2, \dots, B_1$, is smaller than a threshold, the iteration stops. Otherwise, let $j = j + 1$ and go to Step 1.

As we can see, VQ is easy to implement. However, note that to have a good result, N_c has to be large. We now discuss the codeword selection. As mentioned, two methods are commonly used for the codeword selection. The first one calculates the optimum precoder and then selects the codeword having the shortest distance to the optimum precoder. The second method simply tries all the codewords and chooses the one that minimizes a certain criterion. Due to the special problem we consider, we use a method combining the both. The optimum precoder is \mathbf{V} which can be calculated. On the other hand, we want that $\mathbf{V}^H\mathbf{V}_p$ is as close to a diagonal matrix as possible. Let $\bar{\Sigma} = \Sigma\mathbf{V}^H\mathbf{V}_p$. Then, we can rewrite (4.4) as $\mathbf{r} = \bar{\Sigma}\mathbf{F}\mathbf{x} + \mathbf{U}^H\mathbf{n} = \bar{\Sigma}\mathbf{F}\mathbf{x} + \mathbf{n}'$, where $\mathbf{n}' = \mathbf{U}^H\mathbf{n}$. Let $\bar{\Sigma}_A$ denote the matrix where each entry is obtained by $\bar{\Sigma}_A(i, j) = |\bar{\Sigma}(i, j)|$. Hence, we can define a criterion to select \mathbf{V}_p as

$$\mathbf{V}_p = \max_{p \in B_1} \frac{\sum_{i=1}^M \bar{\Sigma}_A(i, i)}{\sum_{i=1}^M \sum_{j=1, j \neq i}^M \bar{\Sigma}_A(i, j)}. \quad (4.7)$$

As seen, $\bar{\Sigma}$ is a complex-valued non-diagonal matrix since the selected \mathbf{V}_p is not equal to \mathbf{V} . As a result, the subprecoders proposed in Chapter 3, designed for diagonal matrices with real values, may not be applied in the limited-feedback system. We now propose a method to solve this problem. We first assume that B_1 is large enough such that the off-diagonal entries in $\bar{\Sigma}_A$ are relatively smaller compared to the diagonal entries in $\bar{\Sigma}_A$. Also, the diagonal entries of $\bar{\Sigma}_A$ are assumed to have a descending order. Using the assumptions, we can use a complex-valued

diagonal matrix, denoted by $\bar{\Sigma}_D$, to approximate $\bar{\Sigma}$. Consider a 2×2 $\bar{\Sigma}_D$ expressed as:

$$\bar{\Sigma}_D = \begin{bmatrix} \bar{\Sigma}(1,1) & 0 \\ 0 & \bar{\Sigma}(2,2) \end{bmatrix} \quad (4.8)$$

$$= \begin{bmatrix} \exp^{j\theta_1} & 0 \\ 0 & \exp^{j\theta_2} \end{bmatrix} \begin{bmatrix} \bar{\Sigma}_A(1,1) & 0 \\ 0 & \bar{\Sigma}_A(2,2) \end{bmatrix} \quad (4.9)$$

$$= \Omega \bar{\Sigma}_A \quad (4.10)$$

where $\bar{\Sigma}(1,1) \geq \bar{\Sigma}(2,2)$. In the following, we will show that $\bar{\Sigma}_A$ can be used for constructing the corresponding subprecoders.

Let \mathbf{F}_{GMD} be the GMD solution for $\bar{\Sigma}_A$. In other words,

$$\bar{\Sigma}_A \mathbf{F}_{\text{GMD}} = \mathbf{Q}_A \mathbf{R}_A \quad (4.11)$$

where \mathbf{Q}_A is a unitary matrix and \mathbf{R}_A is an upper-triangular matrix with equal diagonal entries. Using (4.10) and (4.11), we can have

$$\bar{\Sigma}_D = \Omega \bar{\Sigma}_A = \Omega \mathbf{Q}_A \mathbf{R}_A \mathbf{F}_{\text{GMD}}^H \quad (4.12)$$

It is easy to verify that Ω is a unitary matrix. Hence, we can have

$$\bar{\Sigma}_D = \mathbf{Q}_{A_1} \mathbf{R}_A \mathbf{F}_{\text{GMD}}^H \quad (4.13)$$

where $\mathbf{Q}_{A_1} = \Omega \mathbf{Q}_A$ is also a unitary matrix. From (4.13), it can be seen that \mathbf{F}_{GMD} also serves the GMD solution for $\bar{\Sigma}_D$ since the diagonal entries of \mathbf{R}_A remains unchanged. Using the results in Chapter 3, \mathbf{F}_{GMD} for a 2×2 $\bar{\Sigma}_A$ can be explicitly expressed as:

$$\mathbf{F}_{\text{GMD}} = \sqrt{\frac{P_T}{2}} \begin{bmatrix} \sqrt{\frac{\bar{\Sigma}_A(2,2)}{\bar{\Sigma}_A(1,1)+\bar{\Sigma}_A(2,2)}} & -\sqrt{\frac{\bar{\Sigma}_A(1,1)}{\bar{\Sigma}_A(1,1)+\bar{\Sigma}_A(2,2)}} \\ \sqrt{\frac{\bar{\Sigma}_A(1,1)}{\bar{\Sigma}_A(1,1)+\bar{\Sigma}_A(2,2)}} & \sqrt{\frac{\bar{\Sigma}_A(2,2)}{\bar{\Sigma}_A(1,1)+\bar{\Sigma}_A(2,2)}} \end{bmatrix}. \quad (4.14)$$

It is interesting to observe that the GMD solution of a complex-valued diagonal matrix is a real-valued matrix.

Next, we consider the case when the subprecoder is rank-deficient. Here, we use $\mathbf{F}_{c,1}$ in (3.10) as an example. In this case, we can have

$$\bar{\Sigma}_D \mathbf{F}_{c,1} = \sqrt{P_T} \begin{bmatrix} \bar{\Sigma}(1,1) & 0 \\ 0 & \bar{\Sigma}(2,2) \end{bmatrix} \begin{bmatrix} \cos \theta_{c,1} & \sin \theta_{c,1} e^{j\varphi_{c,1}} \\ 0 & 0 \end{bmatrix}. \quad (4.15)$$

The corresponding free distance for $\bar{\Sigma}_D \mathbf{F}_{c,1}$ can be expressed as

$$d_{\text{free}} = \min_{\mathbf{x}_i, \mathbf{x}_j \in \mathcal{X}^2, \mathbf{x}_i \neq \mathbf{x}_j} \|\bar{\Sigma}_D \mathbf{F}_{c,1} (\mathbf{x}_i - \mathbf{x}_j)\|. \quad (4.16)$$

Then, we can have

$$\begin{aligned} d_{\text{free}} &= \min_{\mathbf{x}_i, \mathbf{x}_j \in \mathcal{X}^2, \mathbf{x}_i \neq \mathbf{x}_j} \sqrt{P_T} \left\| \Omega \begin{bmatrix} \bar{\Sigma}_A(1,1) \cos \theta_{c,1} & \bar{\Sigma}_A(1,1) \sin \theta_{c,1} e^{j\varphi_{c,1}} \\ 0 & 0 \end{bmatrix} (\mathbf{x}_i - \mathbf{x}_j) \right\| \\ &= \min_{\mathbf{x}_i, \mathbf{x}_j \in \mathcal{X}^2, \mathbf{x}_i \neq \mathbf{x}_j} \sqrt{P_T} \left\| \begin{bmatrix} \bar{\Sigma}_A(1,1) \cos \theta_{c,1} & \bar{\Sigma}_A(1,1) \sin \theta_{c,1} e^{j\varphi_{c,1}} \\ 0 & 0 \end{bmatrix} (\mathbf{x}_i - \mathbf{x}_j) \right\| \\ &= \min_{\mathbf{x}_i, \mathbf{x}_j \in \mathcal{X}^2, \mathbf{x}_i \neq \mathbf{x}_j} \|\bar{\Sigma}_A \mathbf{F}_{c,1} (\mathbf{x}_i - \mathbf{x}_j)\|. \end{aligned} \quad (4.17)$$

As discussed, $\theta_{c,1}$ and $\varphi_{c,1}$ in (4.15) yield the maximum free distance for a given $\bar{\Sigma}_D$ when the subprecoder is of rank-deficiency. Note that Ω is unitary. From (4.16) and (4.17), we can see that $\mathbf{F}_{c,1}$ provides the same free distance when $\theta_{c,1}$ and $\varphi_{c,1}$ are designed for $\bar{\Sigma}_A$. Hence, we can conclude that $\bar{\Sigma}_D$ can be replaced by $\bar{\Sigma}_A$ when designing the subprecoders. Although we use $\mathbf{F}_{c,1}$ for illustration, the above result is still valid when the rank-deficient subprecoder is implemented by $\mathbf{F}_{r,1}$ in (3.15).

With the results above, we now can use $\bar{\Sigma}_A$ for deriving the subprecoders. Similar to those in Chapter 3, the i th and $(M - i + 1)$ th subchannels are paired together to form a 2×2 subsystem since the diagonal entries of $\bar{\Sigma}_A$ are assumed to be in descending order. Then, the subprecoder

for the i th subsystem can be expressed as:

$$\mathbf{F}_{p,1,(i)} = \begin{cases} \mathbf{F}_{c,1} = \sqrt{P_T} \begin{bmatrix} \cos \theta_{c,1} & \sin \theta_{c,1} e^{j\varphi_{c,1}} \\ 0 & 0 \end{bmatrix} & \text{for } \gamma_i \leq \gamma_1 \\ \mathbf{F}_{\text{GMD},i} & \text{for } \gamma_i > \gamma_1 \end{cases} \quad (4.18)$$

where $\gamma_i = \tan^{-1} \left(\frac{\bar{\Sigma}_A(M-i+1, M-i+1)}{\bar{\Sigma}_A(i, i)} \right)$, and $\mathbf{F}_{\text{GMD},i}$ is expressed as

$$\mathbf{F}_{\text{GMD},i} = \sqrt{\frac{P_T}{2}} \begin{bmatrix} \sqrt{\frac{\bar{\Sigma}_A(M-i+1, M-i+1)}{\bar{\Sigma}_A(i, i) + \bar{\Sigma}_A(M-i+1, M-i+1)}} & -\sqrt{\frac{\bar{\Sigma}_A(i, i)}{\bar{\Sigma}_A(i, i) + \bar{\Sigma}_A(M-i+1, M-i+1)}} \\ \sqrt{\frac{\bar{\Sigma}_A(i, i)}{\bar{\Sigma}_A(i, i) + \bar{\Sigma}_A(M-i+1, M-i+1)}} & \sqrt{\frac{\bar{\Sigma}_A(M-i+1, M-i+1)}{\bar{\Sigma}_A(i, i) + \bar{\Sigma}_A(M-i+1, M-i+1)}} \end{bmatrix}. \quad (4.19)$$

In the limited-feedback scenario, $\mathbf{F}_{p,1,(i)}$ needs to be quantized also. Let $\cos \theta_i$ and $\sin \theta_i$ be defined as:

$$\cos \theta_i = \sqrt{\frac{\bar{\Sigma}_A(M-i+1, M-i+1)}{\bar{\Sigma}_A(i, i) + \bar{\Sigma}_A(M-i+1, M-i+1)}} \quad (4.20)$$

$$\sin \theta_i = \sqrt{\frac{\bar{\Sigma}_A(i, i)}{\bar{\Sigma}_A(i, i) + \bar{\Sigma}_A(M-i+1, M-i+1)}}. \quad (4.21)$$

Using (4.20) and (4.21), we can rewrite $\mathbf{F}_{\text{GMD},i}$ as

$$\mathbf{F}_{\text{GMD},i} = \sqrt{\frac{P_T}{2}} \begin{bmatrix} \cos \theta_i & -\sin \theta_i \\ \sin \theta_i & \cos \theta_i \end{bmatrix}. \quad (4.22)$$

Note that $\cos \theta_i \leq \sin \theta_i$ when the diagonal entries of $\bar{\Sigma}_A$ are in descending order. Therefore, we have $\frac{\pi}{4} \leq \theta_i \leq \frac{\pi}{2}$. Next, we observe that the structure of $\mathbf{F}_{c,1}$ in (4.18) is independent of the channel matrix. Therefore, the construction for \mathcal{F}_2 can be simplified to the quantization of θ_i . Let $\{\tilde{\theta}_i\}_{i=1}^{B_2-1}$ denote the quantized angles between $\frac{\pi}{4}$ and $\frac{\pi}{2}$. Then, we can have an codebook \mathcal{F}_2 expressed as

$$\mathcal{F}_2 = \left\{ \sqrt{P_T} \begin{bmatrix} \cos \theta_{c,1} & \sin \theta_{c,1} e^{j\varphi_{c,1}} \\ 0 & 0 \end{bmatrix}, \sqrt{\frac{P_T}{2}} \begin{bmatrix} \cos \tilde{\theta}_i & -\sin \tilde{\theta}_i \\ \sin \tilde{\theta}_i & \cos \tilde{\theta}_i \end{bmatrix}, i = 1, 2, \dots, B_2 - 1 \right\} \quad (4.23)$$

Note that the size of \mathcal{F}_2 in (4.23) is equal to B_2 . With \mathcal{F}_2 , we can choose the optimum codeword according to γ_i . It is worth noting that if we use other full-rank subprecoders instead of the GMD method, the quantization of $\mathbf{F}_{p,1,(i)}$ may require more feedback overhead. The reason is that other full-rank subprecoders have more variables and cannot be quantized by only a single angle θ_i .

§ 4.3 Low-Complexity MIMO Detection

In unquantized X-structured precoding, $\bar{\Sigma}$ is a diagonal matrix, i.e., $\bar{\Sigma} = \Sigma$. This property allows a low-complexity detection scheme since each subsystem only requires 2×2 ML detection. However, this advantage cannot be exploited when we consider a limited-feedback scenario. In this section, we propose a group-wise SIC combined with ML detection (GSML) method to overcome this problem.

Consider the received signal expressed as

$$\mathbf{r} = \bar{\Sigma} \mathbf{F}_q \mathbf{x} + \mathbf{n}. \quad (4.24)$$

As mentioned, \mathbf{F}_q is constructed from \mathcal{F}_2 and still has an X-structure. In a limited-feedback system, $\bar{\Sigma}(i, j)$ for $i \neq j$. This indicates that for a subsystem, there will be interference from other subsystems. Therefore, we have to conduct $M \times M$ ML detection at the receiver, which is not desirable. It is well-known that SIC is an effective method to achieve a good trade-off between detection performance and computational complexity. For example, we can let the received signal vector be re-ordered such that \mathbf{F}_q has a block diagonal rather than an X-structure. In doing this, the transmitted symbols for a subsystem are grouped together. Let $\bar{\Sigma}_r$ denote the channel matrix whose entries are re-arranged according to the block-diagonal \mathbf{F}_q . Obviously, $\bar{\Sigma}_r$ still involves interference. To facilitate the use of SIC, we conduct QRD on $\bar{\Sigma}_r$ to obtain an upper-triangular channel matrix. Let the QRD of $\bar{\Sigma}_r$ be expressed as $\bar{\Sigma}_r = \bar{\mathbf{Q}}_r \bar{\mathbf{R}}_r$. Then, use the GSML detection to obtain the estimate of transmitted signal. However, the above method exhibits some problems. First, the ordering of diagonal entries in $\bar{\mathbf{R}}_r$ may be different from that

in $\bar{\Sigma}_r$. Specifically, the diagonal entries of $\bar{\mathbf{R}}_r$ have a trend to be with descending ordering. This may result in performance loss since the subsystem first detected has higher probability to be with smaller channel gains. Second, the subprecoders are designed based on $\bar{\Sigma}_r$ instead of $\bar{\mathbf{R}}_r$. Hence, the QRD operations will make \mathbf{F}_q be far from the optimum solution. To overcome the above problem, we still let \mathbf{F}_q have an X-structure, and propose a method to realize the GSML detection as described in the following.

First, we let the QRD of $\bar{\Sigma}$ be expressed as

$$\bar{\Sigma} = \bar{\mathbf{Q}}\bar{\mathbf{R}}. \quad (4.25)$$

Hence, we can rewrite (4.24) as:

$$\bar{\mathbf{r}} = \bar{\mathbf{Q}}^H \mathbf{r} = \begin{bmatrix} \bar{r}_1 \\ \bar{r}_2 \\ \vdots \\ \bar{r}_M \end{bmatrix} = \bar{\mathbf{R}}\mathbf{F}_q \mathbf{x} + \bar{\mathbf{n}}. \quad (4.26)$$

Note that $\bar{\mathbf{R}}(i, j) = 0$ for $i > j$. Let $\bar{\mathbf{r}}_i$ and \mathbf{x}_i denote the received and transmit signal in the i th subsystem, respectively. Also let $\mathbf{F}_{q,(i)}$ denote the subprecoder for the i th subsystem. Due to the upper-triangular structure of $\bar{\mathbf{R}}$, we can express $\bar{\mathbf{r}}_i$ as follows:

$$\bar{\mathbf{r}}_i = \begin{bmatrix} \bar{\mathbf{R}}(i, i) & \bar{\mathbf{R}}(i, i+1) \\ 0 & \bar{\mathbf{R}}(M-i+1, M-i+1) \end{bmatrix} \mathbf{F}_{q,(i)} \mathbf{x}_i + \mathbf{i}_i + \mathbf{n}_i \quad (4.27)$$

$$= \bar{\mathbf{R}}_i \mathbf{F}_{q,(i)} \mathbf{x}_i + \mathbf{i}_i + \mathbf{n}_i \quad (4.28)$$

where \mathbf{i}_i is the interference vector introduced by other subsystems. Unlike the conventional SIC, we hereby first conduct 2×2 ML detection for the $\frac{M}{2}$ th subsystem. The ML detection searches all possible 2×1 symbol vectors to obtain an estimate $\hat{\mathbf{x}}_{\frac{M}{2}}$ such that

$$\hat{\mathbf{x}}_{\frac{M}{2}} = \min_{\mathbf{x} \in \mathcal{X}^2} \left\| \bar{\mathbf{r}}_{\frac{M}{2}} - \bar{\mathbf{R}}_{\frac{M}{2}} \mathbf{F}_{q,(\frac{M}{2})} \mathbf{x} \right\|. \quad (4.29)$$

Note that $\hat{\mathbf{x}}_{\frac{M}{2}}$ is the $\frac{M}{2}$ th and $(\frac{M}{2} + 1)$ th components of $\hat{\mathbf{x}}$. Since $\mathbf{x}_{\frac{M}{2}}$ has been detected, the rest $\hat{\mathbf{x}}_j$ for $j = 1, 2, \dots, \frac{M}{2} - 1$ can be sequentially obtained with GSML. That is,

$$\hat{\mathbf{x}}_j = \min_{\mathbf{x} \in \mathcal{X}^2} \left\| \bar{\mathbf{r}}_j - \sum_{i=j+1}^{\frac{M}{2}} \bar{\mathbf{R}}_i \mathbf{F}_{q,(i)} \hat{\mathbf{x}}_i - \bar{\mathbf{R}}_j \mathbf{F}_{q,(j)} \mathbf{x} \right\|. \quad (4.30)$$

Also note that $\hat{\mathbf{x}}_j$ is the j th and $(M - 1 + j)$ th components of $\hat{\mathbf{x}}$. Although the GSML method exhibits low-complexity requirement, its performance is limited since we treat \mathbf{i}_i as channel noise when detecting \mathbf{x}_i . Furthermore, the detection errors will propagate. This is an inherent problem in SIC-based detection algorithms [61]. We now propose a method to alleviate the problem.

From (4.29), we can see that if $\mathbf{x}_{\frac{M}{2}}$ in (4.29) is detected incorrectly, this detection error will be propagated to other subsystems. As a result, the reliability of the final output, $\hat{\mathbf{x}}$, can be affected adversely. To solve this problem, we propose using a list-based method combined with GSML detection. The main idea is to reserve K_c candidates for $\hat{\mathbf{x}}$, and choose the one with the maximum likelihood as the final output. Let $\{\hat{\mathbf{x}}_{\frac{M}{2}}^{(k)}\}_{k=1}^{K_c}$ denote the set consisting of candidates for the estimate of $\mathbf{x}_{\frac{M}{2}}$. The list-based GSML detection, referred to as LGSML detection, is summarized as follows.

1. In the $\frac{M}{2}$ th subsystem, use (4.29) to compute the corresponding distance for all possible 2×1 symbol vectors in \mathcal{X}^2 .
2. Construct the set $\{\hat{\mathbf{x}}_{\frac{M}{2}}^{(k)}\}_{k=1}^{K_c}$ in which the vectors provide the first K_c minimum values of distance in Step 1.
3. Conduct GSML detection for each $\hat{\mathbf{x}}_{\frac{M}{2}}^{(k)}$ so that we can have K_c candidates of $\hat{\mathbf{x}}$, denoted by $\{\hat{\mathbf{x}}^{(k)}\}_{k=1}^{K_c}$.
4. Compute $\|\bar{\mathbf{r}} - \bar{\mathbf{R}}\mathbf{F}_q \hat{\mathbf{x}}^{(k)}\|$ for $k = 1, 2, \dots, K_c$.
5. Choose the one with minimum $\|\bar{\mathbf{r}} - \bar{\mathbf{R}}\mathbf{F}_q \hat{\mathbf{x}}^{(k)}\|$ as the final output $\hat{\mathbf{x}}$.

Compared to the GSML detection, the computational complexity of the LGSML method will be increased. However, it is obvious that the detection complexity of the LGSML method is still much lower than that of $M \times M$ ML detection. Therefore, the list-based method can be a good solution from the implementation point of view. The computational complexity comparison for various detection methods is given in Table 4.1.

§ 4.4 Simulation Results

In this section, we report simulation results evaluating the performance of the proposed precoding methods in limited-feedback MIMO systems. In simulations, the flat-fading MIMO channel is considered and each entry of a channel matrix is assumed to be i.i.d. complex Gaussian random variable with zero mean and unit variance. Also, the size of the spatial-multiplexing MIMO system is 4×4 , i.e., $N_t = 4$, $N_r = 4$, and $M = 4$. In addition, we use (3.27) to implement the subprecoder. The QPSK transmission scheme is used and CSI is assumed to be perfectly known at the receiver.

We first evaluate the performance of the quantized right singular matrix. Here, we let the subprecoder, \mathbf{F}_q , be unquantized. For the LGSML detector, the number of candidates is set as 3, i.e., $K_c = 3$. The power allocation between subsystems is not applied (WPA), reducing the feedback overhead. Figure 4.2 shows the simulation results. From the figure, we can see that the codebook with larger size can provide better performance. However, as the the size of the codebook is increased, the improvement become smaller and smaller. For the codebook size of 1024, there is still one dB loss (at BLER of 10^{-3}).

It is simple to see that the computational complexity of the LGSML detector is proportional to the number of candidates. It is then interesting to know that how many candidates we actually needs. Figure 4.3 shows the performance comparison for different K_c . Here, we let $B_1 = 1024$ and $B_2 = 4$. In this case, the overall number of feedback bits is $\log_2(1024) + 2\log_2(4) = 14$. Note that the LGSML detector with $K_c = 1$ is reduced to the original GSML. As we can see, the

performance is improved as K_c is increased. However, for $K_c = 3$, the performance is almost the same as that with 4×4 ML detector. This is to say that three candidates are sufficient for the scenario.

Figure 4.4 shows the performance comparison between the precoded and unprecoded system. In limited-feedback scenarios, we let $B_1 = 1024$ and $B_2 = 4$. Also, let $K_c = 3$ in the LGSML detector. Note that in the unprecoded system, we conduct QR decomposition first and let $\mathbf{x}_{\frac{M}{2}} = [x_{M-1} \ x_M]^T$ be first detected so that there is no interference from other subsystems. As seen in the figure, the precoded systems outperform the unprecoded ones. As discussed, unprecoded systems require 4×4 ML detection and the computational complexity is high. Although we can use the GSML or LGSML detectors in unprecoded systems, its performance will be inferior to that of the precoded systems with the same kind of detectors. For the LGSML detector, the performance gap between the precoded and unprecoded systems is about 2 dB (at BLER of 10^{-3}). Note that we only have to feedback 14 bits in this case. For static or slowly fading channels, the method proposed in this chapter can be a good precoding method for MIMO systems. In Figure 4.4, we also show the performance of the K-best algorithm, a well-known low-complexity ML detection method. Let K_k denote the number of candidates in the K-best algorithm. For unprecoded systems, we can see that the K-best algorithm provides a comparable performance with the LGSML method for the same number of candidates ($K_k = K_c = 3$). Figure 4.5 shows the detection complexity comparison for different values of M . As we can see, the required multiplications of the K-best algorithm are higher than those of the proposed detection methods. The reason is that the K-best algorithm requires to evaluate its candidates at each processing stage; however, the proposed LGSML only needs once.

Table 4.1: Complexity comparisons for detection methods

Detection complexity comparisons		
Scheme	QRD	Number of multiplications
GSML	$\mathcal{O}(N_r N_t^2)$	$3L + 3 + (3L + 3 + M')(M' - 1)$
LGSML	$\mathcal{O}(N_r N_t^2)$	$3L + 3 + (3L + 3 + M')(M' - 1) K_c$
K-best algorithm	$\mathcal{O}(N_r N_t^2)$	$2L^2 + 2L + K_k L (M^2 + M - 6)$
$M \times M$ ML	\times	$L^2 L^M + L$

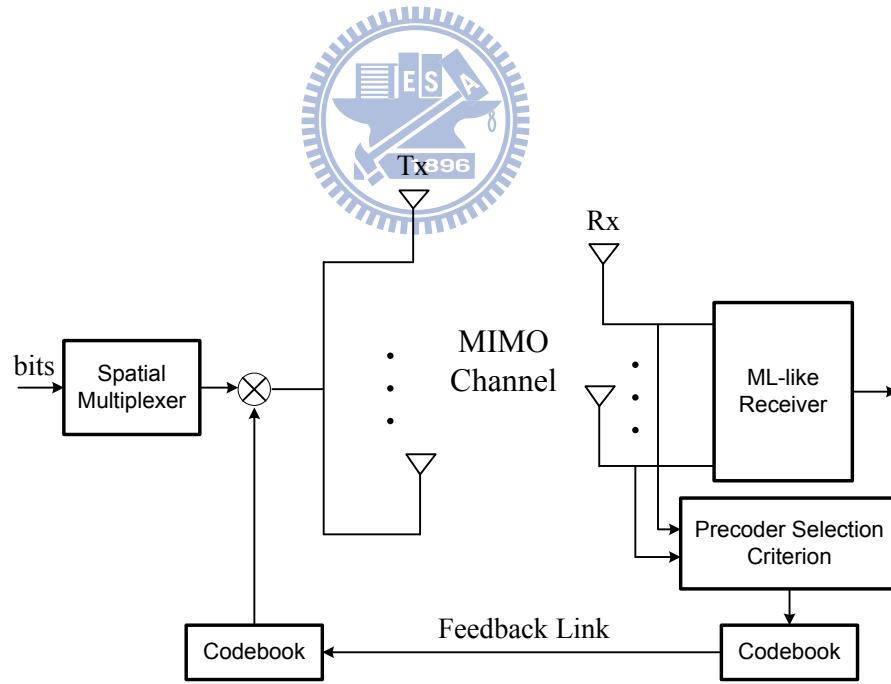


Figure 4.1: System model for a limited-feedback precoding MIMO system.

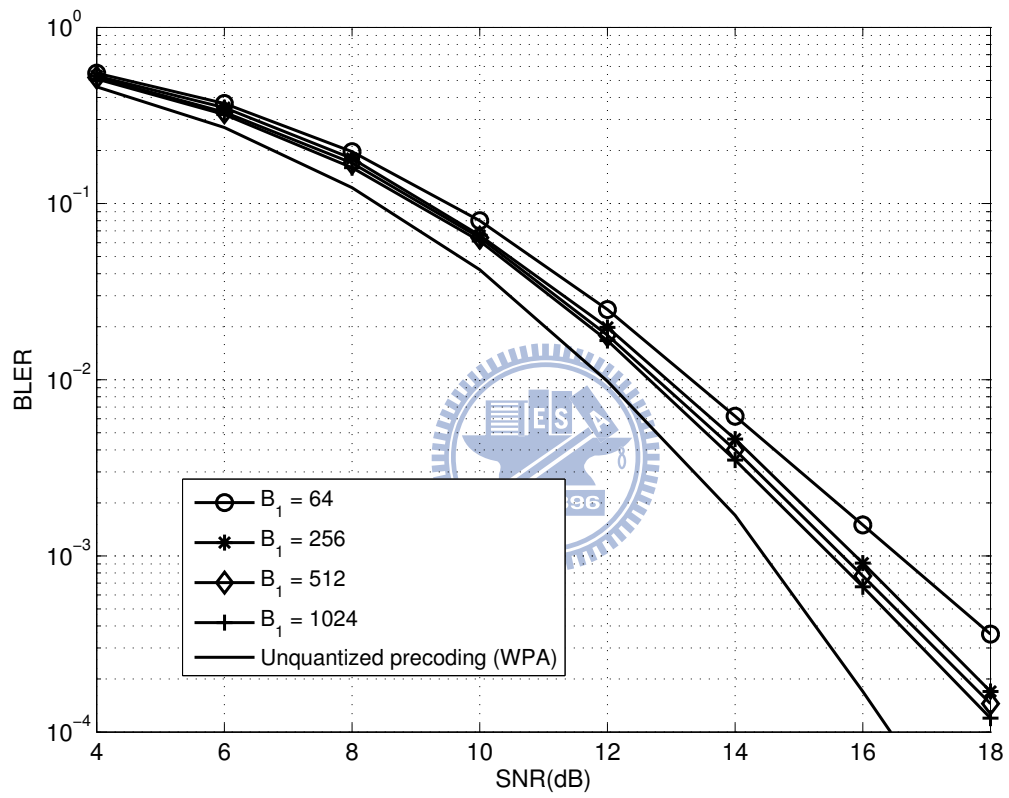


Figure 4.2: Performance comparisons for different sizes of \mathcal{F}_1 .

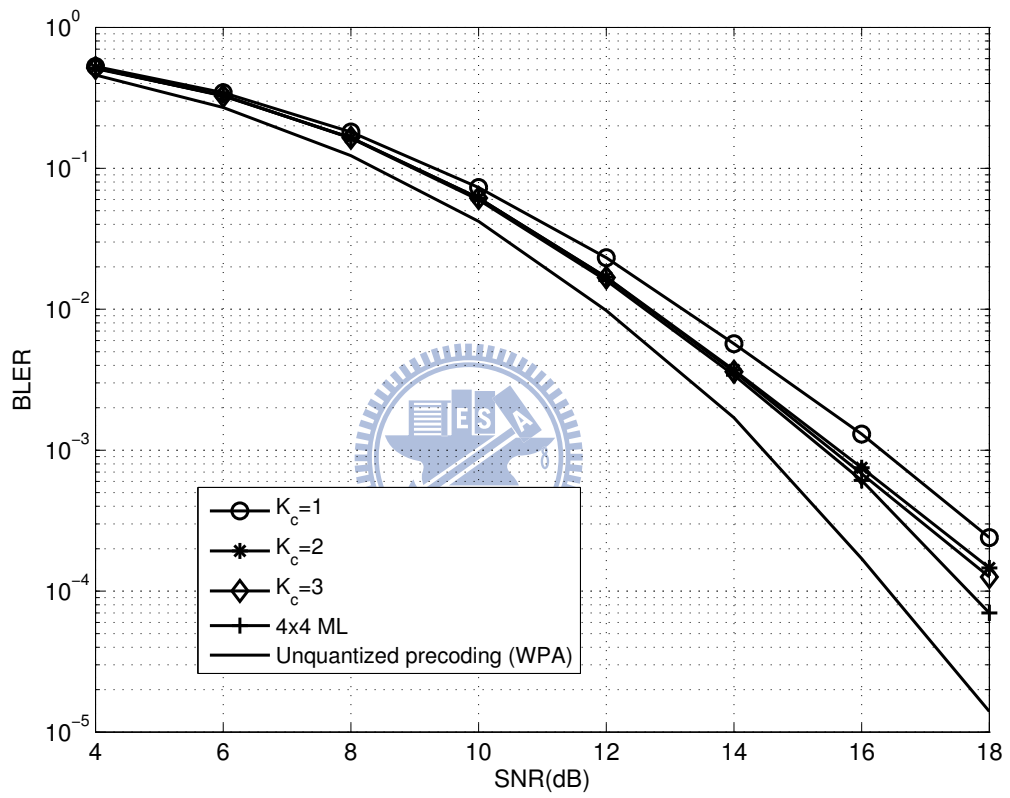


Figure 4.3: Performance comparisons for different values of K_c .

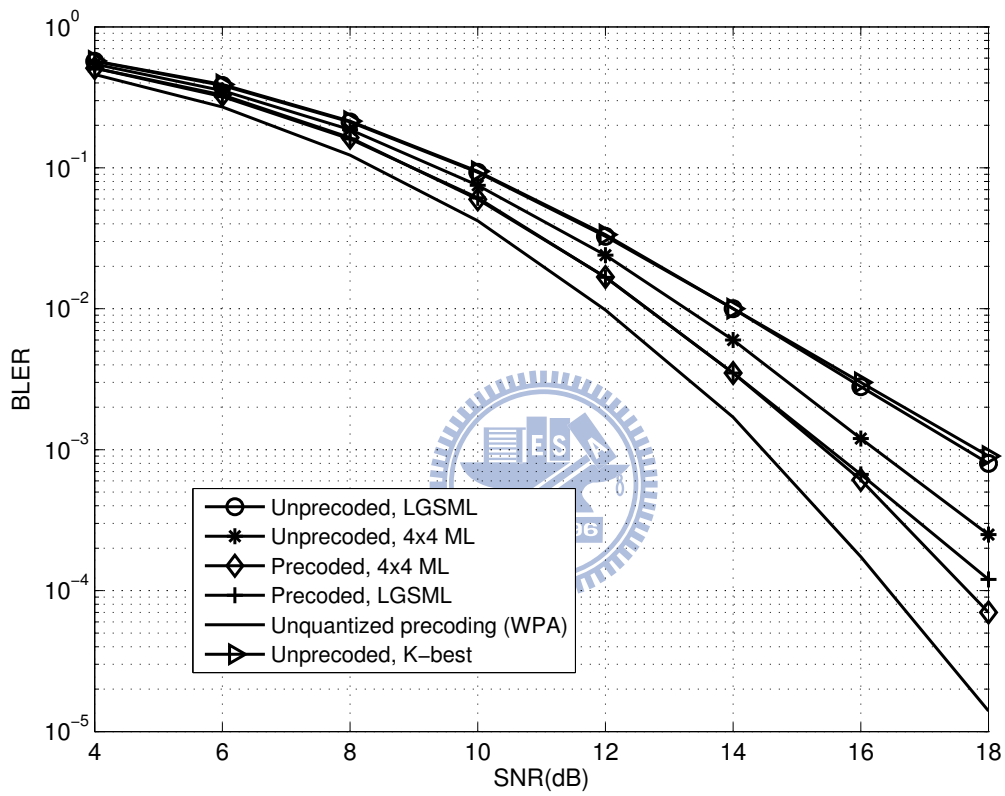


Figure 4.4: Performance comparisons for unprecoded and precoded systems with $N_t = 4$, $N_r = 4$, and $M = 4$.

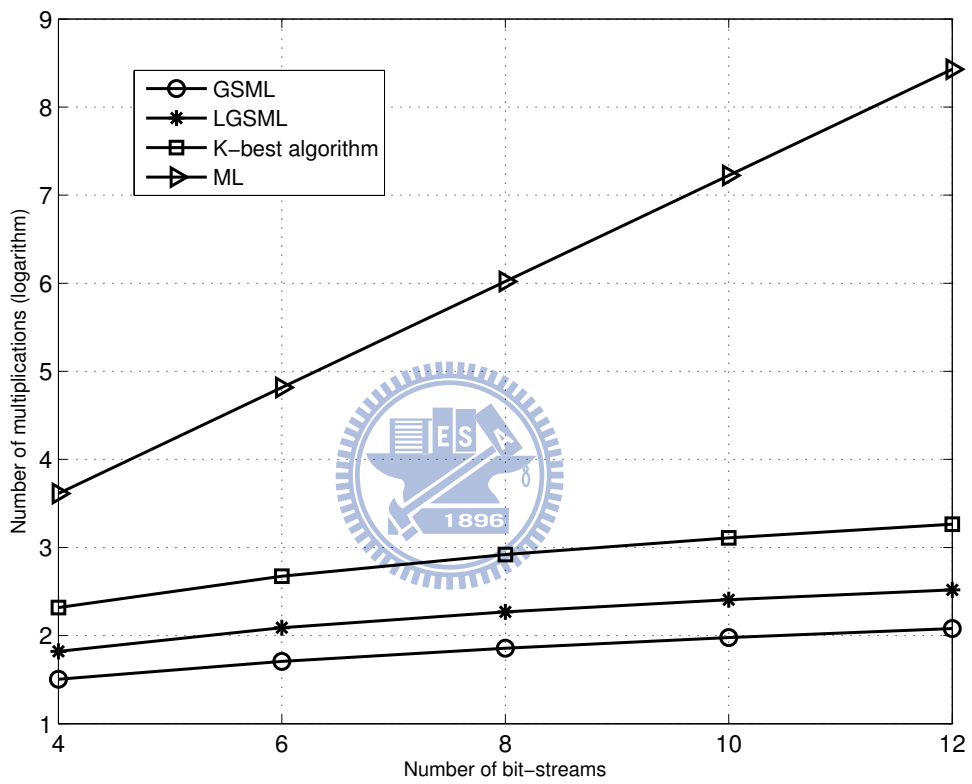
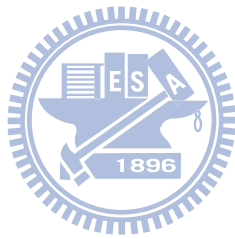


Figure 4.5: Detection complexity comparisons for unprecoded systems with different values of M .



Chapter 5

Conclusions

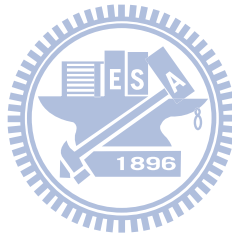
In this dissertation, we have investigated the precoder design for the ML detector in MIMO and MIMO relay systems. It is known that the optimum precoder can be found by maximizing the free distance. However, this optimization problem is difficult to solve. To overcome this problem, we first considered a simplified precoding scheme, namely, transmit antenna selection. Instead of maximizing free distance itself, we proposed using a QRD-based lower bound as the selection criterion. For further performance improvement, a basis-transformation method was proposed so that the QRD-based lower bound can be further tightened. We have shown that the proposed methods can be effectively applied to other scenarios such as receive antenna selection, and joint transmit and receive antenna selection. Although antenna selection is simple, its performance improvement may be limited. We then considered precoding with X-structure, a simple and effective precoding scheme for the ML detector. Most existing subprecoders require numerical searches in design and table look-up operations in run time. To remedy this problem, we proposed using the GMD design method combined with a rank-deficient subprecoder. The proposed method was then extended to the joint precoders design for a two-hop AF MIMO relay system. To facilitate the derivation of the precoders, we applied an iterative method solving the source and relay precoders, repeatedly. With some mild assumptions, the precoders can be efficiently solved by the KKT conditions. Finally, we investigated the X-structured precoder

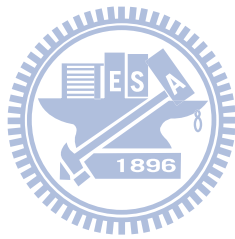
design in the limited-feedback scenario. We proposed a low-complexity detection method so that the performance loss due to quantization error can be mitigated. With a small feedback overhead, the proposed precoders can still be effective in MIMO systems.

In concluding the dissertation, we suggest some possible topics for future research.

1. In this dissertation, we only consider antenna selection in a single-carrier system. Nowadays, multicarrier systems, such as orthogonal frequency division multiplexing (OFDM), are widely used. As a nature extension, the proposed selection method can be applied in such system. However, note that basis-transformation must be conducted in each carrier and this requires high computational complexity. Hence, how to design a low-complexity selection criterion for MIMO-OFDM systems is an interesting future work.
2. In this dissertation, we only study a two-hop AF MIMO relay system. In such system, there is only one relay node. In a general relay system, there may be multiple relay nodes and multi-hops. Hence, how to conduct antenna selection or X-structured precoding in the system can be challenging and deserves for further research.
3. In two-hop AF MIMO relay systems, the relay precoder is derived based on the diagonalization of an equivalent MIMO channel. Although this approach is simple and effective, it may suffer from performance loss due to its sub-optimality. The derivation of the optimum relay precoder is still an open issue and deserves further research.
4. In this dissertation, the proposed precoding method in limited-feedback scenario is simple and easy to realize. However, the number of quantization bits may become large when a large-size MIMO system is considered. How to reduce the feedback overhead with limited performance loss also deserves further studies.
5. In this dissertation, we only consider X-structured precoding in limited-feedback MIMO systems. The extension to a MIMO relay system will be much more difficult and complicated. For example, the CSI of the source-to-relay link may not be available at the destination in real-world systems. How to solve this problem is also an interesting topic.

6. In the limited-feedback scenario, the codeword is selected by evaluating all possible codewords in a codebook. This may lead to high computational complexity for a large-size codebook. Hence, designing an codebook allowing an efficient codeword search also deserves further research.
7. In this dissertation, we only consider single-user environments. In real-world applications, however, the transmitter may serve multiple users. Since multiple-user interference will result, the precoding problem becomes much more involved. Whether or not the X-structure can still be used can server as a subject for further investigation.





Appendix A

§ A.1 SVD-Based Lower Bound with Transformed Symbol Vectors

In what follows, we will show that the SVD-based lower bound can still be used when a transformation is conducted on \mathbf{x} . Starting from (2.16), we can rewrite the free distance as

$$d_{\text{free}} = \min_{\bar{\mathbf{x}}, \bar{\mathbf{x}}' \in \bar{\mathcal{X}}^M, \bar{\mathbf{x}} \neq \bar{\mathbf{x}}'} \frac{\|\bar{\mathbf{H}}_p(\bar{\mathbf{x}} - \bar{\mathbf{x}}')\|}{\|\bar{\mathbf{x}} - \bar{\mathbf{x}}'\|} \|\bar{\mathbf{x}} - \bar{\mathbf{x}}'\|. \quad (\text{A1})$$

Using the Rayleigh-Ritz theorem, we can have the following result:

$$\frac{\|\bar{\mathbf{H}}_p(\bar{\mathbf{x}} - \bar{\mathbf{x}}')\|}{\|\bar{\mathbf{x}} - \bar{\mathbf{x}}'\|} \geq \min_{\bar{\mathbf{x}} \neq \bar{\mathbf{x}}'} \frac{\|\bar{\mathbf{H}}_p(\bar{\mathbf{x}} - \bar{\mathbf{x}}')\|}{\|\bar{\mathbf{x}} - \bar{\mathbf{x}}'\|} = \bar{\lambda}_M \quad (\text{A2})$$

where $\bar{\lambda}_M$ is the minimum singular value of $\bar{\mathbf{H}}_p$. Consequently, we can have the modified SVD-based lower bound expressed as

$$d_{\text{free}} \geq \bar{\lambda}_M d_{\min}(\bar{\mathcal{X}}^M) \quad (\text{A3})$$

where $d_{\min}(\bar{\mathcal{X}}^M)$ is defined as (2.5). From (A3), it can be seen that the SVD-based lower bound is still valid though the entries of $\bar{\mathbf{x}}$ are correlated. However, $d_{\min}(\bar{\mathcal{X}}^M)$ is no longer straightforward to obtain. Finding $d_{\min}(\bar{\mathcal{X}}^M)$ may require an exhaustive search algorithm.

§ A.2 Evaluation of (2.27)

For the ease of description, we assume that the symbol vector is scaled and shifted such that the symbol before and after the transformation are located on the same lattice. As defined, for an $M \times M$ MIMO system, the LR-transformed symbol vector will be $\mathbf{x}_{\text{LR}} = \mathbf{P}^{-1}\mathbf{x}$. Let $\mathbf{x}_{\text{LR}} = [x_{\text{LR},1}, x_{\text{LR},2}, \dots, x_{\text{LR},M}]^T$. Denote the (n, k) th entry of \mathbf{P}^{-1} as $P_{n,k}^I$. Then, the n th entry of \mathbf{x}_{LR} can be obtained by

$$x_{\text{LR},n} = \sum_{k=1}^M P_{n,k}^I x_k. \quad (\text{A4})$$

Note that $P_{n,k}^I$ is a complex integer, and $x_{\text{LR},n}$ is a combination of x_1, x_2, \dots , and x_M . If x_k has S constellation points, $x_{\text{LR},n}$ may have S^M constellation points. As we can see, the number of the constellation points for $x_{\text{LR},n}$ can be greatly increased. As defined, $d_{\min}(\mathcal{X}_{\text{LR},n}) = \min |x_n - x'_n|$. Note that $d_{\min}(\mathcal{X}_{\text{LR},n})$ is changed only when no constellation points are allocated in neighbor. Besides, $d_{\min}(\mathcal{X}_{\text{LR}}^1)$ is changed only when all $d_{\min}(\mathcal{X}_{\text{LR},n})$'s are changed.

We now use an examples to illustrate this property. Consider a 2×2 system with QPSK modulation for each transmit antenna. Let an LR matrix \mathbf{P} be given by

$$\mathbf{P} = \begin{bmatrix} 2 - 1j & 4 + 1j \\ 1 & 1 + 1j \end{bmatrix}.$$

Assume that the minimum distance of the original symbol constellation is g . That is,

$$d_{\min}(\mathcal{X}_1) = d_{\min}(\mathcal{X}_2) = d_{\min}(\mathcal{X}^M) = g.$$

Note that LR makes the transformed vectors located on the original constellation lattice. Therefore, we can have the result that $d_{\min}(\mathcal{X}_{\text{LR},1}) \geq g$ and $d_{\min}(\mathcal{X}_{\text{LR},2}) \geq g$. Figure A1 shows the constellations before and after the transformation. It can be seen that $d_{\min}(\mathcal{X}_{\text{LR},1}) > g$ while $d_{\min}(\mathcal{X}_{\text{LR},2}) = g$. As defined, we have

$$d_{\min}(\mathcal{X}_{\text{LR}}^1) = \min\{d_{\min}(\mathcal{X}_{\text{LR},1}), d_{\min}(\mathcal{X}_{\text{LR},2})\} = g. \quad (\text{A5})$$

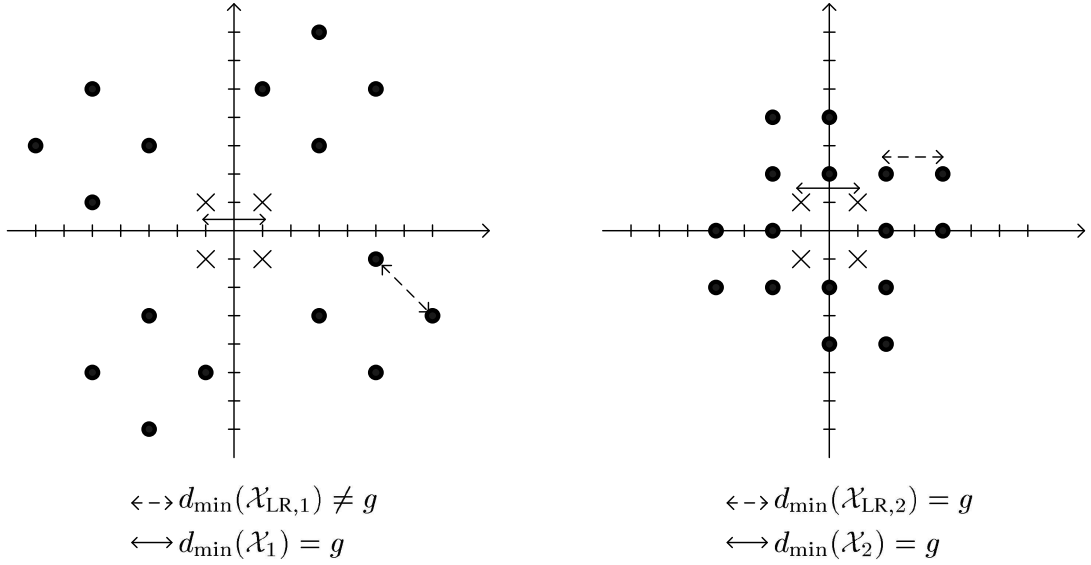


Figure A1: Symbol constellations in which $d_{\min}(\mathcal{X}_{LR}^1) = d_{\min}(\mathcal{X}^M)$ ($M = 2$, \times : original constellation, \bullet : transformed constellation).

From (A5), we can see that $d_{\min}(\mathcal{X}_{LR}^1) = d_{\min}(\mathcal{X}^M)$ when at least one of $\{d_{\min}(\mathcal{X}_{LR,1}), d_{\min}(\mathcal{X}_{LR,2})\}$ is equal to g . This result clearly indicates that $d_{\min}(\mathcal{X}_{LR}^1)$ is larger than g only when all $d_{\min}(\mathcal{X}_{LR,i})$'s are changed simultaneously. Fortunately, the case that all $d_{\min}(\mathcal{X}_{LR,i})$'s are changed can be of very low probability when M increases. From simulations, we found that the probability of $d_{\min}(\mathcal{X}_{LR}^1) \neq g$ is about 10^{-3} for $M = 2$, and it can be lower than 10^{-6} when $M = 3$. Thus, we can assume that the value of $d_{\min}(\mathcal{X}_{LR}^1)$ is the same for all candidate channel matrices.

§ A.3 Proof of (2.28)

In the CLLL algorithm shown in Table 2.2, the reduction operations are performed on two neighbor columns sequentially, from the left to the right column pairs. Consider a candidate channel matrix \mathbf{H}_p with its QRD expressed as $\mathbf{H}_p = \mathbf{Q}\mathbf{R}$. For the $(m - 1)$ th neighbor column pair of \mathbf{R} , the swap will occur when the condition that $\delta |R_{m-1,m-1}|^2 > |R_{m,m}|^2 + |R_{m-1,m}|^2$ is met, where $m = 2, 3, \dots, M$. Let $\mathbf{\Pi}^{(m-1)}$ be a permutation matrix that swaps the $(m - 1)$ th and

m th columns of \mathbf{R} . We can have $\mathbf{H}_p \mathbf{\Pi}^{(m-1)} = \mathbf{Q} \mathbf{R} \mathbf{\Pi}^{(m-1)} = \mathbf{Q} \mathbf{R}'$. Then, the Givens rotation matrix Θ , expressed as

$$\Theta = \begin{bmatrix} \frac{(R'_{m-1,m-1})^H}{\|\mathbf{R}'_{(m-1:m,m-1)}\|} & \frac{R'_{m,m-1}}{\|\mathbf{R}'_{(m-1:m,m-1)}\|} \\ \frac{-R'_{m,m-1}}{\|\mathbf{R}'_{(m-1:m,m-1)}\|} & \frac{R'_{m-1,m-1}}{\|\mathbf{R}'_{(m-1:m,m-1)}\|} \end{bmatrix},$$

is applied so that \mathbf{R}' can be transferred into an upper-triangular matrix denoted as \mathbf{R}'' . Letting

$$\mathbf{R}''_{(m-1:m,m-1:M)} = \Theta \mathbf{R}'_{(m-1:m,m-1:M)},$$

we can have

$$|R''_{1,1}|^2 = \frac{(|R_{m-1,m}|^2 + |R_{m,m}|^2)^2}{w} \quad (\text{A6})$$

$$|R''_{2,2}|^2 = \frac{|R_{m-1,m-1}|^2 |R_{m,m}|^2}{w} \quad (\text{A7})$$

where $w = |R_{m-1,m}|^2 + |R_{m,m}|^2$ is a real-valued number. Then,

$$\begin{aligned} |R''_{1,1}|^2 &= \frac{(|R_{m-1,m}|^2 + |R_{m,m}|^2)^2}{w} \\ &= |R_{m-1,m}|^2 + |R_{m,m}|^2 \\ &\geq |R_{m,m}|^2. \end{aligned} \quad (\text{A8})$$

Notice that $\delta |R_{m-1,m-1}|^2 > |R_{m,m}|^2 + |R_{m-1,m}|^2$, which means $|R_{m-1,m-1}|^2 > |R_{m,m}|^2 + |R_{m-1,m}|^2$ since $0.5 < \delta < 1$. Hence, we have

$$|R''_{1,1}|^2 = |R_{m-1,m}|^2 + |R_{m,m}|^2 < |R_{m-1,m-1}|^2. \quad (\text{A9})$$

From (A8) and (A9), we know

$$|R_{m,m}|^2 \leq |R''_{1,1}|^2 < |R_{m-1,m-1}|^2. \quad (\text{A10})$$

Next, we will show that $|R''_{2,2}|^2$ also has the similar property as that in (A10). First, $|R''_{2,2}|^2$ can be expressed as

$$\begin{aligned} |R''_{2,2}|^2 &= \frac{|R_{m-1,m-1}|^2 |R_{m,m}|^2}{w} \\ &= \frac{|R_{m-1,m-1}|^2 |R_{m,m}|^2}{|R_{m-1,m}|^2 + |R_{m,m}|^2}. \end{aligned} \quad (\text{A11})$$

Using the fact that $|R_{m,m}|^2 + |R_{m-1,m}|^2 < |R_{m-1,m-1}|^2$, we can have

$$|R''_{2,2}|^2 > \frac{|R_{m-1,m-1}|^2 |R_{m,m}|^2}{|R_{m-1,m-1}|^2} = |R_{m,m}|^2. \quad (\text{A12})$$

Second, it is obvious that $|R_{m-1,m}|^2 + |R_{m,m}|^2 \geq |R_{m,m}|^2$. Therefore,

$$\begin{aligned} |R''_{2,2}|^2 &= \frac{|R_{m-1,m-1}|^2 |R_{m,m}|^2}{|R_{m-1,m}|^2 + |R_{m,m}|^2} \\ &\leq \frac{|R_{m-1,m-1}|^2 |R_{m,m}|^2}{|R_{m,m}|^2} \\ &= |R_{m-1,m-1}|^2. \end{aligned} \quad (\text{A13})$$

Combining (A12) with (A13), we have

$$|R_{m,m}|^2 < |R''_{2,2}|^2 \leq |R_{m-1,m-1}|^2. \quad (\text{A14})$$

Using (A10) and (A14), we can see that when the swap operation occurs at the $(m-1)$ th column pair,

$$\begin{aligned} |R_{m,m}|^2 &\leq \min\{|R''_{1,1}|^2, |R''_{2,2}|^2\} \\ &\leq \max\{|R''_{1,1}|^2, |R''_{2,2}|^2\} \\ &\leq |R_{m-1,m-1}|^2. \end{aligned} \quad (\text{A15})$$

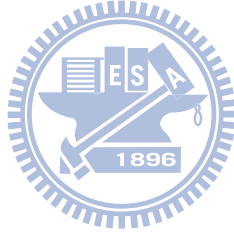
Then, we consider the condition for $\delta |R_{m-1,m-1}|^2 \leq |R_{m,m}|^2 + |R_{m-1,m}|^2$, where the swap operation is not conducted. Obviously, $|R_{m,m}|^2 = |R''_{2,2}|^2$ and $|R_{m-1,m-1}|^2 = |R''_{1,1}|^2$. Note that, in this case, we cannot determine if $|R_{m-1,m-1}|^2$ or $|R_{m,m}|^2$ is larger. Taking this case into consideration, we can have the following inequality:

$$\begin{aligned} &\min\{|R_{m-1,m-1}|^2, |R_{m,m}|^2\} \\ &\leq \min\{|R''_{1,1}|^2, |R''_{2,2}|^2\} \end{aligned} \quad (\text{A16})$$

$$\leq \max\{|R''_{1,1}|^2, |R''_{2,2}|^2\} \quad (\text{A17})$$

$$\leq \max\{|R_{m-1,m-1}|^2, |R_{m,m}|^2\}. \quad (\text{A18})$$

From the results of (A16)-(A18), we observe that the swap operation in the CLLL algorithm can enlarge the value of $\min\{|R_{m-1,m-1}|^2, |R_{m,m}|^2\}$. Let $[\mathbf{R}]_{\min}^{(m-1)}$ denote the minimum diagonal entry of \mathbf{R}'' when the CLLL algorithm has processed the $(m-1)$ th neighbor column pair. Note that $[\mathbf{R}]_{\min}^{(m-1)}$ is not necessarily identical to $\min\{|R_{m-1,m-1}|, |R_{m,m}|\}$. Also let $[\mathbf{R}]_{\min}^{(1)} = [\mathbf{R}]_{\min}$. Besides, we can see that $[\mathbf{R}]_{\min}^{(M-1)} \geq [\mathbf{R}]_{\min}^{(1)}$ when the CLLL algorithm has completed its processing. Since $[\mathbf{R}]_{\min}^{(M-1)} = [\mathbf{R}_{\text{LR}}]_{\min}$, we can conclude that $[\mathbf{R}_{\text{LR}}]_{\min} \geq [\mathbf{R}]_{\min}$.



Appendix B

§ B.1 Proof of (3.57)

Let x be fixed and define two functions $f(y)$ and $g(y)$ as:

$$f(y) = \exp^{-x^{w_1} y^{w_2}} \quad (\text{B1})$$

$$g(y) = w_1 \exp^{-x} + w_2 \exp^{-y} \quad (\text{B2})$$

where we assume $y \geq x \geq 1$ and $w_1 + w_2 = 1$. The problem now is to prove that $f(y) \leq g(y)$. Assume that both $f(y)$ and $g(y)$ are continuous and differentiable for $y \geq x$. Then, we can rewrite $f(y)$ and $g(y)$ as:

$$f(y) = f(x) + \int_x^y f'(t_1) dt_1 \quad (\text{B3})$$

$$g(y) = g(x) + \int_x^y g'(t_1) dt_1 \quad (\text{B4})$$

where $f'(t_1)$ and $g'(t_1)$ denote the first derivative of $f(t_1)$ and $g(t_1)$ respectively. From (B1) and (B2), it is easy to verify that $f(x) = g(x)$. Hence, the problem is equivalent to showing that

$$\int_x^y f'(t_1) dt_1 \leq \int_x^y g'(t_1) dt_1. \quad (\text{B5})$$

It is simple to see that if $f'(t_1) \leq g'(t_1)$ for $t_1 \geq x$, then (B5) holds true. Consequently, $f'(t_1)$ and $g'(t_1)$ can be expressed as:

$$f'(t_1) = -w_2 x^{w_1} \exp^{-x^{w_1} t_1^{w_2}} t_1^{w_2-1} \quad (\text{B6})$$

$$g'(t_1) = -w_2 \exp^{-t_1}. \quad (\text{B7})$$

Since $-w_2 < 0$, we see that the conditions $f'(t_1) \leq g'(t_1)$ and $\frac{-1}{w_2} f'(t_1) \geq \frac{-1}{w_2} g'(t_1)$ are equivalent. It can be seen that both $\frac{-1}{w_2} f'(t_1)$ and $\frac{-1}{w_2} g'(t_1)$ are positive values. Define two functions $f_1(t_1)$ and $g_1(t_1)$ as:

$$f_1(t_1) \triangleq \ln \frac{-f'(t_1)}{w_2} = w_1 \ln x - w_1 \ln t_1 - x^{w_1} t_1^{w_2} \quad (\text{B8})$$

$$g_1(t_1) \triangleq \ln \frac{-g'(t_1)}{w_2} = -t_1. \quad (\text{B9})$$

Hence, the problem now is equivalent to proving $f_1(t_1) \geq g_1(t_1)$. Using the similar method as that in (B3) and (B4), we can first rewrite $f_1(t_1)$ and $g_1(t_1)$ as follows:

$$f_1(t_1) = f_1(x) + \int_x^{t_1} f_1'(t_2) dt_2 \quad (\text{B10})$$

$$g_1(t_1) = g_1(x) + \int_x^{t_1} g_1'(t_2) dt_2. \quad (\text{B11})$$

It can be verified that $f_1(x) = g_1(x)$. Hence, if $f_1'(t_2) \geq g_1'(t_2)$ for $t_2 \geq x$, then $f_1(t_1) \geq g_1(t_1)$. From (B8) and (B9), we have

$$f_1'(t_2) = -\frac{w_1}{t_2} - x^{w_1} t_2^{w_2-1} w_2 \quad (\text{B12})$$

$$g_1'(t_2) = -1. \quad (\text{B13})$$

For $t_2 = x \geq 1$, we have

$$\begin{aligned} f_1'(t_2) |_{t_2=x} &= -\frac{w_1}{x} - x^{w_1} x^{w_2-1} w_2 \\ &= -\frac{w_1}{x} - w_2 \\ &\geq -(w_1 + w_2) = g_1'(t_2). \end{aligned} \quad (\text{B14})$$

For $t_2 > x \geq 1$, we observe that $\frac{x}{t_2} < 1$ and

$$\begin{aligned}
f_1'(t_2) |_{t_2 > x} &= -\frac{w_1}{t_2} - x^{w_1} t_2^{w_2-1} w_2 \\
&= -\frac{w_1}{t_2} - w_2 \left(\frac{x}{t_2}\right)^{w_1} \\
&\geq -w_1 - w_2 \left(\frac{x}{t_2}\right)^{w_1} \\
&> -w_1 - w_2 = g_1'(t_2).
\end{aligned} \tag{B15}$$

From (B14) and (B15), we can see that $f_1'(t_2) \geq g_1'(t_2)$ for any given $t_2 \geq x$. With this result, we can conclude that $f(y) \leq g(y)$ for $y \geq x \geq 1$, which completes the proof of this lemma.

§ B.2 Proof of (3.58)

Using Lemma 3.1, we now can use mathematical induction to prove Lemma 3.2. Without loss of generality, we can assume that $d_{\text{free},1}^2 \geq d_{\text{free},2}^2 \geq \dots \geq d_{\text{free},M'}^2$. Letting $w_1 = w_2 = \frac{1}{2}$, $y = \frac{d_{\text{free},1}^2}{4}$, and $x = \frac{d_{\text{free},2}^2}{4}$, we have the following inequality:

$$\exp^{-\sqrt{\frac{d_{\text{free},1}^2}{4} \frac{d_{\text{free},2}^2}{4}}} \leq \frac{1}{2} \exp^{-\frac{d_{\text{free},1}^2}{4}} + \frac{1}{2} \exp^{-\frac{d_{\text{free},2}^2}{4}}. \tag{B16}$$

From (B16), it is obvious that (3.58) is true for $M' = 2$. Then, we assume that the statement in Lemma 3.2 is true for $M' - 1$ ($M' > 3$). That is,

$$\exp^{-\frac{1}{4} \left(d_{\text{free},1}^2 d_{\text{free},2}^2 \dots d_{\text{free},M'-1}^2 \right)^{\frac{1}{M'-1}}} \leq \frac{1}{M'-1} \left(\exp^{-\frac{d_{\text{free},1}^2}{4}} + \exp^{-\frac{d_{\text{free},2}^2}{4}} + \dots + \exp^{-\frac{d_{\text{free},M'-1}^2}{4}} \right). \tag{B17}$$

Now, for the MIMO system with M' subsystems, we can have the following equivalence:

$$\exp^{-\frac{1}{4} \left(d_{\text{free},1}^2 d_{\text{free},2}^2 \dots d_{\text{free},M'}^2 \right)^{\frac{1}{M'}}} = \exp^{-\left(\frac{1}{4} \left(d_{\text{free},1}^2 d_{\text{free},2}^2 \dots d_{\text{free},M'-1}^2 \right)^{\frac{1}{M'-1}} \right)^{\frac{M'-1}{M'}}} \left(\frac{1}{4} d_{\text{free},M'}^2 \right)^{\frac{1}{M'}}. \tag{B18}$$

Using Lemma 3.1 again, we obtain

$$\begin{aligned}
& \exp^{-\left(\frac{1}{4}(d_{\text{free},1}^2 d_{\text{free},2}^2 \cdots d_{\text{free},M'-1}^2)^{\frac{1}{M'-1}}\right)^{\frac{M'-1}{M'}}} \left(\frac{1}{4}d_{\text{free},M'}^2\right)^{\frac{1}{M'}} \\
& \leq \frac{M'-1}{M'} \exp^{-\left(\prod_{i=1}^{M'-1} \frac{d_{\text{free},i}^2}{4}\right)^{\frac{1}{M'-1}}} + \frac{1}{M'} \exp^{-\frac{d_{\text{free},M'}^2}{4}}. \tag{B19}
\end{aligned}$$

Substituting (B17) into (B19), we can have the following inequality as:

$$\begin{aligned}
\exp^{-\frac{1}{4}(d_{\text{free},1}^2 d_{\text{free},2}^2 \cdots d_{\text{free},M'}^2)^{\frac{1}{M'}}} & \leq \frac{M'-1}{M'} \frac{1}{M'-1} \sum_{i=1}^{M'-1} \exp^{-\frac{d_{\text{free},i}^2}{4}} + \frac{1}{M'} \exp^{-\frac{d_{\text{free},M'}^2}{4}} \\
& = \frac{1}{M'} \sum_{i=1}^{M'-1} \exp^{-\frac{d_{\text{free},i}^2}{4}} + \frac{1}{M'} \exp^{-\frac{d_{\text{free},M'}^2}{4}} \\
& = \frac{1}{M'} \sum_{i=1}^{M'} \exp^{-\frac{d_{\text{free},i}^2}{4}}. \tag{B20}
\end{aligned}$$

It can be verified that the equality in (B20) can be held when all $d_{\text{free},i}$ are equal. From (B20), we can have

$$\sum_{i=1}^{M'} \exp^{-\frac{d_{\text{free},i}^2}{4}} \geq M' \exp^{-\frac{1}{4}\left(\prod_{i=1}^{M'} d_{\text{free},i}^2\right)^{\frac{1}{M'}}} \tag{B21}$$

which completes the proof of Lemma 3.2.

§ B.3 Derivation of (3.68)

The Lagrangian function in (3.67) can be express as:

$$\mathcal{L} = -\sum_{i=1}^M \frac{\sigma_{R,i}^2 \sigma_{rd,i}^2}{\sigma_{R,i}^2 \sigma_{rd,i}^2 \sigma_{n,r}^2 + \sigma_{n,d}^2} + \frac{1}{\mu} \left(\sum_{i=1}^M \sigma_{R,i}^2 (\sigma_{n,r}^2 + \mathbf{B}(i,i) \sigma_{sr,i}^2) - P_{R,T} \right) - \sum_{i=1}^M \mu_i \sigma_{R,i}^2 \tag{B22}$$

where $\mu \geq 0$ and $\mu_i \geq 0$. By the KKT conditions for all $i = 1, 2, \dots, M$, we can have

$$\begin{aligned} \frac{d\mathcal{L}}{d\sigma_{R,i}^2} &= -\frac{\sigma_{R,i}^2 \sigma_{rd,i}^2 \sigma_{n,r}^2 + \sigma_{n,d}^2 \sigma_{rd,i}^2 (\sigma_{R,i}^2 \sigma_{rd,i}^2 \sigma_{n,r}^2 + \sigma_{n,d}^2) - \sigma_{R,i}^2 \sigma_{rd,i}^4 \sigma_{n,r}^2}{\sigma_{R,i}^2 \sigma_{rd,i}^2 (\sigma_{n,r}^2 + \mathbf{B}(i, i) \sigma_{sr,i}^2) - \mu_i \sigma_{R,i}^2} \\ &+ \frac{1}{\mu} (\sigma_{n,r}^2 + \mathbf{B}(i, i) \sigma_{sr,i}^2) - \mu_i \sigma_{R,i}^2 = 0; \end{aligned} \quad (\text{B23})$$

$$\mu, \mu_i, \sigma_{R,i}^2 \geq 0; \quad (\text{B24})$$

$$\mu_i \sigma_{R,i}^2 = 0; \quad (\text{B25})$$

$$\frac{1}{\mu} \left(\sum_{i=1}^M \sigma_{R,i}^2 (\sigma_{n,r}^2 + \mathbf{B}(i, i) \sigma_{sr,i}^2) - P_{R,T} \right) = 0. \quad (\text{B26})$$

Using (B23), (B24), (B25), and (B26), we can have

$$\sigma_{R,i}^2 = \sqrt{\frac{\mu \sigma_{n,d}^2}{\sigma_{rd,i}^2 \sigma_{n,r}^2 (\sigma_{n,r}^2 + \mathbf{B}(i, i) \sigma_{sr,i}^2)} + \left(\frac{\sigma_{n,d}^2}{2\sigma_{rd,i}^2 \sigma_{n,r}^2} \right)^2} - \frac{\sigma_{n,d}^2}{2\sigma_{rd,i}^2 \sigma_{n,r}^2}.$$

§ B.4 Derivation of (3.80)

Similarly, the Lagrangian function in (3.79) can be express as:

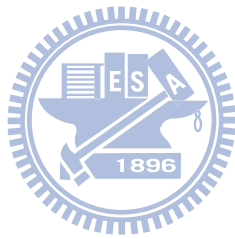
$$\mathcal{L} = -\sum_{i=1}^r \frac{\kappa_i \sigma_{R,i}^2 \sigma_{rd,i}^2}{\sigma_{R,i}^2 \sigma_{rd,i}^2 \sigma_{n,r}^2 + \sigma_{n,d}^2} + \frac{1}{\mu} \left(\sum_{i=1}^r \sigma_{R,i}^2 (\sigma_{n,r}^2 + \mathbf{B}(i, i) \sigma_{sr,i}^2) - P_{R,T} \right) - \sum_{i=1}^r \mu_i \sigma_{R,i}^2 \quad (\text{B27})$$

where $\mu \geq 0$, $\mu_i \geq 0$, and κ_i is defined in (3.78). By the KKT conditions, we can have

$$\frac{\kappa_i}{\sigma_{R,i}^2} \frac{\sigma_{n,d}^2}{\sigma_{R,i}^2 \sigma_{rd,i}^2 \sigma_{n,r}^2 + \sigma_{n,d}^2} = \frac{1}{\mu} (\sigma_{n,r}^2 + \mathbf{B}(i, i) \sigma_{sr,i}^2). \quad (\text{B28})$$

Let $\bar{\mu}_i = \mu \kappa_i$ for $i = 1, 2, \dots, r$. From (B28), it can be easily verified that $\sigma_{R,i}^2$ can be expressed as:

$$\sigma_{R,i}^2 = \sqrt{\frac{\bar{\mu}_i \sigma_{n,d}^2}{\sigma_{rd,i}^2 \sigma_{n,r}^2 (\sigma_{n,r}^2 + \mathbf{B}(i, i) \sigma_{sr,i}^2)} + \left(\frac{\sigma_{n,d}^2}{2\sigma_{rd,i}^2 \sigma_{n,r}^2} \right)^2} - \frac{\sigma_{n,d}^2}{2\sigma_{rd,i}^2 \sigma_{n,r}^2}.$$



Bibliography

- [1] G. J. Foschini, "Layered space-time architecture for wireless communication in a fading environment when using multiple antennas," *Bell Labs. Tech. J.*, vol. 1, no. 2, pp. 41-59, 1996.
- [2] L. Zheng, and D. N. C. Tse, "Diversity and multiplexing: A fundamental tradeoff in multiple-antenna channels," *IEEE Trans. Inform. Theory*, vol. 49, no. 5, pp. 1073-1096, May 2003.
- [3] A. Lozano, A. M. Tulino, and S. Verdu, "Optimum power allocation for parallel Gaussian channels with arbitrary input distributions," *IEEE Trans. Inform. Theory*, vol. 52, no. 7, pp. 3033-3051, Jul. 2006.
- [4] F. P. Cruz, M. R. D. Rodrigues, and S. Verdu, "MIMO Gaussian channels with arbitrary inputs: Optimal precoding and power allocation," *IEEE Trans. Inform. Theory*, vol. 56, no. 3, pp. 1070-1084, Mar. 2010.
- [5] P. Stoica and G. Ganesan, "Maximum-SNR spatial-temporal forming designs for MIMO channels," *IEEE Trans. Signal Process.*, vol. 50, no. 12, pp. 3036-3042, Dec. 2002.
- [6] H. Sampath, P. Stoica, and A. Paulraj, "Generalized linear precoder and decoder design for MIMO channels using the weighted MMSE criterion," *IEEE Trans. Commun.*, vol. 49, no. 12, pp. 2198-2206, Dec. 2001.

- [7] A. Scaglione, P. Stoica, S. Barbarossa, G. B. Giannakis, and H. Sampath, "Optimal designs for space-time linear precoders and decoders," *IEEE Trans. Signal Process.*, vol. 50, no. 5, pp. 1051-1064, May 2002.
- [8] D. P. Palomar, J. M. Cioffi, and M. A. Lagunas, "Joint Tx-Rx beamforming design for multicarrier MIMO channels: A unified framework for convex optimization," *IEEE Trans. Signal Process.*, vol. 51, no. 9, pp. 2381-2401, Sep. 2003.
- [9] Y. Jiang, J. Li, and W. W. Hager, "Joint transceiver design for MIMO communications using geometric mean decomposition," *IEEE Trans. Signal Process.*, vol. 53, no. 10, pp. 3791-3803, Oct. 2005.
- [10] J.-K. Zhang, A. Kavčić, and K. M. Wong, "Equal-diagonal QR decomposition and its application to precoder design for successive-cancellation detection," *IEEE Trans. Inform. Theory*, vol. 51, no. 1, pp. 154-172, Jan. 2005.
- [11] Y. Jiang, J. Li, and W. W. Hager, "Uniform channel decomposition for MIMO Communications," *IEEE Trans. Signal Process.*, vol. 53, no. 11, pp. 4283-4294, Nov. 2005.
- [12] S. Bergman, D. P. Palomar, and B. Ottersten, "Joint bit allocation and precoding for MIMO systems with decision feedback detection," *IEEE Trans. Signal Process.*, vol. 57, no. 11, pp. 4509-4521, Nov. 2009.
- [13] C.-C. Weng, C.-Y. Chen, and P. P. Vaidyanathan, "MIMO transceivers with decision feedback and bit loading: Theory and optimization," *IEEE Trans. Signal Process.*, vol. 58, no. 3, pp. 1334-1346, Mar. 2010.
- [14] S. Sanayei and A. Nosratinia, "Capacity of MIMO channels with antenna selection," *IEEE Trans. Inform. Theory*, vol. 53, no. 11, pp. 4356-4362, Nov. 2007.
- [15] R. W. Heath, S. Sandhu, and A. Paulraj, "Antenna selection for spatial multiplexing systems with linear receivers," *IEEE Commun. Lett.*, vol. 5, no. 4, pp. 142-144, Apr. 2001.

- [16] C. Mun, "Transmit-antenna selection for spatial multiplexing systems with ordered successive interference cancellation," *IEEE Trans. Commun.*, vol. 54, no. 3, pp. 423-429, Mar. 2006.
- [17] F. Kharrat-Kammoun, S. Fontenelle, S. Rouquette, and J. Boutros, "Antenna selection for MIMO systems based on an accurate approximation of QAM error probability," in *Proc. IEEE Vehicular Technology Conf.*, Stockholm, Sweden, May 2005, pp. 206-210.
- [18] R. W. Heath Jr. and A. Paulraj, "Antenna selection for spatial multiplexing systems based on minimum error rate," in *Proc. IEEE Int. Conf. Communications*, Helsinki, Finland, Jun. 2001, pp. 2276-2280.
- [19] H. Yao and G. W. Wornell, "Lattice-reduction-aided detectors for MIMO communication systems," in *Proc. IEEE Global Telecommunications Conf.*, Taipei, Taiwan, Nov. 2002, pp. 424-428.
- [20] D. Wübben, R. Böhnke, V. Kühn, and K. D. Kammeyer, "Near-maximum-likelihood detection of MIMO systems using MMSE-based lattice-reduction," in *Proc. IEEE Int. Conf. Communications*, Paris, France, Jun. 2004, pp. 798-802.
- [21] I. Berenguer and X. Wang, "MIMO antenna selection with lattice-reduction-aided linear receivers," *IEEE Trans. Veh. Technol.*, vol. 53, no. 5, pp. 1289-1302, Sep. 2004.
- [22] A. Gorokhov, D. A. Gore, and A. J. Paulraj, "Receive antenna selection for MIMO spatial multiplexing: theory and algorithms," *IEEE Trans. Signal Process.*, vol. 51, no. 11, pp. 2796-2807, Nov. 2003.
- [23] K. T. Phan and C. Tellambura, "Receive antenna selection based on union-bound minimization using convex optimization," *IEEE Signal Process. Lett.*, vol. 14, no. 9, pp. 609-612, Sep. 2007.

- [24] A. F. Molisch, M. Z. Win, and J. H. Winters, "Capacity of MIMO systems with antenna selection," *IEEE Trans. Wireless Commun.*, vol. 4, no. 4, pp. 1759-1772, Jul. 2005.
- [25] T. Gucluoglu and T. M. Duman, "Performance analysis of transmit and receive antenna selection over flat fading channels," *IEEE Trans. Wireless Commun.*, vol. 7, no. 8, pp. 3056-3065, Aug. 2008.
- [26] J. N. Laneman, D. N. C. Tse, and G. W. Wornell, "Cooperative diversity in wireless networks: Efficient protocols and outage behavior," *IEEE Trans. Inform. Theory*, vol. 50, no. 12, pp. 3062-3080, Dec. 2004.
- [27] B. Wang, J. Zhang, and A. Host-Madsen, "On the capacity of MIMO relay channels," *IEEE Trans. Inform. Theory*, vol. 51, no. 1, pp. 29-43, Jan. 2005.
- [28] B. Vrigneau, J. Letessier, P. Rostaing, L. Collin, and G. Burel, "Extension of the MIMO precoder based on the minimum Euclidean distance: A cross-form matrix," *IEEE J. Sel. Topics Signal Process.*, vol. 2, no. 2, pp. 135-146, Apr. 2008.
- [29] S. K. Mohammed, E. Viterbo, Y. Hong, and A. Chockalingam, "MIMO precoding with X- and Y-codes," *IEEE Trans. Inform. Theory*, vol. 57, no. 6, pp. 3542-3566, Jun. 2011.
- [30] K. P. Srinath and B. S. Rajan, "A low ML-decoding complexity, full-diversity, full-rate MIMO precoder," *IEEE Trans. Signal Process.*, vol. 59, no. 11, pp. 5485-5498, Nov. 2011.
- [31] L. Collin, O. Berder, P. Rostaing, and G. Burel, "Optimal minimum distance-based precoder for MIMO spatial multiplexing systems," *IEEE Trans. Signal Process.*, vol. 52, no. 3, pp. 617-627, Mar. 2004.
- [32] Q.-T. Ngo, O. Berder, and P. Scalart, "Minimum Euclidean distance based precoders for MIMO systems using rectangular QAM constellations," *IEEE Trans. Signal Process.*, vol. 60, no. 3, pp. 1527-1533, Mar. 2012.

- [33] Q.-T. Ngo, O. Berder, and P. Scalart, "Minimum Euclidean distance-based precoding for three-dimensional multiple input multiple output spatial multiplexing systems," *IEEE Trans. Wireless Commun.*, vol. 11, no. 7, pp. 2486-2495, Jul. 2012.
- [34] X. Tang and Y. Hua, "Optimal design of non-regenerative MIMO wireless relays," *IEEE Trans. Wireless Commun.*, vol. 6, no. 4, pp. 1398-1407, Apr. 2007.
- [35] R. Mo and Y. H. Chew, "Precoder design for non-regenerative MIMO relay systems," *IEEE Trans. Wireless Commun.*, vol. 8, no. 10, pp. 5041-5049, Oct. 2009.
- [36] W. Guan and H. Luo, "Joint MMSE transceiver design in non-regenerative MIMO relay systems," *IEEE Commun. Lett.*, vol. 12, no. 7, pp. 517-519, Jul. 2008.
- [37] F.-S. Tseng, W.-R. Wu and J.-Y. Wu, "Joint source/relay precoder design in nonregenerative cooperative systems using an MMSE criterion," *IEEE Trans. Wireless Commun.*, vol. 8, no. 10, pp. 4928-4933, Oct. 2009.
- [38] R. Mo and Y. H. Chew, "MMSE-based joint source and relay precoding design for amplify-and-forward MIMO relay networks," *IEEE Trans. Wireless Commun.*, vol. 8, no. 9, pp. 4668-4676, Sep. 2009.
- [39] F.-S. Tseng and W.-R. Wu, "Linear MMSE transceiver design in amplify-and-forward MIMO relay systems," *IEEE Trans. Veh. Technol.*, vol. 59, no. 2, pp. 754-765, Feb. 2010.
- [40] C. Song, K.-J. Lee, and I. Lee, "MMSE based transceiver designs in closed-loop non-regenerative MIMO relaying systems," *IEEE Trans. Wireless Commun.*, vol. 9, no. 7, pp. 2310-2319, Jul. 2010.
- [41] C. Xing, S. Ma, and Y.-C. Wu, "Robust joint design of linear relay precoder and destination equalizer for dual-hop amplify-and-forward MIMO relay systems," *IEEE Trans. Signal Process.*, vol. 58, no. 4, pp. 2273-2283, Apr. 2010.

- [42] Y. Rong, "Robust design for linear non-regenerative MIMO relays with imperfect channel state information," *IEEE Trans. Signal Process.*, vol. 59, no. 5, pp. 2455-2460, May 2011.
- [43] S. Boyd and L. Vandenberghe, *Convex Optimization*, Cambridge University Press 2004.
- [44] D. J. Love and R. W. Heath Jr., "Grassmannian beamforming for multiple-input multiple-output wireless systems," *IEEE Trans. Inform. Theory*, vol. 49, no. 10, pp. 2735-2747, Oct. 2003.
- [45] D. J. Love and R. W. Heath Jr., "Limited feedback unitary precoding for orthogonal space-time block codes," *IEEE Trans. Signal Process.*, vol. 53, no. 1, pp. 64-73, Jan. 2005.
- [46] D. J. Love and R. W. Heath Jr., "Limited feedback unitary precoding for spatial multiplexing systems," *IEEE Trans. Inform. Theory*, vol. 51, no. 8, pp. 2967-2976, Aug. 2005.
- [47] Y. Fu, C. Tellambura, and W. A. Krzymien, "Limited-feedback precoding for closed-loop multiuser MIMO OFDM systems with frequency offsets," *IEEE Trans. Wireless Commun.*, vol. 7, no. 11, pp. 4155-4165, Nov. 2008.
- [48] Q. Gao, X.-D. Zhang, J. Li, and W. Shi, "Linear precoding and finite rate feedback design for V-BLAST architecture," *IEEE Trans. Wireless Commun.*, vol. 7, no. 12, pp. 4976-4986, Dec. 2008.
- [49] Y. Linde, A. Buzo, and R. Gray, "An algorithm for vector quantizer design," *IEEE Trans. Commun.*, vol. 28, no. 1, pp. 84-95, Jan. 1980.
- [50] T. Guess, "Optimal sequences for CDMA with decision-feedback receivers," *IEEE Trans. Inform. Theory*, vol. 49, no. 4, pp. 886-900, Apr. 2003.
- [51] R. A. Horn and C. R. Johnson, *Matrix Analysis*. New York: Cambridge Univ. Press, 1985.
- [52] A. W. Marshall and I. Olkin, *Inequalities: Theory of Majorization and Its Applications*. New York: Academic, 1991.

- [53] G. Golub and C. F. Van Loan, *Matrix Computations*. 3rd ed. Baltimore, MD: Johns Hopkins Univ. Press, 1996.
- [54] N. Balakrishnan and A. C. Cohen, *Order Statistics and Inference Estimation Methods*. New York: Academic, 1991.
- [55] W. Zhao and G. B. Giannakis, "Reduced complexity closest point decoding algorithms for random lattices," *IEEE Trans. Wireless Commun.*, vol. 5, no. 1, pp. 101-111, Jan. 2006.
- [56] X. Ma and W. Zhang, "Performance analysis for MIMO systems with lattice-reduction aided linear equalization," *IEEE Trans. Commun.*, vol. 56, no. 2, pp. 309-318, Feb. 2008.
- [57] J.-Y. Wu, W.-R. Wu, and N.-C. Lien, "Low-complexity MIMO detection using a list projection technique," in *Proc. IEEE Int. Conf. Signal Processing and Communication Systems*, Gold Coast, Australia, Dec. 2008.
- [58] N. Al-Dhahir and J. M. Cioffi, "Optimum finite-length equalization for multicarrier transceivers," *IEEE Trans. Commun.*, vol. 44, no. 1, pp. 56-64, Jan. 1996.
- [59] F.-S. Tseng and W.-R. Wu, "Nonlinear transceiver designs in MIMO amplify-and-forward relay systems," *IEEE Trans. Veh. Technol.*, vol. 60, no. 2, pp. 528-538, Feb. 2011.
- [60] C.-T. Lin and W.-R. Wu, "QRD-based precoder selection for maximum-likelihood MIMO detection," in *Proc. IEEE Int. Symposium on personal, Indoor, and Mobile Radio Communications*, Istanbul, Turkey, Sep. 2010, pp. 455-460.
- [61] D. Tse and P. Viswanath, *Fundamentals of Wireless Communication*, Cambridge University Press 2005.

個人資料

姓名：林鈞陶

性別：男

出生年月日：民國 68 年 2 月 19 日

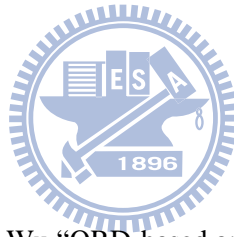
籍貫：台灣台南市

經歷：國立中正大學電機系畢業

國立交通大學電信工程研究所碩士班畢業

博士論文題目：Precoder Designs for Maximum-Likelihood
Detectors in MIMO and MIMO Relay Systems

Publication list:



A. Journal paper

1. **Chun-Tao Lin** and Wen-Rong Wu, "QRD-based antenna selection for ML detection of spatial multiplexing MIMO systems: Algorithms and Applications," *IEEE Trans. Vehicular Technology*, vol. 60, no. 7, pp. 3178-3191, Sep. 2011.
2. **Chun-Tao Lin** and Wen-Rong Wu, "X-structured precoder designs for spatial-multiplexing MIMO and MIMO relay systems," in preparation.

B. Conference paper

1. **Chun-Tao Lin** and Wen-Rong Wu, "Clipping ratio estimation for OFDM receivers," in *Proc. IEEE Vehicular Technology Conf. (VTC)*, Stockholm, Sweden, May 2005, pp.797-800.
2. **Chun-Tao Lin** and Wen-Rong Wu, "Receiver signal clipping for OFDM systems," in *Proc. International Conference on Signal and Systems*, Kaohsiung, Taiwan, Apr. 2005.
3. **Chun-Tao Lin** and Wen-Rong Wu, "QRD-based antenna selection for maximum-likelihood MIMO detection," in *Proc. IEEE Int. Symposium on personal, Indoor, and Mobile Radio Communications (PIMRC)*, Tokyo, Japan, Sep. 2009, pp.2016-2020.
4. **Chun-Tao Lin** and Wen-Rong Wu, "Joint mode switching and antenna selection for MIMO transmission," in *Proc. The 9th IEEE VTS Asia Pacific Wireless Communications Symposium (APWCS)*, Kaohsiung, Taiwan, Aug. 2010.

5. **Chun-Tao Lin** and Wen-Rong Wu, “QRD-based precoder selection for maximum-likelihood MIMO detection,” in *Proc. IEEE Int. Symposium on personal, Indoor, and Mobile Radio Communications (PIMRC)*, Istanbul, Turkey, Sep. 2010, pp.455-460.
6. **Chun-Tao Lin** and Wen-Rong Wu, “QRD-based antenna grouping for MIMO transmission,” in *Proc. IEEE Vehicular Technology Conf. (VTC)*, San Francisco, USA, Sep. 2011, pp.1-5.
7. **Chun-Tao Lin** and Wen-Rong Wu, “X-structured precoder design for spatial multiplexing MIMO systems,” to appear in *Proc. IEEE Global Telecommunications Conf. (GLOBECOM)*, Anaheim, USA, Sep. 2012.

C. Patent

1. TW patent, I308431, 估計正交分頻多工系統之截波參數的裝置及方法 (2009/04/01 公告核准)

